Sorting through the JuNK: Using Chemical and Genetic Tools to Probe c-Jun N-Terminal Kinase Allostery and Scaffolding, as well as a General Methodology for Studying Localized Kinase Biology

Chloe Lombard

A dissertation

submitted in partial fulfillment of the

requirements for the degree of

Doctor of Philosophy

University of Washington

2019

Reading Committee:

Dustin Maly, Chair

Jesse Zalatan

Gojko Lalic

Program Authorized to Offer Degree:

Chemistry

University of Washington

Abstract

Sorting through the JuNK: Using Chemical and Genetic Tools to Probe c-Jun N-Terminal Kinase Allostery and Scaffolding, as well as a General Methodology for Studying Localized Kinase Biology

Chloe Lombard

Chair of the Supervisory Committee:
Dustin Maly, PhD
Chemistry

This dissertation explores the complicated nature of protein kinase allostery and the use of ATP-competitive inhibitors as tools to study kinase function. Much of this work focuses on the c-Jun N-Terminal Kinases (JNKs), a subfamily of the Mitogen Activate Protein Kinases (MAPK), which are involved in a broad range of signaling processes, including those that are involved in both cell survival and cell death. The JNKs possess docking surfaces, distal to their ATP-binding sites, that engage with scaffold proteins, upstream activators, and downstream substrates. Prior work indicated that binding of certain regulatory proteins to a specific docking surface, termed the D-recruitment site (DRS), could allosterically modulate the conformation of the ATP-binding site of the JNKs. We used a diverse panel of ATP-competitive inhibitors to further investigate the allosteric relationship between the ATP-binding pockets and DRSs of JNKs. We showed that by changing the ATP-binding site occupancy, we could allosterically enhance or decrease binding of

JNKs to the scaffold protein JIP1. Strikingly, the lowest and highest affinity JNK-inhibitor complexes showed a greater than 50-fold difference in dissociation constant. We also found that scaffolding of activated JNKs by JIP1 could prevent specific ATP-competitive inhibitors of JNKs, but not others, from binding. Additionally, we discovered that ATP-competitive inhibitors of JNKs could promote or attenuate activation loop phosphorylation by JNK's upstream activators, MKK4 and MKK7. Given that JIP1, MKK4, and MKK7 all interact with JNK DRSs, these results demonstrate that there is functional allostery between the ATP-binding sites and DRSs of these kinases. Further, our data indicates that the type of JNK inhibitor used in cells may influence the resulting cellular phenotype, and also, that the cellular state of JNKs may affect their ability to bind to certain inhibitors. However, it remains difficult to study JNK regulation in vivo using ATP-competitive inhibitors, mainly due to their promiscuity. To achieve additional selectivity of kinase inhibitors in cells, our lab has designed orthogonal, conformation selective inhibitors that are mono-selective for mutant kinases. We have shown here that they can selectively interact with mutant JNKs, thus providing an attractive tool-set to selectively study these allosteric changes in vivo, in each of the individual JNK isoforms. Finally, we present the development of ATP-competitive inhibitor tools and methodology that will allow further exploration into the spatial regulation of these complex signaling mediators. We have functionalized ATP-competitive inhibitors such that they can be tethered to locally expressed SNAP-tag fusion proteins in vivo. By modifying the specific kinase inhibitor used, or by using different SNAP-fusions to alter the region of SNAP expression, this methodology could be used to study a broad range of kinase -or other protein- targets, and can be employed in any region of interest for which there is a known localization domain.

TABLE OF CONTENTS

LIST OF FIGURES

LIST OF TABLES

LIST OF SCHEMES

ACKNOWLEDGEMENTS

I would like to start off by thanking everyone who helped me along the way. Getting to this point required a village. If I were to thank all of you, I am realizing I would need to write another dissertation, so unfortunately, I may not address each of you directly. However, I will be forever grateful to the *countless* individuals who are responsible for my success.

The person I most need to acknowledge is my late mother, Heidi Lombard, my biggest supporter throughout most of my life. She gave me unconditional love and acceptance that allowed me to experience life knowing that failure was better than never stepping outside the arena. She showed me that it was okay to laugh loudly, laugh often, and *especially* to laugh at yourself. She herself knew, more than anyone, that she was flawed, and she was not afraid to acknowledge or laugh about it. Her openness was what made her exceptional; regrettably, however, I did not fully appreciate that fact until recently. Now, her courage will continue to give me my own, as I learn to express myself and share my heart without fear or reservation. My mother also went above and beyond to positively shape my education and creative pursuits. She even went as far as to open the Pocatello Community Charter School -a school that focused on hands-on learning- with other community parents. I fortunate enough to attend the PCCS from 1st to 8th grade. I doubt I would have my true love and passion for learning -something that, thankfully, will never end- without her efforts.

I would like to thank my husband, Joseph Humphries, who has assumed my mom's role as my biggest supporter, a role that is not always easy to have. We met at the PCCS, when we were both in grade school. In middle school, my mom told me that I should marry him (or someone like him), with her main point being that he would treat me how he treats his mother. However, I assumed his feelings towards me were never anything other than platonic, and we remained friends

throughout high school, before going in different directions for a while. We reconnected during the last year of my undergraduate studies and confessed our mutual affection for one another. Not long after, we began a journey that eventually lead to our marriage in 2019. His love, acceptance, and encouragement were essential in overcoming not only the challenges of graduate school, but also the unpredictable obstacles that life can bring. In a world full of uncertainty, the security of our love has allowed me to accomplish things I feared impossible, and I have no doubt that it will continue to do so throughout our lives. My only regret is that my mom passed away before getting to remind me that she had been right all along.

I am incredibly grateful that my high school chemistry teacher, Susan Mayo, encouraged me to apply for the American Chemical Society (ACS) Project SEED fellowship at Idaho State University. This program allowed me to work in Dr. Andrew Holland's lab the summer following my junior year in high school. I would like to thank Andrew Holland for the experience I had in his lab, which was so instrumental in validating my desire to pursue a PhD in chemistry. I also want to thank my lab mate from Dr. Holland's lab, Zed Platt. Our shared passion for bench science made each day feel more like play than work, and I always have immense joy recalling our adventures.

Working in my undergraduate lab at Boise State University, for Dr. Don Warner, gave me a sense of purpose when I was at a very trying time in my life, and for that, I cannot thank him enough. As I was facing the death of my mother from Stage IV colorectal cancer, working in his lab -which studies specific chemotherapeutics- helped to remind me that I could use my education to help people like my mom. This knowledge gave me the motivation to continue my education, even when it felt like I had no more left to give. There are many professors at BSU who were a huge source of support during that time. The hours I spent talking to them about life and science

were perhaps more influential than anything I learned in class, and those lessons will stay with me for a lifetime. Dr. Ken Cornell was particularly influential in my interest in protein allostery.

I want to offer deep gratitude to the family and friends who were willing to step-up and help during times of challenge in graduate school. I truly could not have made it to where I am without their support and kindness. I would like to specifically thank my grandfather, Paul Anderson, my aunt, Suzy Anderson, my late grandmother, Kathryn Rossiter, and my friends Laura Murphy, Sujata Chakraborty, Jeffrey Paz Buenaflor, and Erin Fagnan.

Throughout the university, there were *many* wonderful professors, classmates, and lab-mates, who not only taught me a great deal about science, but about life. The Chemistry Department administration and staff were also incredibly kind and helpful throughout my time here, especially Paul Miller, Eric Camp, Paul Isaac, Kim Quigley, Diana Knight, and Lochlan Hickok. My "gut instinct," when I arrived to visit the UW Chemistry Department was: "Wow, they *really* seem to care about their graduate students!" I am grateful for my choice to come to UW for my graduate studies every day, because my instinct was spot-on.

I had the privileged of being in the Molecular Biophysics Training Program (MBTP) at UW, where I was able to further my exposure to invaluable research and techniques. The MBTP is funded by the National Institute of Health (Grant #T32GM008268). I am grateful to all the people I met in the MBTP, as well as in the Biological Physics, Structure & Design (BPSD) Program, who offered unique and enriching perspectives that added to my current work and will aid my thinking in the future.

My graduate advisor, Dustin Maly, has been such a wonderful source of support and encouragement these last five years. I feel his greatest lessons were in teaching me how to be an unbiased observer. I recall the first time I generated data that was inconsistent with our prior

hypothesis, and I went to him feeling like I had failed. He looked at me, rather surprised, and asked why I was upset. I said, “The data doesn’t show what we want it to show.” He replied, “What do you mean, ‘what we want it to show?’ We will follow the data wherever it may lead. The data is the data, and we will tell our story based on the data.” In that moment, I changed as a scientist and a person. I realized that you will rarely be able to do good science without first stripping yourself of your bias and your assumptions, which has been much of my focus during my time here.

Graduate school is notoriously challenging, but having a supportive environment (both in and out of the lab) made this experience one that I will genuinely miss. Thank you all.

Chapter 1. INTRODUCTION TO PROTEIN KINASES AND PROTEIN KINASE ALLOSTERY

1.1 Introduction to Protein Kinases and Their Study

Protein kinases are a class of phosphotransferase enzymes that catalyze the transfer of the γ-phosphate of ATP to various cellular substrates, in order to cause functional change to the cellular output. There are 538 protein kinases in the human body, each of which can have dozens of different substrates.[1, 2] It is necessary that kinases phosphorylate the correct substrate at the correct place and time, in response to a specific cellular input (stimulus), in order to produce a desired output (change in the cellular state). Misregulation of kinase signaling often leads to disease, which makes kinases attractive drug targets.[3] Over a decade ago, it was estimated that pharmaceutical companies were spending about 30% of R&D on kinase inhibitors, and though current estimates are unavailable, interest in kinase inhibitors has shown little sign of slowing down.[4, 5] Kinases are now the second most investigated drug target, behind G-protein coupled receptors. There are 37 FDA approved kinase inhibitor drugs already on the market, and as of 2018, there were 150 more in clinical trials.

Kinases are as challenging to study as they are enticing. These essential signaling enzymes are incredibly diverse, and can have many levels of regulation, some of which are especially arduous to investigate. Kinases and their roles in cells are frequently investigated using "knockouts" or "knockdowns" which remove or reduce the expression level of a kinase.[6] After removal or expression level reduction, effect(s) under specific conditions can be observed, and inferences about the function of the kinase can be made. Alternatively, there are several techniques that allow catalytically inactive (dead) kinases to replace the endogenous kinase, such that the kinase is still present in the cell but unable to phosphorylate its substrates.

Increasingly, we are discovering that kinases can have effects beyond just those mediated via direct phosphorylation.[7] In certain situations, this means that replacing a kinase with a catalytically inactive version is more ideal than removing it, as it is more closely approximates the native conditions. In the last couple of decades, selective, ATP-competitive kinase inhibitors have been similarly employed to study kinase biology, as they also result in a loss of catalytic activity for the targeted kinase.[6] Though we have many tools to study the purpose of kinase phosphorylation, studying protein kinase allostery has remained challenging.

1.2 Protein Kinase Allostery and ATP-Competitive Inhibitors as Tools

Protein kinase architecture consists of a bi-local catalytic domain, with an ATP-binding site residing in the cleft between the two lobes.[8] Kinases can have many other regulatory domains, in addition to the main catalytic site. These regulatory domains allow kinases to achieve a broad range of outputs using relatively simple protein components. Upon protein or ATP binding, or phosphorylation of the kinase's regulatory sites, the kinase can experience a change in the conformation of its catalytic and/or regulatory domain(s).[7-9] These conformational changes can modulate the location of the kinase in the cell, the binding of other effectors, their affinity and catalytic efficiency for ATP, and many other aspects of kinase behavior. Each kinase family, and even different isoforms within a subfamily, appear to be fairly unique in their mechanism(s) of control.

Although we are starting to understand how important kinase conformation is for mediating these kinase non-catalytic functions, it often remains difficult to investigate. To study a specific aspect of a kinase's regulation there must be a technique that allows for its perturbation. By modulating a system, and then observing the resulting effect, we can better understand the endogenous process. In this way, scientists have investigated kinase catalytic activity by removing

it. Similarly, scientists have started using chemical tools that can modulate a kinase's conformation in vitro or in vivo, such that we can better understand the native role of those conformational changes in cells. Generally, these tools are ATP-competitive inhibitors. The use of ATP-competitive kinase inhibitors is two-fold. They can be used as drugs to treat specific diseases and, importantly, they can also help us understand the native role of their target kinase(s).[6] While these tools do target the kinase's ATP-binding site, and can often be used solely to achieve kinase inhibition, they can be used to exploit and study the allostery between the regulatory domains and the ATP-binding site.[7, 10-16] Due to the bi-directionality of allostery, stabilizing different ATP-binding site conformations can influence the conformation of distal kinase domains. In doing so, ATP-competitive inhibitors can influence the overall behavior of the kinase, and thus the behavior of the in vitro or in vivo system. By studying the changes to the output, we can better understand non-catalytic aspects of a kinase's biology. For a review highlighting the diversity in the allosteric regulation and non-catalytic functions of protein kinases, as well as the ways ATP-competitive inhibitors can modulate those aspects of their regulation, see Kung *et al.* (2016).[7]

Due to modulation of kinase allostery, even highly selective ATP-competitive inhibitors of a single kinase will often have different and even opposing effects in a cell, if they stabilize different kinase conformations.[7, 17] While drug discovery work can be challenging for that very reason, methodical characterization can yield knowledge that may allow a framework for tuning specific effects, mediated by conformational control of the kinase of interest. Without a thorough understanding of kinase allostery or the many other forms of kinase regulation, however, drug discovery work will often remain a shot in the dark. Since mis-regulation of kinases can lead to a diseased state, the logic behind using kinase inhibitors as drugs is sound and, with high-throughput screening methods, it is often possible to find selective, potent kinase inhibitors. However, the

more we know about the importance of kinase allostery, the less we can ignore the fact that inhibitors may influence significant aspects of a kinase's biology other than its phosphorylation activity, leading to differing effects for inhibitors of the same kinase. Thus, especially when designing inhibitors as drugs, testing many functional outputs may be even more important than designing around inhibitor structures. This is especially true if assumptions about the target kinase allostery are based on the regulation a different kinase, as even isoforms within the same family can have significant variations.

1.3 Using ATP-Competitive Inhibitors to Study JNKs

The c-Jun N-Terminal Kinases (JNKs) are a subfamily of the Mitogen Activated Protein Kinases (MAPKs) and are involved in cell migration, differentiation, proliferation, and apoptosis.[18-22] Due to their importance in these vital processes, it is unsurprising that their misregulation often leads to disease. Despite being the target of intense research for the last couple of decades, their complexity makes them challenging to target in disease treatment. In Chapters 2 and 3, the JNKs are used as a model kinase family to explore some of the diverse effects that ATP-competitive inhibitors can have on kinase behavior.[10] Our studies show that ATP-competitive inhibitors of JNKs are able to allosterically influence in vitro binding of important regulators, including the scaffold protein, JNK Interacting Protein 1 (JIP1), which has been shown to potentiate JNK activation. Certain ATP-competitive inhibitors of the JNKs were able to enhance or decrease activation by their upstream activators, MKK4 or MKK7, in vitro. Further, we found that scaffolding of activated JNKs by JIP1 can prevent some ATP-competitive inhibitors from binding JNKs. Our results add JNKs to a growing list of kinases that are known to be modulated allosterically with ATP-competitive inhibitors. They also indicate that the type of JNK inhibitor

used in cells may influence the resulting cellular phenotype, and that the cellular state of JNKs may affect their ability to bind to certain inhibitors.

Although we were able to probe allosteric modulation of JNKs by ATP-competitive inhibitors in vitro, it remains difficult to study JNKs using ATP-competitive inhibitors in vivo. This is mainly due to the promiscuity of many JNK inhibitors in cells. Not only do many inhibitors frequently bind off-targets like p38, but they also regularly fail to discriminate between JNK family members, which have high sequence homology.[10, 23, 24] To achieve additional selectivity of kinase inhibitors in cells, members of the Maly lab have designed orthogonal, conformation-selective inhibitors that are mono-selective for mutant kinases.[17] In Chapter 3, we show that orthogonal, conformation-selective inhibitors can selectively interact with mutant, sensitized JNKs. This provides an attractive new toolset to selectively study these allosteric changes in each of the individual JNK isoforms in vivo.[25]

1.4 Achieving Enhanced Spatial Resolution of Inhibitor-Based Tools

While ATP-competitive inhibitors are valuable tools for understanding kinase regulation, it remains difficult to probe variations in regulation and function between different subcellular populations of the same kinase. In Chapter 4, we show the development of tools and a methodology that will allow further exploration of the spatial regulation of these complex singling mediators. These tools will allow researchers to more selectively probe localization as a means of kinase regulation and function, something that is difficult to do using global kinase inhibition. In the future, it would be exciting to use the orthogonal, conformation-selective ligands (presented in Chapter 3),[17, 25] in combination with the methodology from Chapter 4. Using these techniques in tandem would allow the selective study of localized signaling, for individual JNK isoforms.

Further, it would allow the investigation of allosteric perturbations in localized populations of JNKs, or other protein kinases.

Chapter 2. ATP-COMPETITIVE INHIBITORS CAN MODULATE JNK DOCKING-SITE INTERACTIONS[1]

2.1 INTRODUCTION TO C-JUN N-TERMINAL KINASES

The c-Jun N-terminal kinases (JNKs) are a multi-functional subfamily of the mitogen activated protein kinases (MAPKs) that play critical roles in cell migration, differentiation, proliferation, and apoptosis.[18, 20-22, 26] The JNK family consists of three distinct but highly homologous isoforms, JNK1, JNK2, and JNK3, which have more than ten total splice variants.[26, 27] The sequences of JNK1 and JNK3 are 92% similar, and they possess only one residue difference in the 23 residues comprising their ATP-binding sites. The sequences of JNK1 and JNK2 are 83% similar, and they also possess only one residue difference in the 23 residues comprising their ATP-binding sites.[28-30] JNK1 and JNK2 are expressed ubiquitously, while JNK3 is expressed mainly in the brain, heart, and testes.[31] JNKs exist in a predominately inactivate, non-phosphorylated state, but are activated by a variety of extracellular stimuli, including UV radiation, oxidative stress, and inflammatory cytokines.[26, 31, 32] Following cellular stimulation, JNKs are predominately activated by their upstream MAPK kinases (MKKs), MKK4 and/or MKK7, via dual phosphorylation of the Thr/Pro/Tyr (TPY) motifs within their activation loops.[31, 33, 34] Activated JNKs then phosphorylate a variety of downstream substrates.[26, 31, 32] Due to their contribution to diverse signaling pathways, which can often determine cell fate, JNK activity is tightly controlled. Aberrant JNK signaling has been associated with cancer, insulin resistance, neurodegeneration, and the development of autoimmune conditions.[26, 35-42]

---

[1] Reprinted (adapted) with permission from Lombard, C. K., Davis, A. L., Inukai, T., and Maly, D. J. (2018) Allosteric Modulation of JNK Docking Site Interactions with ATP-Competitive Inhibitors, *Biochemistry 57*, 5897-5909. Copyright [2018] American Chemical Society.[1]

The structural architecture of JNKs is relatively simple, consisting of a single bi-lobal kinase domain with an ATP-binding cleft at its center.[32] Phospho-acceptor substrates of JNKs bind in an extended conformation, adjacent to the JNK ATP-binding site. While JNKs display substrate preferences based on the primary sequence of the phospho-acceptor, multiple docking surfaces–distal to the site of phosphate transfer–are utilized to discriminate between cellular substrates.[26, 27, 43, 44] These docking interactions provide enhanced specificity in signaling. Many JNK substrates, and other protein binding partners, contain short interacting motifs known as docking-domains (D-domains). D-domains typically consist of a few basic residues and a hydrophobic (φ) motif, surrounding a one to six residue spacer (K/R_{2-3}-X_{1-6}-φ-X-φ).[45, 46] Proteins with D-domains bind to JNK D-recruitment sites (DRS), which are located on the face opposite of the ATP-binding site, mainly on the C-terminal lobe (**Figure 2.1A**). The DRSs of JNKs are multi-functional and mediate interactions with scaffolds, upstream activating MKKs, and a number of substrates.[43-45, 47, 48]

There is believed to be allosteric communication between the ATP-binding sites and DRSs of JNKs, although the full extent of this communication has not yet been determined. Evidence to suggest the existence of allostery between the DRSs and ATP-binding sites of JNKs lies largely in studies exploring the interactions of JNK interacting proteins (JIPs). JIPs are a family of scaffold proteins that have been shown to interact directly with the DRSs of JNKs.[49, 50, 51] Prior work identified an eleven amino acid peptide, derived from the D-domain of JIP1 (RPKRPTTLNLF; JIPtide), that is capable of interacting with the DRSs of JNKs, like the full-length scaffold.[52] Structural alignments of *apo*-JNK3 with either JNK1-JIPtide or JNK3-JIPtide complexes, shows that the N-terminal lobes of JIPtide-bound JNKs are rotated ~15˚ relative to the C-lobe (**Figure 2.2**).[30, 53] Additionally, comparisons of *apo*-JNK3 and JNK3 complexed with other D-domain peptides–derived from JNK substrates–also show significant conformational differences.[53]

Furthermore, JIPtide binding has been demonstrated to modestly affect the affinities of JNKs for ATP.[30, 54, 55] Given that the conformation of kinase ATP-binding sites can be modulated by ligand binding, we were curious whether ATP-competitive inhibitors could alter the ability of both scaffold proteins and upstream MKKs to interact with and act upon the JNKs, by allosterically modulating the behavior of their DRSs. To probe this, we selected ten diverse ATP-competitive inhibitors of the JNKs and systemically probed how they influence the behavior of JIP1, MKK4, and MKK7 (**Figure 2.1B**). We found that ATP-competitive compounds can either *enhance* or *diminish* JNK-JIP1 interactions, and either *activate* or *attenuate* activation by MKK4 or MKK7.

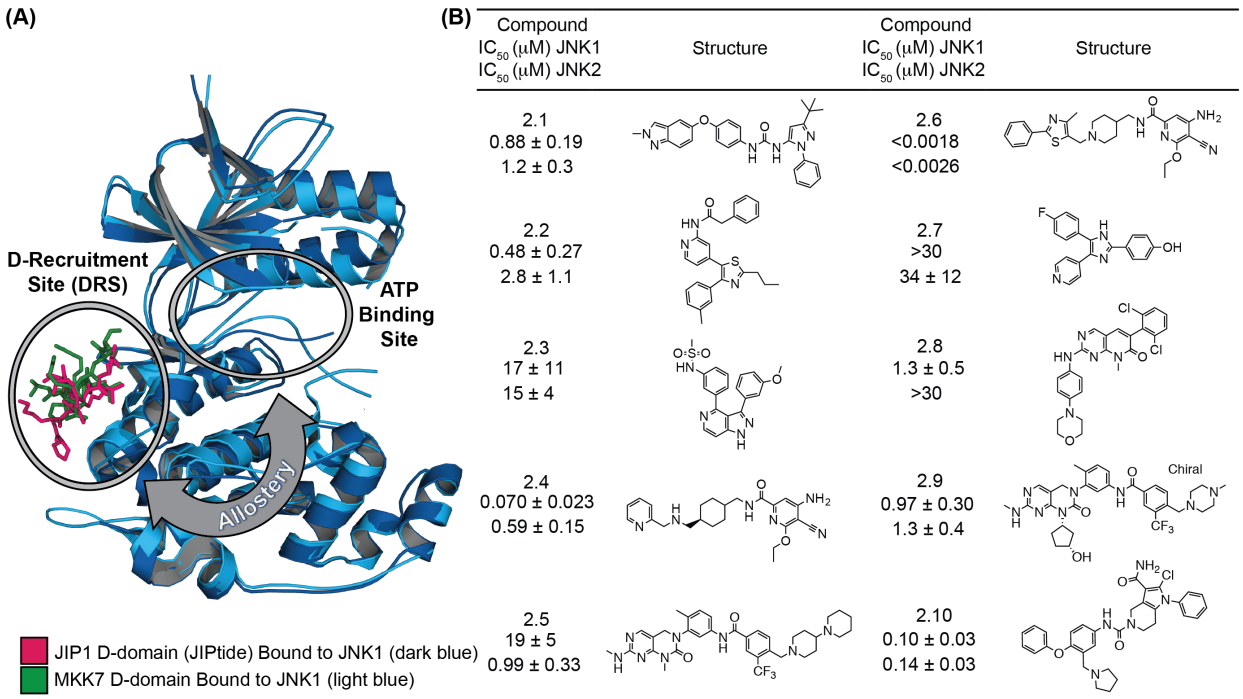

Figure 2.1. *Allosteric communication between the DRSs and ATP-binding sites of JNKs.* (A) Structure of JNK1 bound to JIPtide (blue, PDB ID: 4E73) or the D-domain of MKK7 (green, PDB ID: 4UX9). The DRS and ATP-binding site of JNK1 are circled. (B) The ten ATP-competitive JNK compounds that were used in this study and their IC_{50} values for JNK1 and JNK2 in a TR-FRET activity assay.

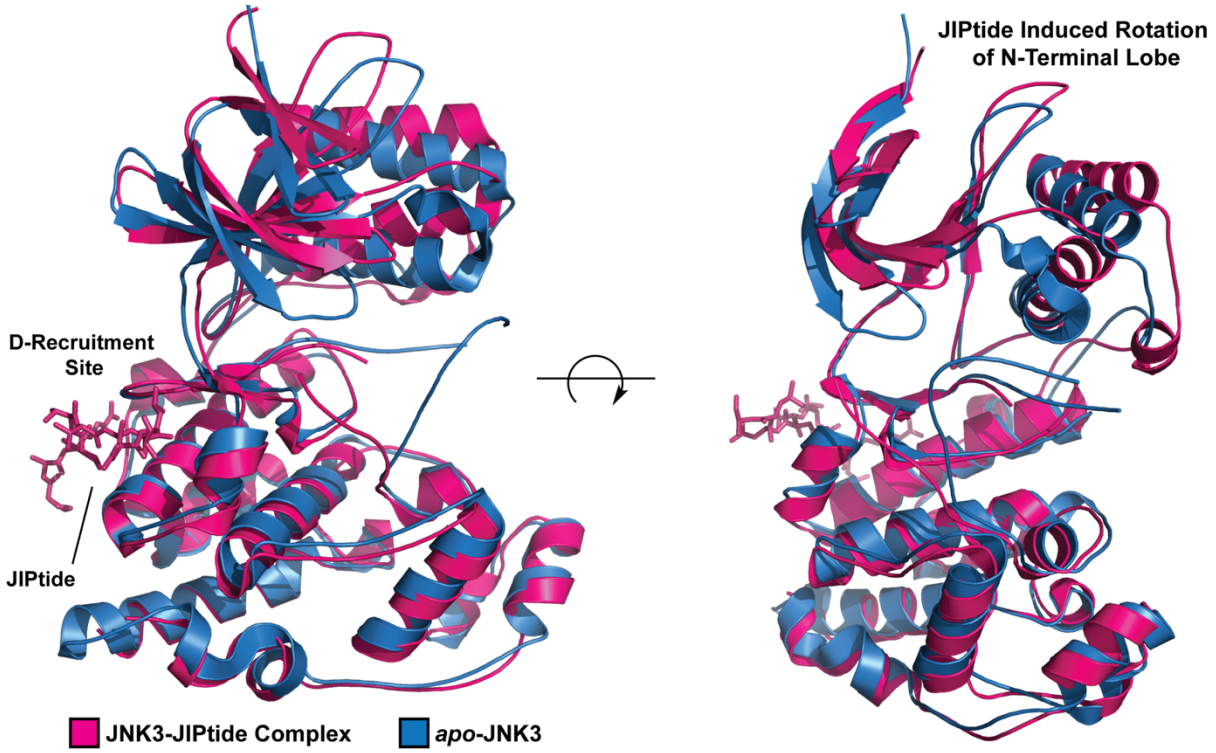

Figure 2.2. *JIPtide induces interlobe rotation in JNK3 crystal structures.* Alignment of apo-JNK3 (Purple) with JNK3 in complex with JIPtide (Pink).[30, 53] JIPtide binding to DRS (D-recruitment site) of JNK3 induces an ~15° rotation of the N-terminal lobe, relative to the C-terminal lobe (PDB IDs: 4KKG (apo), 4H39 (JIPtide)).

2.2 Allosteric Communication Between the DRSs and ATP-Binding Sites of JNKs

To facilitate our investigation of how ATP-binding site occupancy affects the docking interactions of JNKs, we assembled a diverse panel of ten ATP-competitive inhibitors of the JNKs (**Figure 2.1B**). These compounds are based on several different scaffolds that should make differential interactions with variable regions of JNK ATP-binding sites. Because we were interested in exploring how JIP1 and MKKs interact with non-phosphorylated JNKs, which possess almost undetectable catalytic activity, we first confirmed that each compound binds to the ATP-binding site of non-phosphorylated JNK1. To do this, we developed a Time-Resolved

Fluorescence Energy Transfer (TR-FRET) competition assay, that can be used to determine the affinities of ATP-binding site ligands, independent of kinase activation state (**Figure 2.3A**). This assay measures the ability of compounds to block TR-FRET between a europium-labeled antibody–bound to the N-terminal His_6-tag of JNK1–and a cyanine 5 (Cy5)-labeled, ATP-binding site ligand (**Figures 2.3B, 2.3C**). The inhibitory constants (K_is) of our ten ATP-competitive inhibitors for non-phosphorylated JNK1 are shown in **Figure 2.3D**.

All ten inhibitors in our panel were capable of competitively displacing the Cy5-probe from the ATP-binding site of non-phosphorylated JNK1 (**Figure 2.3D**). Furthermore, we found that the IC_{50} values for all ten ATP-competitive compounds for inhibition of activated phospho-JNK1 correlated well with their K_is in the binding assay with non-phosphorylated JNK1. Most importantly, we found that all ten ATP-competitive inhibitors in our panel bind with high enough affinity to non-phosphorylated JNK1 that near quantitative JNK-inhibitor complexes can be generated for biochemical studies.

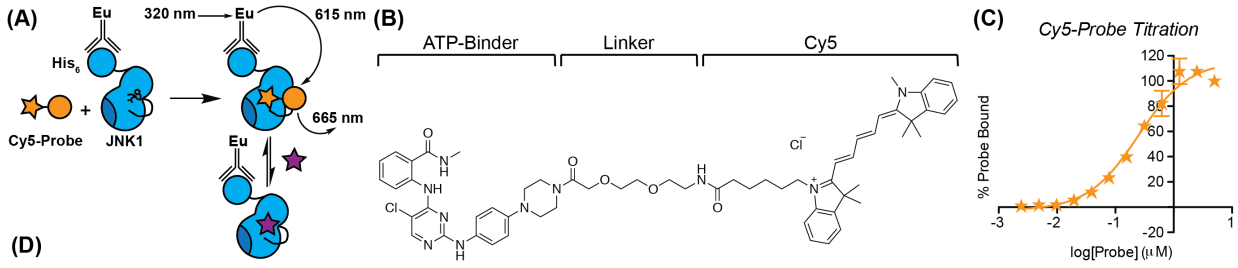

(D)

Compound	K_i (μM) JNK1	Compound	K_i (μM) JNK1
2.1	0.27 ± 0.01	**2.6**	0.015 ± 0.002
2.2	0.20 ± 0.03	**2.7**	3.2 ± 0.3
2.3	0.88 ± 0.12	**2.8**	0.40 ± 0.06
2.4	0.080 ± 0.011	**2.9**	0.41 ± 0.02
2.5	3.8 ± 1.6	**2.10**	0.11 ± 0.05

Figure 2.3. *A competitive binding assay for determining the affinities of JNK inhibitors for non-phosphorylated JNKs*. (A) Schematic of the TR-FRET-based competition binding assay. (B) Structure of the Cy5-labeled, ATP-binding site probe (Cy5-Probe). (C) Titration curve of the Cy5-probe's binding interaction with non-phosphorylated JNK1. (D)

Inhibitory constants (K_is) of compounds **2.1-2.10** for non-phosphorylated JNK1. Values shown are mean ± SEM (n=3).

2.3 ATP-Competitive Inhibitors Modulate JNK1's Affinity for the D-Domain of JIP1

We next investigated whether ATP-binding site occupancy of JNK1 could allosterically modulate the interaction of its DRS with JIP1. To do this, we used a fluorescence polarization (FP) binding assay to measure the affinity of non-phosphorylated JNK1 and a 6-carboxytertamethylrhodamine(TMR)-peptide containing the D-domain of JIP1 (TMR-JIPtide). (**Figures 2.4A, 2.4B**).[52, 56] Titration of non-phosphorylated *apo*-JNK1 against a fixed concentration of TMR-JIPtide provided a dissociation constant (K_D) for these two species of 0.89 ± 0.09 μM (**Figure 2.4C**), which is consistent with prior studies.[56] We performed the same titration with ATP-bound JNK1 and found that this complex bound two-fold more tightly to JIPtide than *apo*-JNK1 (**Figure 2.4D**)

Next, we performed similar titrations with JNK1 complexed to each of the inhibitors in our panel, to determine how different modes of ATP-binding site occupancy affect JNK1's affinity for JIPtide. Titration of different JNK1-inhibitor complexes across a fixed concentration of TMR-JIPtide revealed that ATP-binding site occupancy can either strengthen or weaken JIPtide binding (**Figure 2.4**). Six out of the ten JNK1-inhibitor complexes tested showed a modest–but significant–increase in affinity for TMR-JIPtide, with the JNK1-**2.1** complex demonstrating the largest overall enhancement (**Figure 2.4E**). We observed that three JNK1-inhibitor complexes demonstrated significantly diminished affinity for TMR-JIPtide relative to the *apo* or the ATP-bound forms of the kinase. Binding of inhibitor **2** caused the largest decrease in JIPtide affinity, with the JNK1-**2.2** complex exhibiting an ~30-fold higher K_D for TMR-JIPtide compared to JNK1-ATP (**Figure**

2.4F). Overall, we found that the affinity of JNK1 for JIPtide can differ by ~50-fold, depending on the ligand occupying the ATP-binding site (**Figure 2.4G**).

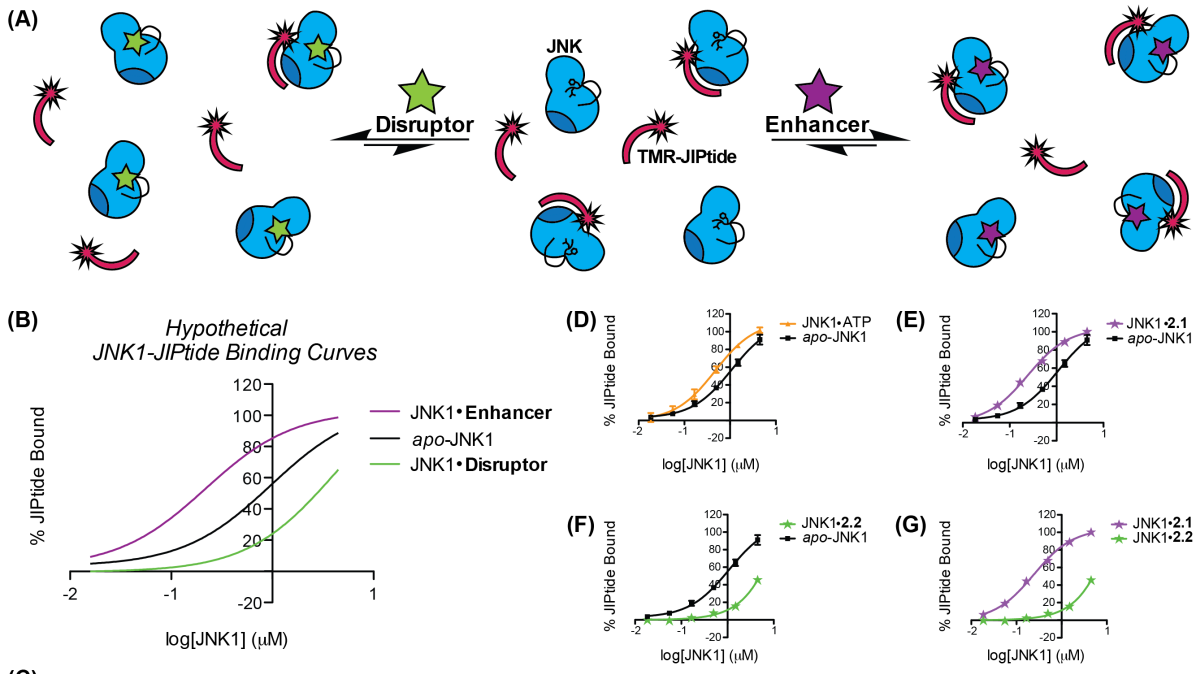

(C)

Complex	JIPtide K_D(μM) for JNK Complex	Complex	JIPtide K_D(μM) for JNK Complex	Complex	JIPtide K_D(μM) for JNK Complex	Complex	JIPtide K_D(μM) for JNK Complex
apo-JNK1	0.89 ± 0.09	JNK1•**2.2**	14 ± 1	JNK1•**2.5**	0.68 ± 0.10	JNK1•**2.8**	0.31 ± 0.01
JNK1•ATP	0.40 ± 0.07	JNK1•**2.3**	0.25 ± 0.02	JNK1•**2.6**	3.2 ± 0.4	JNK1•**2.9**	0.45 ± 0.02
JNK1•**2.1**	0.23 ± 0.03	JNK1•**2.4**	1.5 ± 0.1	JNK1•**2.7**	3.6 ± 0.1	JNK1•**2.10**	0.44 ± 0.09

Figure 2.4. *Influence of JNK ATP-binding site occupancy on JIPtide affinity*. (A) Two modes of how ATP-competitive inhibitors can modulate the affinity of JNKs for TMR-JIPtide. Disruptors reduce the affinity of JNKs for TMR-JIPtide by allosterically stabilizing a docking site conformation with reduced complementary to TMR-JIPtide. Enhancers increase the affinity of JNKs for TMR-JIPtide by allosterically stabilizing a docking site conformation with increased complementary to JIPtide. (B) Schematic of how JNK-enhancer and JNK-disruptor complexes behave in the TMR-JIPtide FP assay. (C) K_Ds of JIPtide for *apo*-JNK1 and JNK1-inhibitor complexes. Values shown are mean ± SEM (n=3). (D-G) Titration curves of *apo*-JNK1 and JNK1-inhibitor complexes against TMR-JIPtide.

2.4 ATP-Competitive Compounds Modulate JIPtide Binding to Non-Phosphorylated JNK2 and JNK3

We performed similar binding assays with TMR-JIPtide and non-phosphorylated JNK2 and JNK3 to investigate any similarities or differences in how ATP-binding site occupancy influences JIPtide affinity amongst the JNKs. In general, we found that most of the inhibitors we tested have similar effects on all JNK isoforms (**Table 2.1**). For example, the **2.2**- and **2.6**-bound forms of all three JNKs demonstrated lower affinity for TMR-JIPtide relative to their *apo* forms. Furthermore, several inhibitors enhanced the interaction between TMR-JIPtide and all three JNK isoforms.

However, some inhibitors demonstrated divergent effects on the JNK isoforms. Consistent with the high sequence homology between JNK1 and JNK3 (92%),[29, 30] we observed the most similarity between these two isoforms in how ATP-binding site occupancy affected JIPtide binding affinity. JNK2 displayed the lowest affinity for TMR-JIPtide (K_D = 7.9 ± 0.8 μM) and the most divergent behavior in how ATP-competitive ligands influenced its affinity for JIPtide. For example, compound **2.5** slightly increased JNK1's and JNK3's affinity for JIPtide but reduced the strength of the JNK2-JIPtide interaction by ~4 fold. Furthermore, JNK2 displayed the smallest fold differences between JIPtide's affinity for different ligand-bound complexes. These differences may reflect divergences in allosteric regulation between JNK family members.

Table 2.1. JNK/TMR-JIPtide K_Ds (μM) ± 30 μM compound, determined using a fluorescence polarization binding assay.

Compound	JNK1	JNK2	JNK3
DMSO	0.89 ± 0.09	7.9 ± 0.8	1.9 ± 0.2
2.1	0.23 ± 0.03	4.6 ± 0.4	0.48 ± 0.01
2.2	14 ± 1	17 ± 2	12 ± 2
2.3	0.25 ± 0.01	3.0 ± 0.2	0.64 ± 0.08
2.4	1.5 ± 0.1	6.0 ± 0.8	2.8 ± 0.2
2.5	0.68 ± 0.09	37 ± 8	1.7 ± 0.2
2.6	3.2 ± 0.4	15 ± 1	4.6 ± 0.2
2.10	0.44 ± 0.09	5.1 ± 0.2	1.5 ± 0.1

2.5 Effects of ATP-Binding Site Occupancy on JNK1's Interaction with Full Length JIP

We were curious whether the allosteric influence that our panel of inhibitors had on JNK1's interaction with JIPtide would also hold for full-length JIP1. To this end, we developed a JNK1 pull-down assay using immobilized, full-length JIP1 (**Figure 2.5A**). We used quantitative western blotting of retained JNK1 to determine the relative affinities of *apo*-JNK1 and different JNK1-inhibitor complexes for immobilized JIP1 (**Figure 2.6**). Consistent with the minimized JIPtide peptide behaving like the full-length protein scaffold, we observed that all ten inhibitors have a similar influence on JNK1's interaction with full-length JIP1 and JIPtide (**Figure 2.5B**). JNK1 complexed to compounds **2.1**, **2.3**, **2.5**, and **2.10** showed a significant increase in retained JNK1 relative to *apo*-JNK1, which reflects the higher binding affinities of these JNK1-inhibitor complexes for JIPtide. Furthermore, all four JNK1-inhibitor complexes that demonstrated reduced affinities for JIPtide also showed diminished retention by immobilized JIP1. Notably, the relative amounts of JNK1-**2.2**, JNK1-**2.4**, JNK1-**2.6**, and JNK1-**2.7** retained in the pull-down assay correlates with the binding affinities of these JNK1-inhibitor complexes for TMR-JIPtide. Given that we were unable to perform JNK1 titrations in the pull-down assay due to technical limitations,

quantitative differences in affinities between different JNK1-inhibitor complexes for full-length JIP1 could not be determined. However, our results demonstrate that TMR-JIPtide is a suitable surrogate for performing quantitative studies on the allosteric relationship between ATP-binding site occupancy and the DRSs of JNKs.

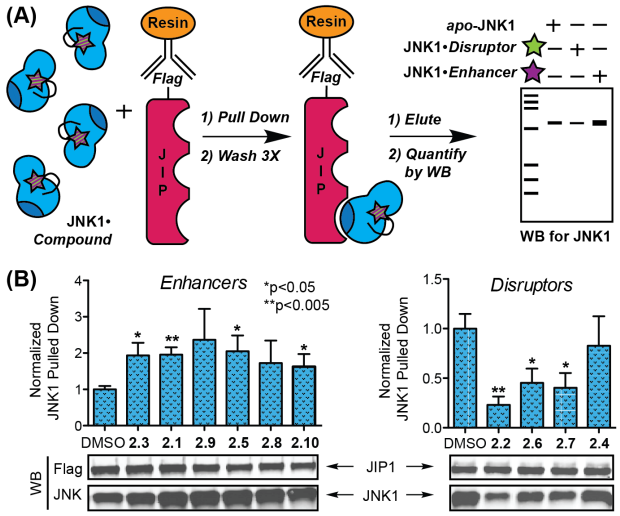

Figure 2.5. *Effects of ATP-binding site occupancy on JNK1's interaction with full-length JIP1.* (A) Schematic of the pull-down assay. (B) Full-length Flag-JIP1 (0.6 μM) was immobilized and then incubated with either 200 nM JNK1 (left) or 500 nM JNK1 (right), ± 10 μM ATP-competitive inhibitor. The JNK1-JIP1 complexes were washed and remaining JNK1-JIP1 was eluted from the beads. JIP1 and JNK1 were detected by western blotting for total JNK (JNK1) and Flag (JIP1). Values shown are mean ± SEM (n=3). Statistical significance was determined by a two-tailed, unpaired t-test. See **Figure 2.6** for JNK1 western blot linearity curves, which allow quantitative comparisons.

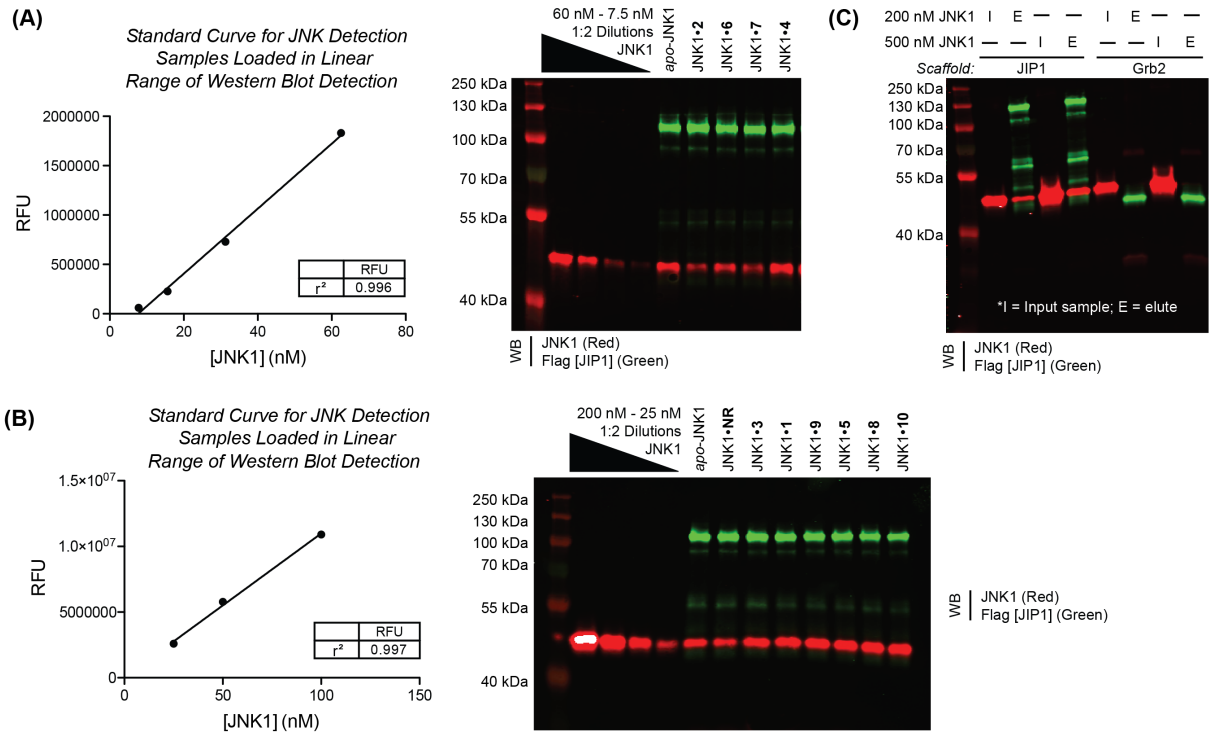

Figure 2.6. *Control experiments for JNK1-JIP1 pull-down assays* (**Figure 2.5**). (A) Standard JNK1 samples were used to validate that the eluted JNK1 in our pull-down samples was loaded in the linear range of western blot detection. Purified JNK1 dilutions were loaded on the gel used for western blot analysis of the compounds which disrupt JIP1 binding. JNK1 standard dilutions from 60 nM to 7.5 nM were quantified, and samples from the pull-down lie within the linear range of the signal for the standards. (B) As in (A), purified JNK1 dilutions were loaded on the gel used for western blot analysis of the compounds which enhance JIP1 binding. Quantified JNK1 standard dilutions range from 100 nM to 25 nM and samples from the pull-down lie within the linear range of the signal for the standards. (C) Control pull-downs were conducted using either Flag-JIP1 or Flag-Grb2 (an alternative, non-JNK binding scaffold). The scaffolds were incubated with either 200 nM JNK1 or 500 nM JNK1 (the two concentrations used in our pull downs), to validate that there was no detectable nonspecific binding of JNK1 to Flag-Grb2 under our pull-down conditions.

2.6 Assay for Quantitative Determination of JNK1 Phospho-State

MKK4 and MKK7 activate JNKs by phosphorylation of the TPY motif within their activation loops.[33, 34] Like JIP1, MKK4 and MKK7 use D-domains to interact with JNKs, but whether these binding events are allosterically coupled to the ATP-binding sites of JNKs has not been explored.[26, 43, 44] We were thus interested in using our inhibitors to determine how ATP-binding site occupancy affects the ability of MKK4 and MKK7 to phosphorylate the activation loops of JNKs. However, the mechanism by which MKK4 and MKK7 activate the JNKs is complex. While each of these MKKs have been shown to be capable of fully activating JNKs via dual phosphorylation of the TPY motif, this process is inefficient. In many circumstances, both MKKs are believed to be needed to achieve efficient dual phosphorylation. Therefore, prior to performing our studies, we developed a quantitative assay for measuring all phospho-forms of JNKs. To this end, we used Phos-tag sodium dodecyl sulfate polyacrylamide gel electrophoresis (Phos-tag SDS-PAGE), which allows phospho-forms of a protein to be separated and visualized based on the retarded migration of phosphorylated species by a polyacrylamide-immobilized manganese ion. (**Figure 2.7A**).[57, 58] We felt this assay would be ideal for our studies because it would allow us to quantify the ratio of non-, mono-, and dual-phosphorylated species.

We first determined whether Phos-tag SDS-PAGE could be used to separate JNK isoforms by activating JNK1 with a low or a high concentration of MKK4 (**Figure 2.7B**). Both activation conditions showed three bands when separated by Phos-tag SDS-PAGE and visualized with a total JNK antibody. For JNK1 activated with the lower concentration of MKK4, we observed a lower band that corresponds to non-phosphorylated JNK1, a middle band that is positive for phospho-Tyr but not dual phosphorylation, and a top band that is positive for dual-phosphorylated JNK1 (**Figure 2.7B**). Subjection of JNK1 to the higher concentration of MKK4 led to a significant

increase in the top band, which corresponds to dual-phosphorylated JNK1, and diminution of the middle mono-phosphorylated JNK1 band. JNK1 activated with low or high concentrations of MKK7 produced similar distributions of JNK1 phospho-forms. However, under both activation regimes the middle band was not positive for phospho-Tyr, unlike MKK4-activated JNK1, which implies that this species is likely JNK1 mono-phosphorylated on Thr183. Our results are consistent with prior studies demonstrating MKK4's preference for Tyr185 and MKK7's preference for Thr183, even though both MKKs have been shown to be capable of achieving dual phosphorylation of JNKs in vitro.[33]

Having demonstrated that Phos-tag SDS-PAGE can separate all phospho-forms of JNK1, we next sought a more reproducible and quantitative method for determining JNK1 phospho-state. To this end, we created TMR-JNK1 (**Figure 2.7C**), using the transpeptidase Sortase A to transfer TMR-LPTY–from a TMR-labeled, substrate peptide–to the free N-terminus of JNK1 (**Figure 2.7D** and **Figure 2.8**).[59]

This method allowed us to separate the JNK1 phospho-forms using Phos-tag SDS-PAGE, and directly visualize them using fluorescence imaging of the TMR-JNK1. We observed that high concentrations of MKK4 or MKK7 led to similar ratios of phospho-states for TMR-JNK1 and unlabeled-JNK1, demonstrating that the fluorescently-labeled construct behaves like untagged JNK1 (**Figure 2.7E**).

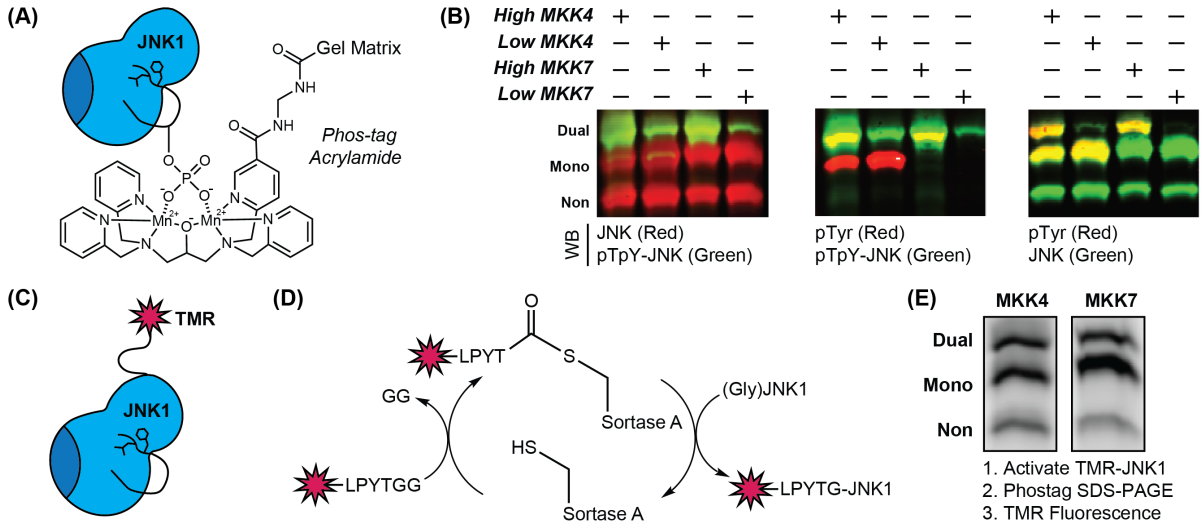

Figure 2.7. *Assay for quantitative determination of JNK1 phospho-state.* (A) Phos-tag SDS-PAGE was used to separate and quantify non-, mono-, and dual-phosphorylated JNK1. (B) JNK1 (200 nM) was activated with either high (900 nM) or low (30 nM) MKK4 or MKK7 concentrations, and the reaction was separated by Phos-tag SDS-PAGE. Western blotting for total JNK, pT183/pY185 JNK (dual phosphorylation), and pTyr was used confirm the identity of the JNK1 phospho-forms. (C) Structure of TMR-labeled JNK1. (D) Sortase A method for labeling the N-terminus of JNK1 with TMR (for gels showing creation and purification of TMR-JNK1, see **Figure 2.8**). (E) TMR-JNK1 (200 nM) was activated with either 900 nM MKK4 or MKK7, separated by Phos-tag SDS-PAGE, and imaged using fluorescence scanning.

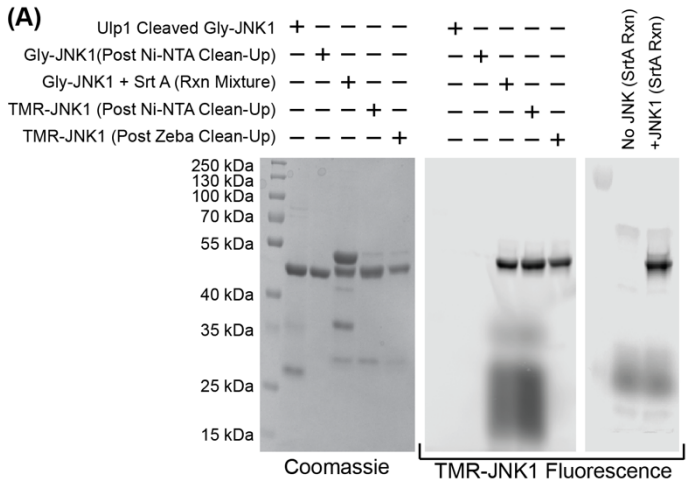

Figure 2.8. *Creation and purification of TMR- JNK1α1.* The Left and Middle gels are the same, visualized using either Coomassie staining (Left) or TMR-fluorescence (Middle). His_6–SUMO-JNK1α1 was treated with His_6-Ulp1 during O.N. dialysis to yield JNK1α1 for subsequent Sortase A labeling [Ulp1 Cleaved Gly-JNK1]. His_6-Ulp1 and His_6-SUMO were removed by Ni-NTA [Gly-JNK1(Post Ni-NTA Clean-Up)]. Gly-JNK1α1 (10 μM) was then combined with Sortase A (SrtA; 20 μM) and Rhodamine-LPETGG (200 μM), in SrtA labeling buffer, for 1.5 hr, at 4°C, in the dark [Gly-JNK1 + Srt A (RXN Mixture)]. The His_6–SrtA was then removed by Ni-NTA [TMR-JNK1 (Post Ni-NTA Clean-Up)] and the remaining peptide was removed using Zeba columns (Thermo Fisher), which also allowed exchange into our standard dialysis buffer [TMR-JNK1 (Post Zeba Clean-Up)]. "TMR-JNK1 (Post Zeba Clean-Up)" was used in all experiments and is referred to as TMR-JNK1.

2.7 Kinetic Analysis of JNK1 Activation

Prior to performing studies on how ATP-binding site occupancy affects the activation of JNKs, we used our new assay to provide the first quantitative look at the generation of mono- and dual-phosphorylated JNK1 by MKK4 and MKK7 (**Figure 2.9A**). We began by conducting titrations with MKK4 or MKK7 to determine how generation of mono- and dual-phosphorylated TMR-JNK1 correlates to the activities of these enzymes (**Figure 2.9B**). We observed a graded increase in the amount of mono-phosphorylated JNK1 generated as MKK4 concentrations were elevated, until a sufficient amount of mono-phosphorylated JNK1 was formed that higher concentrations of

MKK4 converted to the dual-phosphorylated species. We saw a similar effect with the MKK7 titration, except the transitions from the non-phosphorylated to the mono-phosphorylated species and from the mono-phosphorylated to the dual-phosphorylated species were more stepwise than graded. Thus, MKK4 and MKK7 show distinct behaviors in the amount of activity required to generate different phospho-forms of JNK1.

We then conducted time courses for TMR-JNK1 activation using three MKK concentrations that span the activation regimes we observed at the single, one hour timepoint in **Figure 2.9B**. We found that the lowest concentration of MKK4 led to a near linear increase in mono-phosphorylated TMR-JNK1 over time, with a similar linear increase observed for MKK7 as well (**Figures 2.9C, 2.9D**). Activation of TMR-JNK1 with a 30-fold higher concentration of MKK4 led to rapid formation–within five minutes–of mono-phosphorylated JNK1 that minimally increased over time, and barely detectable dual-phosphorylated JNK1 at the last timepoint (**Figure 2.9E**). An almost identical kinetic behavior was observed for activation of TMR-JNK1 with an intermediate concentration of MKK7 (**Figure 2.9F**). Interestingly, co-activation of TMR-JNK1 with both MKK4 and MKK7 at the same intermediate concentrations led to rapid–within 30 seconds–generation of mono- and dual-phosphorylated JNK1 that was converted predominately to the dually phosphorylated species over time (**Figure 2.9G**). This observation is consistent with prior studies showing that MKK4 and MKK7 likely work synergistically to achieve efficient full (dual) activation of JNK in cells.[33, 34] The highest concentration of MKK4 led mainly to mono-phosphorylated TMR-JNK1 at the first timepoint tested (30 seconds), followed by an almost linear conversion of the mono-phosphorylated species to dual over 20 min (**Figure 2.9H**). Again, we observed an almost identical kinetic behavior for activation of TMR-JNK1 by the highest concentration of MKK7 (**Figure 2.9I**). Thus, although MKK4 and MKK7 demonstrate differences

in the amount of activity required to transition between different JNK1 phospho-forms (**Figure 2.9B**) and in the identity of the mono-phosphorylated species that they generate (**Figure 2.9B**), their kinetic behavior in the activation of JNK1 appears to be quite similar.

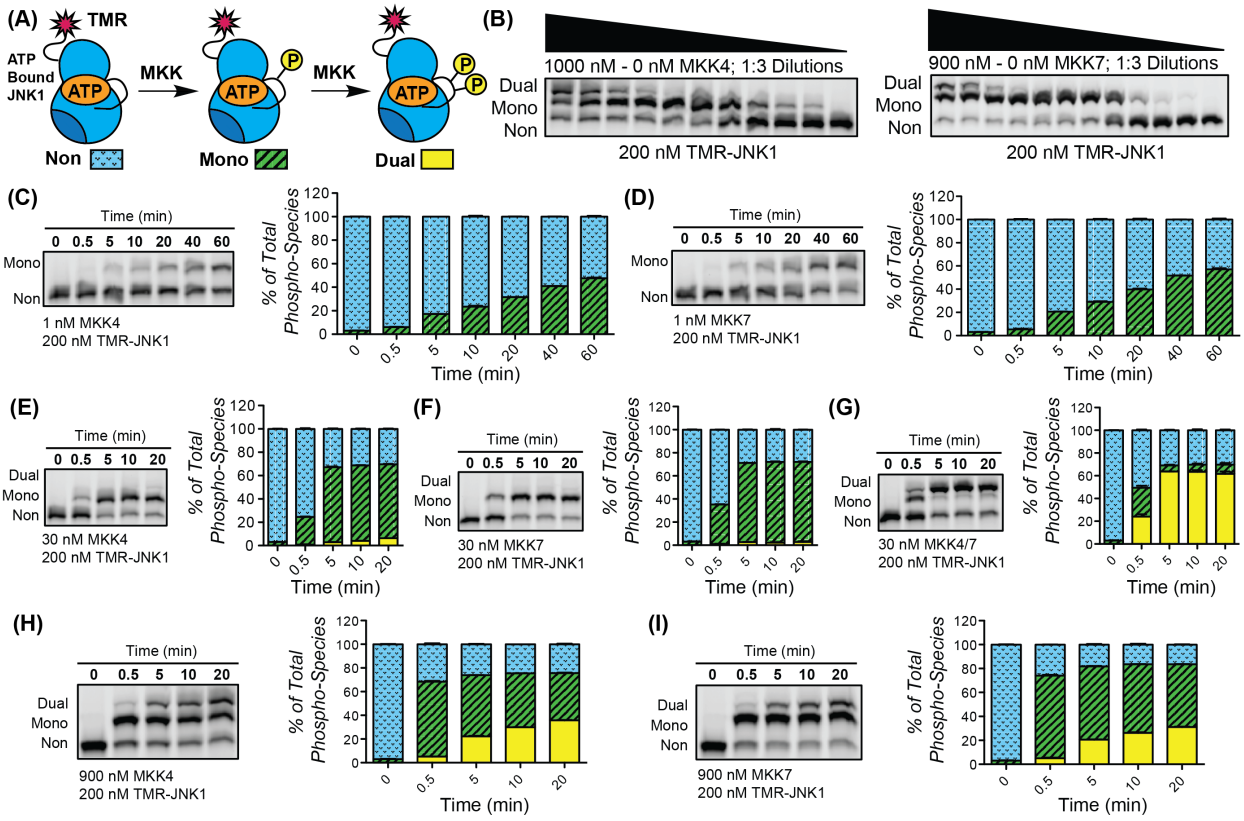

Figure 2.9. *Quantitative analyses of TMR-JNK1 phosphorylation by MKK4 and MKK7.* (A) TMR-JNK1 was activated under varying conditions and resulting phospho-forms were quantified with fluorescence scanning following Phos-tag SDS-PAGE. (B) Varying concentrations of MKK4 or MKK7 were used to activate TMR-JNK1 for one hour and JNK1 phospho-forms were resolved with Phos-tag SDS-PAGE. (C-H) Kinetic analyses of TMR-JNK1 activation under different MKK4 and MKK7 concentration regimes. Values shown are mean ± SEM (n=3). (C) TMR-JNK1 activation by 1 nM MKK4. (D) TMR-JNK1 activation by 1 nM MKK7. (E) TMR-JNK1 activation by 30 nM MKK4. (F) TMR-JNK1 activation by 30 nM MKK7. (G) TMR-JNK1 activation by 30 nM MKK4 and 30 nM MKK7. (H) TMR-JNK1 activation by 900 nM MKK4. (I) TMR-JNK1 activation by 900 nM MKK7.

2.8 ATP-Competitive Inhibitors Can Enhance or Diminish JNK1 Activation Loop Phosphorylation by MKK7

Next, we sought to determine how varying the occupancy of JNK1's ATP-binding site influenced the ability of MKK7 to generate mono- and dual-phosphorylated JNK1 (**Figure 2.10A**). First, we measured how much mono- and dual-phosphorylated JNK1 were produced when different JNK1-inhibitor complexes were activated with a high concentration of MKK7, relative to JNK1 that was not bound to an ATP-competitive inhibitor (**Figure 2.10B)**. Using this activation regime, we observed that the dual-phosphorylation of JNK1's activation loop by MKK7 is either enhanced, diminished, or unaffected when it is bound to ATP-competitive inhibitors. Inhibitors **2.2**, **2.4**, **2.5**, **2.7**, and **2.10** had only a small effect on the amount of mono- and dual-phosphorylated JNK1 generated, while JNK1 bound to **2.1**, **2.3**, **2.8**, or **2.9** was more readily converted to the dual-phosphorylated species relative to JNK1 in the absence of an ATP-competitive inhibitor. Notably, **2.1**, **2.3**, **2.8**, and **2.9** also increase the affinity of the JIP1 scaffold protein for JNK1 (**Figures 2.10C, 2.10B**), suggesting that MKK7's interaction with JNK1 may be strengthened by a similar mechanism.

Our JNK1 activation results at a high concentration of MKK7 demonstrated that compounds **2.1**, **2.3**, **2.8**, and **2.9** enhanced generation of the dual-phosphorylated species at the expense of the mono-phosphorylated form. Therefore, we next measured how efficiently the activation loops of different JNK1-inhibitor complexes were phosphorylated by a concentration of MKK7 that does not generate the dual-phosphorylated form (**Figure 2.10B**). Under this activation regime, we found that compounds **2.1**, **2.3**, and **2.8** had little or no effect on MKK7's ability to generate mono-phosphorylated JNK1 (**Figure 2.10C**). In contrast, compound **2.9** dramatically decreased the amount of mono-phosphorylated JNK1 generated, despite promoting the production

of dual-phosphorylated JNK1 at a higher MKK7 concentration. These results suggest that unphosphorylated JNK1's interaction with **2.1**, **2.3**, **2.8**, or **2.9** does not make it a better substrate for MKK7 relative to JNK1 in the absence of an ATP-competitive inhibitor. However, once these inhibitor-bound JNK1 complexes become mono-phosphorylated, they are more readily converted to the dual-phosphorylated species by MKK7. JNK1 bound to compound **2.9** is the most striking example of this trend; the JNK1-**2.9** complex is a poor substrate for MKK7, but the mono-phosphorylated JNK1-**2.9** complex is efficiently converted to the dual-phosphorylated species.

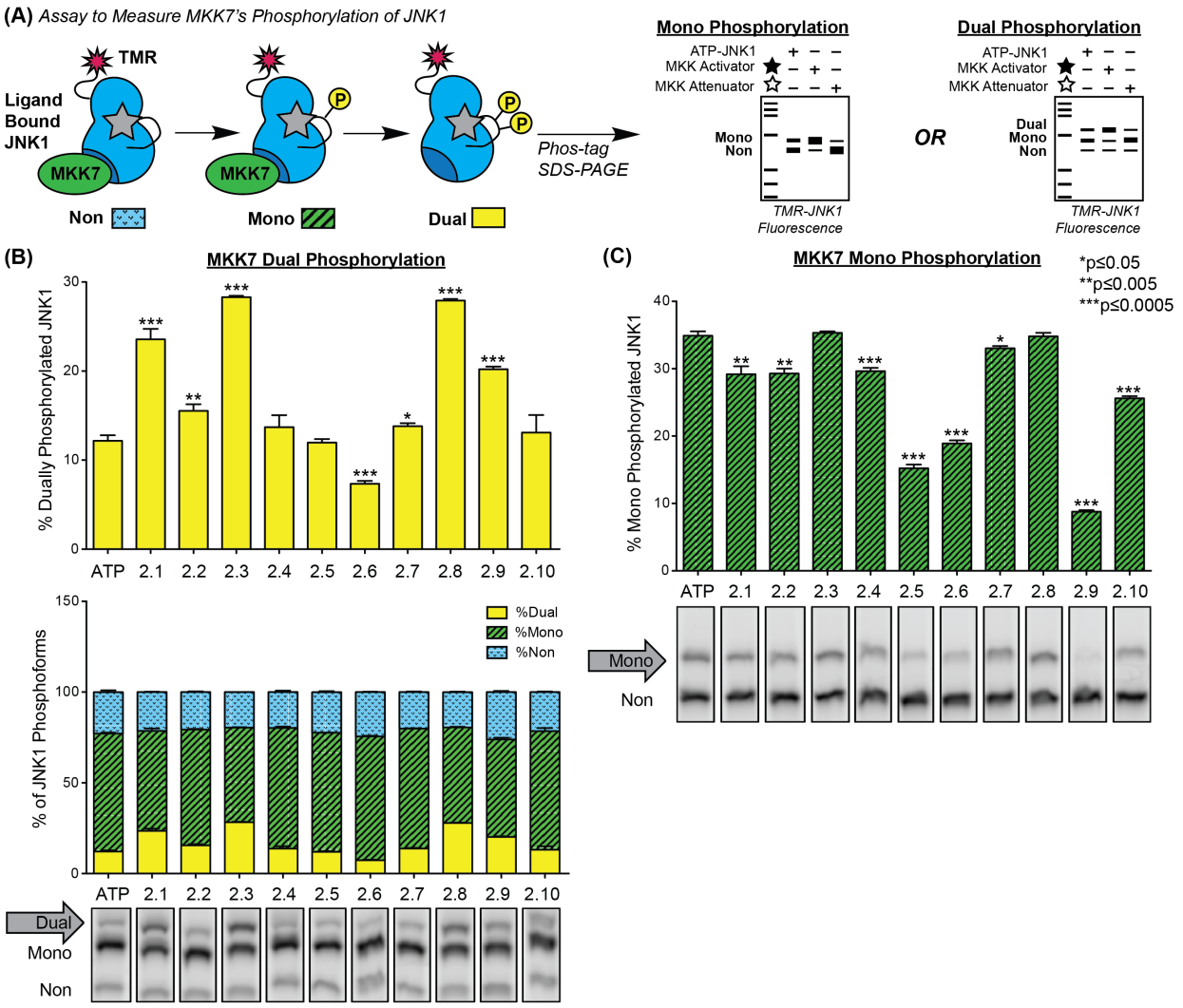

Figure 2.10. *Quantitative assessment of how ATP-competitive inhibitors affect JNK1 phosphorylation by MKK7.* (A) Assay to assess how the ATP-binding site occupancy of JNK1 influences its activation by MKK7. (B) TMR-JNK1 was incubated with ATP and different ATP-competitive inhibitors, followed by the addition of MKK7 (150 nM). After one hour of incubation, JNK1 phospho-forms were separated by Phos-tag SDS-PAGE, detected, and quantified using fluorescence scanning. Values shown are mean ± SEM (n=3). Statistical significance was determined by a two-tailed, unpaired t-test. (C) Experiments conducted as in (B), except with 0.25 nM MKK7.

2.9 ATP-Competitive Inhibitors Can Enhance or Diminish JNK1 Activation Loop Phosphorylation by MKK4

We next determined whether MKK4's ability to generate mono- and dual-phosphorylated JNK1 was similarly influenced by JNK1's interaction with ATP-competitive inhibitors (**Figure 2.11A**). Like with MKK7, we first measured how much mono- and dual-phosphorylated JNK1 were produced when different JNK1-inhibitor complexes were activated with a high concentration of MKK4, relative to JNK1 that was not bound to an ATP-competitive inhibitor. Using this activation regime, we found that most inhibitor-bound JNK1 complexes were similarly acted upon by MKK4 and MKK7 (**Figure 2.11B**). For example, inhibitors **2.2**, **2.4**, **2.5**, and **2.7** had only a small effect on the amount of mono- and dual-phosphorylated JNK1 generated by MKK4, while JNK1 bound to **2.3**, **2.8**, or **2.9** was more readily converted to the dual-phosphorylated species relative to *apo*-JNK1. Furthermore, the JNK1-**2.6** complex was a poor substrate for MKK4, like it was for MKK7. The only major difference between MKK4 and MKK7 was their relative abilities to generate mono- and dual-phosphorylated species of the JNK1-**2.1** complex. JNK1's interaction with **2.1** makes it a better substrate for MKK7, while this ligand makes it an inferior substrate for MKK4.

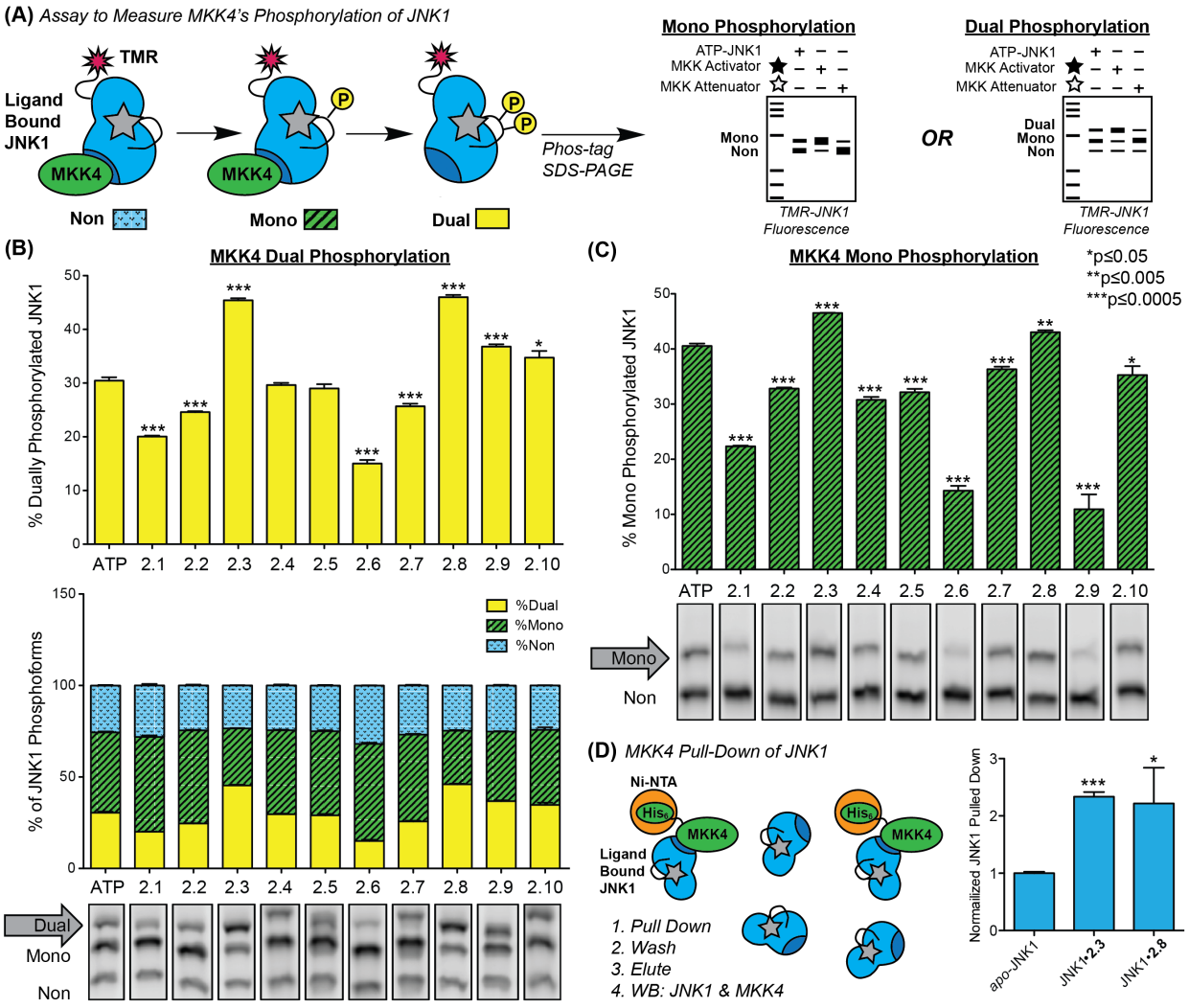

Figure 2.11. *Quantitative assessment of how ATP-competitive inhibitors affect JNK1 phosphorylation by MKK4.* (A) Assay to assess how the ATP-binding site occupancy of JNK1 influences its activation by MKK4. (B) TMR-JNK1 was incubated with ATP and different ATP-competitive inhibitors, followed by the addition of MKK4 (250 nM). After one hour of incubation, JNK1 phospho-forms were separated by Phos-tag SDS-PAGE, detected, and quantified using fluorescence scanning. Values shown are mean ± SEM (n=3). Statistical significance was determined by a two-tailed, unpaired t-test. (C) Experiments conducted as in (B), except with 0.25 nM MKK4. (D) Schematic of the JNK1-MKK4 pull-down assay (left) and quantification of TMR-JNK1 pull-down in the absence or presence of compounds **2.3** and **2.8** (right).

Like with MKK7, we next measured how efficiently the activation loops of different JNK1-inhibitor complexes were phosphorylated by a concentration of MKK4 that does not generate the dual-phosphorylated form (**Figure 2.11C**). Under this activation regime, we found that MKK4 behaved similarly to MKK7 with some small differences. In contrast to MKK7, compounds **2.3** and **2.8** slightly increased the amount of mono-phosphorylated JNK1 produced by MKK4. However, consistent with the unique behavior observed for the JNK1-**2.9** complex with MKK7, JNK1's interaction with **2.9** dramatically decreased the amount of mono-phosphorylated JNK1 generated by the lower concentration of MKK4, despite promoting the production of dual-phosphorylated JNK1 at the higher MKK4 concentration. Furthermore, the JNK1-**2.6** complex appears to be a poor substrate for low and high concentrations of MKK4, like it is for MKK7. One possible mechanism for **2.1** and **2.6** to reduce the activation loop phosphorylation of JNK1 is through direct inhibition of MKK4. To exclude this possibility, we conducted inhibition assays with both compounds using an alternative MKK4 substrate, the MAPK p38α (**Figure 2.12**).[60] Consistent with both **2.1** and **2.6** diminishing activation loop phosphorylation through their interaction with JNK1 and not MKK4, neither compound reduced the ability of MKK4 to phosphorylate p38α. Therefore, JNK1's interaction with ATP-competitive inhibitors can make it either a less or more efficient substrate for MKK4.

One possible explanation for why some inhibitors, like **2.3** and **2.8**, make JNK1 a better substrate for MKK4 and MKK7 is that these inhibitor-bound complexes have higher affinities for MKKs, like they do for JIP1. To test this possibility, we performed pull-down assays with *apo*-JNK1 and inhibitor-bound complexes using MKK4 as an immobilized bait (**Figure 2.11D**). We observed that both the JNK1-**2.3** and JNK1-**2.8** complexes, which are more efficiently converted to the dual phosphorylated form by both MKK4 and MKK7, were pulled down more efficiently

by MKK4 than *apo*-JNK1. Therefore, it appears that JNK1's interactions with upstream activators can be allosterically modulated through its ATP-binding site like its interactions with scaffold proteins. Because ATP-competitive inhibitors that modulate the phosphorylation of JNK1 by MKK4 and MKK7 promote dual over mono-phosphorylation, the enhanced affinity we observe most likely influences processivity, instead of the first phosphorylation event.

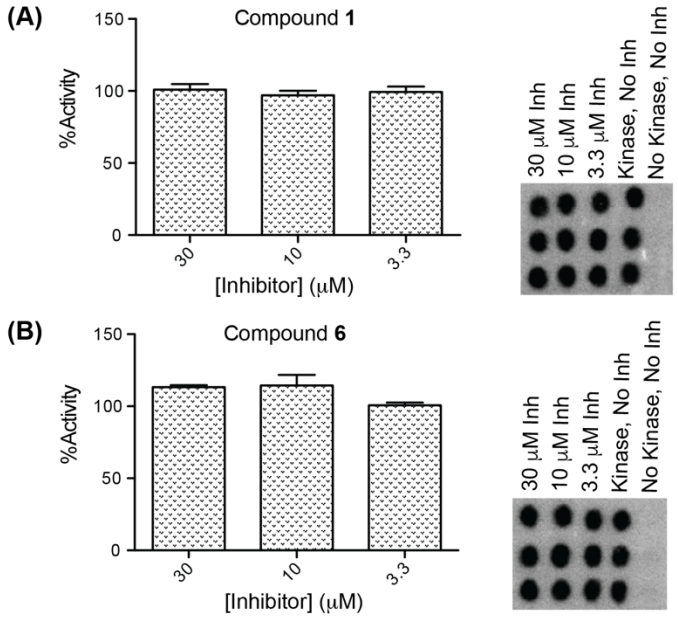

Figure 2.12. *Determine if compounds that decrease MKK4β phosphorylation of JNK1 are inhibiting MKK4β directly using [γ-^{32}P]ATP kinase assays.* (A) Percent activity of MKK4β against an alternative substrate, p38α, in the presence of compound 2.**6**. (B) Percent activity of MKK4β against p38α in the presence of compound 2.**1**.

2.10 DISCUSSION

The JNKs play diverse roles in many cellular signaling processes, including those involved in determining cellular fate. JNKs have been shown to interact with the D-domains of scaffolds, downstream substrates, and their upstream activators via their DRSs, which are distal to the site of ATP binding. Previous structural studies suggested that D-domain interactions with the DRSs of JNKs allosterically influence the conformation of JNK ATP-binding sites. However, the full extent

of the allosteric communication between the DRSs and the ATP-binding sites of JNKs has not been previously explored. Here, we systematically investigated the effects of ten ATP-competitive JNK inhibitors on DRS interactions. First, we investigated how ATP-site occupancy affected binding of a peptide containing the D-domain of JIP1 (JIPtide). Using a quantitative fluorescence polarization binding assay, we demonstrated that the interactions of JNKs with JIPtide can either be strengthened or weakened through the ATP-binding site. In general, we found that most of the ATP-competitive inhibitors we tested had similar effects on all JNK isoforms. We observed a high amount of similarity between JNK1 and JNK3 but noted some differences in how JNK2's affinity for JIPtide was modulated. These results are consistent with the higher sequence homology of JNK1 and JNK3, compared to JNK2, and likely indicate that there are differences in allostery across the JNK family. After determining the effects of JNK ATP-binding site occupancy on JIPtide binding, we validated that these effects were similar for the full-length scaffold protein with a pull-down assay using immobilized JIP1. Together, these results demonstrated that JIPtide is a suitable surrogate of full-length JIP1 for studies exploring allosteric communication between the DRSs and ATP-binding sites of JNKs and that different inhibitor-bound JNK complexes can have large differences in their affinities for scaffold proteins.

We then explored how the ATP-binding site occupancy of JNKs influenced the abilities of MKK4 and MKK7 to phosphorylate their activation loops. To do this, we developed a Phos-tag SDS-PAGE based assay that allowed us to separate the phospho-forms of JNK1, which we had site-specifically labeled with a fluorophore. This technique allowed us to ratio-metrically quantitate the phosphorylation of JNK1's activation loop. We first used this new assay to conduct a quantitative kinetic study of MKK4's and MKK7's activation of JNK1. These kinetic analyses validated previous studies showing that MKK4 and MKK7 are likely to work synergistically to

achieve efficient dual phosphorylation in cells. We then investigated how the interactions of our ten inhibitors with the ATP-binding site of JNK1 influenced the ability of MKK4 and MKK7 to phosphorylate the activation loop of JNK1. These studies showed that different JNK1-inhibitor complexes were significantly better or worse substrates for MKK4 and MKK7. Consistent with certain inhibitors generally promoting higher affinity interactions between D-domain binding partners and the DRSs of JNKs, many of the inhibitors that strengthened JNK1's affinity for JIP1 led to enhanced activation loop phosphorylation by MKK4 and MKK7. Our results further validate the existence of allostery between the ATP-binding sites of JNKs and their distal D-recruitment sites. This may have functional implications in the cell, where the type of occupancy at the ATP-binding site could alter the ability of JNKs to interact with cellular binding partners.

2.11 CONCLUSIONS

This study adds the JNKs to the growing list of kinases whose interactions with protein-binding partners can be divergently modulated through allostery with ATP-competitive inhibitors.[7, 11, 12, 14-16, 61-63] How divergently modulating interactions with MKK4, MKK7, and JIP1 affects the behavior of JNKs in cells will need to be empirically determined, but several predictions can be made. It would be expected that inhibitors that promote dual phosphorylation of JNK1 by MKK4 and MKK7 would result in hyperactivation of JNK signaling under drug wash-out conditions, which occurs during most in vivo drug treatments. Furthermore, in most cellular environments, where JNKs are expressed in excess of JIP1, isoform-selective inhibitors that promote the interaction of inhibitor-bound JNKs with JIP1 would be predicted to prevent scaffold-mediated activation of uninhibited JNK isoforms. Finally, on the basis of the bidirectional nature of allosteric networks, it is likely that JIP1-bound JNKs will be more or less sensitive to certain ATP-competitive inhibitors than their uncomplexed forms. JNKs have been shown to interact with

the D-domains of numerous scaffolds, downstream substrates, and upstream activators via their DRSs; therefore, ATP-competitive inhibitors could significantly alter their interactions with a number of cellular binding partners.

2.12 Materials and Methods

Cloning and mutagenesis. Bacterial expression plasmids containing genes encoding His_6-JNK1α1 (JNK1), His_6-SUMO-JNK1α1 (His_6-SUMO-JNK1), His_6-JNK2α1 (JNK2), His_6-JNK3α1 (JNK3), His_6-SUMO-MKK4β (MKK4), His_6-SUMO-MKK7β1 (MKK7), Flag-JIP1b-His_6 (JIP1), into pMCSG7 vectors were created using Gibson assembly.[64] The genes for MKK4β, MKK7β1, and Flag-JIP1b were obtained as gifts from Roger Davis and were provided in pcDNA3 (Addgene plasmid #s MKK4β: 15517; MKK7β1: 14622; Flag-JIP1b: 52123). The gene for His_6–Ulp1 (Ulp1) was synthesized as a G-block (Integrated DNA Technologies). The pTH1–SaSrtA–A (Sortase A) plasmid was obtained as a gift from Teruyuki Nagamune (Addgene plasmid # 64979). His_6–p38α and His_6–GST–MAP3K1 were provided by Hari, *et al.* in bacterial expression vectors.[65] Uniprot IDs, DNA, and protein sequences for constructs we modified are provided in **Table 2.2**.

Protein expression and purification (Figure 2.13). His_6-JNK1α1, His6-SUMO-JNK1α1, His_6-JNK2α1, His_6-JNK3α1, His_6-SUMO-MKK4β, His_6-SUMO-MKK7β1, His_6–MAP3K1, His_6–p38α, Flag-JIP1b-His_6, His_6–Ulp1, and His_6–Sortase A were expressed in *Escherichia coli* BL21(DE3) cells in LB Miller broth. Cells were induced between OD_{600} 0.65-0.75 with 400 μM isopropyl β-D-thiogalactoside at 18 °C overnight. All purification steps were carried out at 4 °C. Cells were lysed with sonication in 2 mL/gram pellet weight of wash/lysis buffer consisting of 50 mM HEPES (pH 7.5), 300 mM NaCl, 20 mM imidazole, 10% glycerol and 1 mM phenylmethylsulfonyl fluoride. The lysate was centrifuged at 10000 **g** for 20 min and the supernatant was allowed to batch bind for 60 min with 0.4 ml/L cell culture of Ni-NTA (Ni^{2+}-

nitrilotriacetate) resin. The resin was collected by centrifugation at 500 **g** for 5 min and washed with 20 mL of wash/lysis buffer per liter of culture. The wash step was repeated three times. The protein was eluted using ~4 mL of elution buffer (50 mM HEPES (pH 7.5), 300 mM NaCl, 200 mM imidazole and 10% glycerol) per liter of culture. Then, the eluate was dialyzed against 50 mM HEPES (pH 7.5), 200 mM NaCl, 5% glycerol and 1 mM dithiothreitol (DTT). His_6-JNK1α1, His_6-SUMO-JNK1α1, His_6-JNK2α1, and His_6-JNK3α1 were expressed in their inactive forms. The aliquoted proteins were flash-frozen and stored at −80 °C. His_6-SUMO-MKK7β1 was co-expressed with MAP3K1, to allow purification of the active MKK7β1 which was then subjected to overnight Ulp1 cleavage. His_6-SUMO-MKK4β was expressed alone and subsequently activated by MAP3K1 in vitro, during overnight Ulp1 cleavage. Flag-JIP1b-His_6 was purified using sequential Ni-NTA and Anti-Flag purification. After elution from Ni-NTA, Flag-JIP1b-His_6 was bound to Anti-Flag M2 magnetic beads (Sigma), washed twice using 5 CV of TBS (50 mM tris(hydroxymethyl)aminomethane (Tris)/HCl (pH 7.5), 150 mM NaCl), and eluted using 1 mg/mL 3X Flag peptide (MDYKDHDGDYKDHDIDYKDDDDK) in TBS. His_6-SUMO-JNK1α1 was treated with Ulp1 during O.N. dialysis to yield Gly-JNK1α1 for subsequent Sortase A labeling.

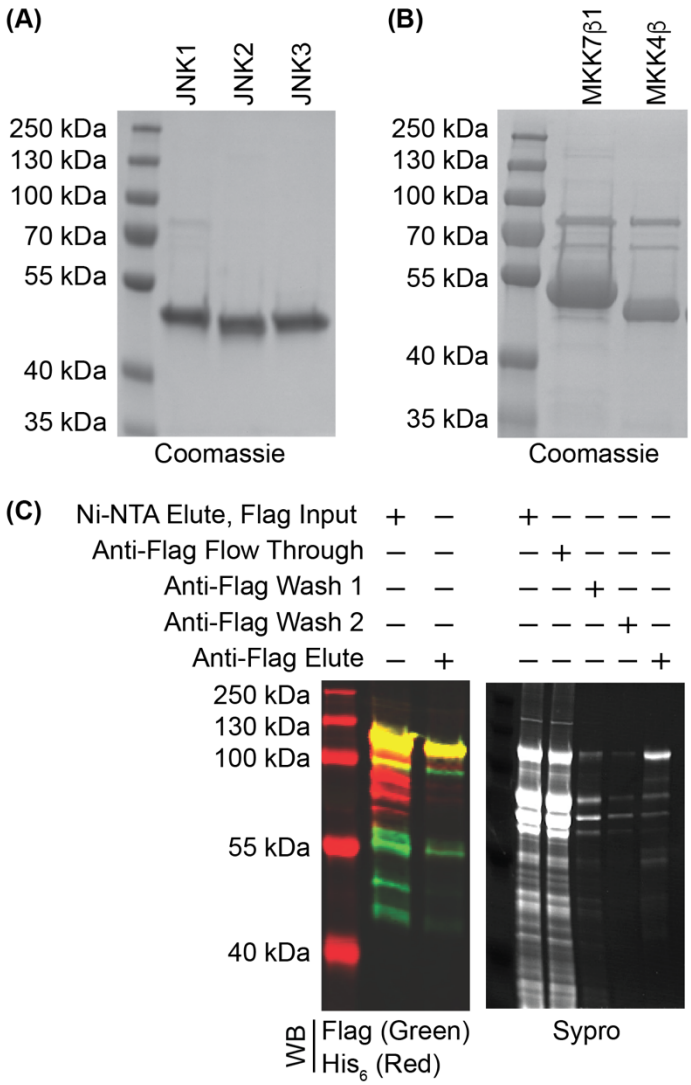

Figure 2.13. *SDS-PAGE analysis of recombinant proteins.* (A-C) His_6-SUMO-MKK4β, His_6-SUMO-MKK7β1, His_6–JNK1α1, His_6–JNK2α1, His_6–JNK3α1, Flag-JIP1b-His_6, were expressed in E. coli BL21 cells and purified using Ni-NTA chromatography. (A) His_6–JNK1α1, His_6–JNK2α1, His_6–JNK3α1 were expressed in their inactive forms. (B) His_6-SUMO-MKK7β1 was co-expressed with MKKK1, to allow purification of the active MKK7β1, following overnight Ulp1 cleavage. His_6-SUMO-MKK4β was expressed alone and subsequently activated by MKKK1 in vitro, during overnight Ulp1 cleavage. (C) Flag-JIP1b-His_6 was purified using sequential Ni-NTA and Anti-Flag purification.

Sortase A labeling of Gly-JNK1α1 (Figure 2.8). Labeling was completed using a method modified from Theile, et al. (2013).[59] After O.N. dialysis, Gly-JNK1α1 was dialyzed against 1 mM β-mercaptoethanol (BME), and the His_6–Ulp1 (used to generate the free terminal Gly-JNK1α1) and cleaved His_6-SUMO, were removed by Ni-NTA. 10 μM of Gly-JNK1α1 was combined with 20 μM Sortase A and 200 μM TMR-LPETGG (TMR: 6-carboxytetramethylrhodamine) in dimethyl sulfoxide (DMSO; 4% v/v final in assay) in Sortase A labeling buffer (50 mM Tris/HCl (pH 7.5), 150 mM NaCl, 20 mM imidazole, 10% glycerol, and 1 mM BME). The labeling took place over 1.5 hr at 4°C in the dark. The His_6–Sortase A was then removed by Ni-NTA and the remaining peptide was removed using a Zeba column (Thermo Fisher), which also allowed exchange into our standard dialysis buffer, containing 1 mM DTT.

Peptides. All peptides were synthesized by Genscript and purified by High Performance Liquid Chromatography (HPLC). The peptide for the fluorescence polarization assays, containing the D-domain of JIP1 (JIPtide), was synthesized with a TMR label at the N-terminus and a free acid at the C-terminus (TMR-JIPtide). The sequence for the JIP 11-mer was RPKRPTTLNLF (amino acids 153–163 of JIP1). The Sortase A peptide for the N-terminal labeling of JNK1α1 was synthesized with a TMR label at the N-terminus and a free acid at the C-terminus (TMR-LPETGG).

Instrumentation. FP and TR-FRET assays were conducted using 384-well plates and detected using a PerkinElmer Envision 2104 Multi-label Reader. Western blots were imaged on a LiCor Odyssey gel image scanner using both 680 nm and 780 nm channels.

Binding Assays. To measure binding of the compounds to the ATP-site of non-phosphorylated His_6-JNKs, serial dilutions (1:3) of compounds in DMSO (4% v/v final in assay) were prepared at 750 μM starting (30 μM final in assay). Compounds were added to 33 nM JNKs in buffer (50 mM

Tris/HCl (pH 8), 100 mM NaCl), 100 nM Cy5-Probe (**Figure 2.3B**), and 1 nM europium Anti-His_6 in a 384-well plate (20 μL per well). TR-FRET was determined using an excitation wavelength of 320 nm and emission wavelengths of 615 nm (Eu^{3+}) and 665 nm (Cy5). Compounds were titrated in triplicate and JNK-compound K_Ds were determined, and subsequently the K_is, using the K_D of the probe for JNK1α1 (0.39 ± 0.24 μM).

FP assays. To measure the binding of the JIP1 11-mer (JIPtide) with JNKs (± ATP-competitive compound), 30 μM compounds were pre-incubated with non-phosphorylated JNKs and 30 nM TMR-JIPtide in a 384-well plate (30 μL per well) for 60 min at room temperature in the assay buffer (10 mM HEPES (pH 7.4), 150 mM NaCl, 10 mM $MgCl_2$, 0.005% Brij-35, 0.1% 2-mercaptoethanol and 0.05% bovine serum albumin (BSA)). A total of 6 JNK concentrations (above and below the K_Ds) were screened in triplicate, and JNK-JIPtide K_Ds (± ATP-competitive compound) were determined. FP assays used 595 nm excitation and emission filters.

Full length JNK1α1-JIP1b pull-downs. Each pull-down contained 20 μL of Anti-Flag M2 magnetic beads (Sigma) in 120 μL total volume. Full length Flag-JIP1b was bound to the beads at a final concentration of 0.6 μM throughout the pull-down (or Flag-Grb2 as a control scaffold; see **Figure 2.6**). JNK1α1 was incubated with the JIP1b bound beads, in buffer (50 mM Tris/HCl (pH 7.5), 150 mM NaCl, 0.01% (v/v) Tween 20, 10 mM $MgCl_2$, and 0.1 mg/mL BSA), containing 10 μM ATP-competitive compound with 4% (v/v final) DMSO (or DMSO alone as a control). Either 500 nM or 200 nM JNK1α1 was allowed to bind JIP1b for compounds that disrupt or enhance binding, respectively, for 1 hr at RT. Free JNK1α1 was washed from the pull-downs using three sequential washes with TBS (50 mM Tris/HCl (pH 7.5), 150 mM NaCl). The remaining JNK1α1-JIP1b was eluted using 1 mg/mL 3X Flag peptide in TBS. JIP1b and JNK1α1 were detected by western blotting for Flag and total JNK, respectively.

Activation of JNKs by MKK4β/MKK7β1. Phosphorylation of TMR-JNK1α1 was carried out in 60 µL reactions containing 200 nM JNK1α1 in buffer (50 mM Tris/HCl (pH 7.5), 0.01% (v/v) Tween 20, 10 mM $MgCl_2$, and 0.1 mg/mL BSA), 400 µM ATP, 10 µM ATP-competitive compound in DMSO (or DMSO alone as a control) 4% (v/v final), and either activated MKK4β or MKK7β1, at concentrations in the linear range for either the dual or mono phosphorylation event. These concentrations for MKK7β1 were 150 nM and 0.25 nM, respectively. These concentrations for MKK4β were 250 nM and 0.5 nM, respectively. There was a 30 min pre-incubation of JNK1α1, ATP-competitive compound, and ATP before starting the assay by addition of MKKs. The reactions proceeded for 1 hr. TMR-JNK1α1 was separated using Phos-tag SDS-PAGE and imaged using fluorescence.

Phos-tag SDS-PAGE. Gels were freshly prepared on the day of the experiment using a Biorad mini-PROTEAN Tetra Handcast system. Resolving gels contained 0.35 M bis-Tris/HCl (pH 6.8), 7% acrylamide (37.5:1 acrylamide: bis-acrylamide), 0.1 mM $MnCl_2$, 0.05 mM Phos-tag acrylamide, 0.05% ammonium persulfate, and 0.001% TEMED. Stacking gels contained 0.35 M bis-Tris/HCl (pH 6.8), 4% acrylamide (37.5:1 acrylamide: bis-acrylamide), 0.05% ammonium persulfate, and 0.001% TEMED. Each layer was allowed to polymerize for 1 hr at RT. Gels were run in buffer (pH 7.8) containing 50 mM MOPS, 50 mM Tris base, 0.1% SDS, and 5 mM sodium bisulfite (added fresh from a 1 M solution) at 150 V. Samples were prepared in EDTA-free SDS loading buffer and throughout sample generation, EDTA was avoided to prevent distortion of the protein's travel. All wells were loaded with an equal volume of sample, containing similar buffer conditions. Unused wells were filled with mock samples containing buffer and loading dye.

MKK4β inhibition assays using p38α as a substrate. Kinase assays for MKK4β were conducted in 30 µL assay volume containing the compound in DMSO (4% v/v final), 100 nM MKK4β, 0.007

μCi/μL [γ-^{32}P]ATP, and 3.9 μM p38α as a substrate in assay buffer (50 mM Tris/HCl (pH 7.5), 0.01% (v/v) Tween 20, 10 mM $MgCl_2$, 2 mM DTT, 1 mM EGTA, 0.05 mg/mL BSA). MKK4β activity was linear at 100 nM. Assays were run for 2 hr (RT) and quenched by spotting 4.6 μL of each reaction onto phosphocellulose membranes (Reaction Biology). The membranes were subjected to three sequential washes in 0.5% phosphoric acid for 10 min, dried, and exposed O.N. to a phosphor screen (GE Healthcare). Blots were scanned using a phosphor scanner (GE Typhoon FLA 9000). Spots were quantified using ImageQuant.

MKK4β pull-downs. Each pull-down contained 20 μL of Ni-NTA in 120 μL total volume. Full length His_6- SUMO-MKK4β was bound to the beads at a final concentration of 0.6 μM throughout the pull-down. JNK1α1 was incubated with the MKK4β bound beads in buffer (50 mM HEPES (pH 7.5), 150 mM NaCl, 20 mM imidazole) containing 30 μM compound with 4% (v/v final) DMSO (or DMSO alone as a control). 500 nM JNK1α1 was allowed to bind MKK4β, for 1 hr at RT. Free JNK1α1 was washed from the pull-downs using three sequential washes with buffer (50 mM HEPES (pH 7.5), 150 mM NaCl, 20 mM imidazole). The remaining JNK1α1-MKK4β was eluted using buffer (50 mM HEPES (pH 7.5), 150 mM NaCl, 200 mM imidazole). MKK4β and JNK1α1 were detected by western blotting for MKK4 and total JNK, respectively.

Activation of JNK1 for activity assays. Activated JNKs were prepared and activated using purified, activated MKK4α. 900 nM JNK1 or 2.7 μM JNK2 were pre-activated with 150 nM MKK4α for 1 hour at RT in (50 mM Tris/HCl (pH 7.5), 0.01% (v/v) Tween 20, 10 mM MgCl2, 2 mM DTT, 1 mM EGTA, 0.1 mg/mL BSA) with 400 μM ATP. JNKs were diluted to 15 nM for activity assays.

TR-FRET based activity assays. The activated JNKs were tested using the Lance Ultra time-resolved fluorescence resonance energy transfer assay (TR-FRET) (Perkin Elmer). Serial dilutions

(1:3) of compounds in DMSO (4% v/v final in assay) were prepared at 750 μM starting (30 μM final in assay). Compounds were added to 15 nM activated JNKs in buffer (50 mM Tris/HCl (pH 7.5), 0.01% (v/v) Tween 20, 10 mM $MgCl_2$, 2 mM DTT, 1 mM EGTA, 0.1 mg/mL BSA) with either 100 μM or 1 mM ATP, +/- 10 μM JIPtide. To initiate the reaction following an initial 30-min pre-incubation with the inhibitors and ATP, 25 nM (for JNK2) or 50 nM (for JNK1) ulight labeled myelin basic peptide (ulight-MBPtide) was added. The reaction mixture was incubated in a volume of 15 μL per well in a 384-well plate at room temperature for 4 h, then quenched with 10 mM EDTA in modified Lance Detect Buffer (40 mM Tris-HCl [pH 7.5] and 100 mM NaCl). After a 5 min incubation with the quench reagents, 0.5 nM europium labeled Anti-phospho-MBPtide was added in Lance Detect Buffer. After 1 h of incubation, the plates were read on an Envision Multilabel Reader. Titrations were run in triplicate. Inhibition experiments +/- full-length JIP were conducted with 30 nM JNK1 and 380 nM JIP. TR-FRET was determined using an excitation wavelength of 320 nm and emission wavelengths of 615 nm (Eu^{3+}) and 665 nm (ulight-MBPtide). Relative amounts of activity were calculated using the ratio of 665 nm light to 615 nm light.

Data Analysis. For all experiments, there were linear relationships between signal and enzyme concentration or time. IC_{50}s and K_Ds were fitted to data by unweighted nonlinear regression using GraphPad Prism. When fitting equations to data, the parameter values, x (concentration of enzyme or compound), were replaced by $\log_{10}x$. Data was reported as Average ± S.E.M.

Inhibitor Characterization: Proton NMR spectra were carried out on 300 or 600 MHz spectrometers. Chemical shifts (δ) are reported in parts per million (ppm) with chemical shifts reported to internal standards: $CDCl_3$ (7.26 ppm) and DMSO-d_6 (2.50 ppm) Coupling constants (J) are reported in Hertz (Hz) and multiplicities are abbreviated as singlet (s), doublet (d), triplet

(t), multiplet (m), doublet of doublets (dd), and doublet of triplets (dt). Fast atom bombardment high resolution mass spectra (FAB-MS, HRMS) (HRMS) were obtained were obtained on a JEOL JMS-700 spectrometer. All final compounds were assessed for purity by ultra high performance liquid chromatography (UHPLC) on Waters Acquity UPLC I-Class system with photodiode array (PDA) detector, MS and ELSD via the following conditions. Column: YMC Triart C18 2.0 mm × 30 mm, 1.9 μm. Mobile phase A: 0.10% TFA in water (v/v). Mobile phase B: 0.10% TFA in MeCN (v/v). Gradient: 95.0% water/5.0% MeCN linear to 5% water/95% MeCN in 1.2 min, HOLD at 5% water/95% MeCN to 1.5 min. Flow: 1.0 mL/min.

2.1: ^{1}H NMR (300 MHz, $CDCl_3$) ppm 1.36 (s, 9 H), 4.21 (s, 3 H), 6.30 (s, 1 H), 6.39 (s, 1 H), 6.58 (s, 1 H), 6.94 (d, J=9.0 Hz, 2 H), 7.03 (dd, J=9.0, 2.2 Hz, 1 H), 7.10 (d, J=2.2 Hz, 1 H), 7.21 (d, J=9.0 Hz, 2 H), 7.49 - 7.29 (m, 5 H), 7.68 (d, J=9.0 Hz, 1 H), 7.80 (s, 1 H); HRMS calculated for $C_{28}H_{29}N_6O_2$ $[M+H]^+$ 481.2352, found 481.2344. UHPLC purity: 95.2% (UV, 254 nm), 98.3% (ELSD).

2.2: ^{1}H NMR (300 MHz, $CDCl_3$) ppm 1.07 (t, J=7.5 Hz, 3 H) 1.79 - 1.97 (m, 2 H) 2.31 (s, 3 H) 3.01 (t, J=7.5 Hz, 2 H) 3.75 (s, 2 H) 6.82 (dd, J=5.4, 1.5 Hz, 1 H) 7.25 - 7.07 (m, 3 H) 7.47 - 7.28 (m, 6 H) 7.96 (s, 1 H) 8.01 (dd, J=5.4, 0.9 Hz, 1 H) 8.32 (s, 1 H); HRMS calculated for $C_{26}H_{26}N_3OS$ $[M+H]^+$ 428.1797, found 428.1786. UHPLC purity: 99.0% (UV, 254 nm), 91.8% (ELSD).

2.3: ^{1}H NMR (600 MHz, DMSO-d_6) δ ppm 13.76 (s, 1 H), 9.67 (s, 1 H), 8.45 (d, J=5.4 Hz, 1 H), 7.58 (d, J=6 Hz, 1 H), 7.28 (dd, J=1.8, 1.8 Hz, 1 H), 7.14 – 7.04 (m, 3 H), 6.92 – 6.86 (m, 2 H), 6.79 (dd, J=2.4, 1.8 Hz, 1 H), 6.56 (dd, J=3, 1.8 Hz, 1 H), 3.46 (s, 3 H), 2.85 (s, 3 H)); HRMS calculated for $C_{20}H_{19}N_4O_3S$ $[M+H]^+$ 395.1166, found 395.1178. UHPLC purity: 98.0% (UV, 254 nm), 96.4% (ELSD).

2.4: ^{1}H NMR (600 MHz, DMSO-d_6) δ ppm 8.47 (d, J=4.8 Hz, 1 H), 8.41 (t, J=6.2 Hz, 1 H), 7.73

(td, J=7.6, 1.8 Hz, 1 H), 7.40 (br d, J=7.6 Hz, 1 H), 7.36 - 7.16 (m, 3 H), 7.02 (s, 1 H), 4.46 (q, J=7.0 Hz, 2 H), 3.78 (br s, 2 H), 3.10 (t, J=6.5 Hz, 2 H), 2.47 - 2.32 (m, 2 H), 1.78 (d, J=13.2 Hz, 2 H), 1.68 (d, J=13.2 Hz, 2 H), 1.57 - 1.41 (m, 1 H), 1.40 - 1.33 (m, 1 H), 1.30 (t, J=7.0 Hz, 3 H), 0.96 - 0.79 (m, 4 H); HRMS calculated for $C_{23}H_{31}N_6O_2$ $[M+H]^+$ 423.2499, found 423.2508. UHPLC purity: 88.1% (UV, 254 nm), 97.9% (ELSD).

2.5: ^{1}H NMR (300 MHz, DMSO-d_6) δ ppm 10.55 (s, 1 H), 9.15 (br s, 1 H), 8.34 - 8.23 (m, 2 H), 8.02 (s, 1 H), 7.95 (d, J=5.8 Hz, 1 H), 7.80 (d, J=2.2 Hz, 1 H), 7.61 (dd, J=9.5, 2.2 Hz, 1 H), 7.31 (d, J=9.5 Hz, 1 H), 4.63 (d, J=13.2 Hz, 1 H), 4.46 (d, J=13.2 Hz, 1 H), 3.50 - 3.19 (m, 8 H), 3.03 - 2.83 (m, 6 H), 2.47 - 2.37 (m, 2 H), 2.12 (s, 3H), 2.10 - 1.99 (m, 2 H), 1.91 - 1.55 (m, 8 H), 1.49 - 1.30 (m, 1 H); HRMS calculated for $C_{34}H_{42}F_3N_8O_2$ $[M+H]^+$ 651.3383, found 651.3379. UHPLC purity: 98.5% (UV, 254 nm), 97.4% (ELSD).

2.6: ^{1}H NMR (600 MHz, DMSO-d_6) δ ppm 8.45 (t, J=6.3 Hz, 1 H), 7.86 (dd, J=8.1, 1.5 Hz, 2 H), 7.52 - 7.37 (m, 3 H), 7.28 (br s, 2 H), 7.02 (s, 1 H), 4.46 (q, J=7.0 Hz, 2 H), 3.60 (s, 2 H), 3.15 (br t, J=6.5 Hz, 2 H), 2.86 (br d, J=10.9 Hz, 2 H), 2.33 (s, 3 H), 1.97 (br t, J=11.1 Hz, 2 H), 1.63 - 1.51 (m, 3 H), 1.30 (t, J=7.0 Hz, 3 H), 1.25 - 1.12 (m, 2 H); HRMS calculated for $C_{26}H_{31}N_6O_2S$ $[M+H]^+$ 491.2218, found 491.2229. UHPLC purity: 99.6% (UV, 254 nm), 96.7% (ELSD).

7: SB-202190 is commercially available from Sigma (catalog #S7067).

2.8: PD-173952 is commercially available from Sigma (catalog #PZ0113). UHPLC purity: 99.5% (UV, 254 nm), 99.2% (ELSD).

2.9: ^{1}H NMR (300 MHz, $CDCl_3$) δ ppm 8.10 (s, 1 H), 8.05 - 7.88 (m, 4 H), 7.74 (dd, J=18.1, 2.0 Hz, 1 H), 7.35 (td, J=7.9, 2.0 Hz, 1 H), 7.24 - 7.19 (m, 1 H), 5.47 - 5.20 (m, 2 H), 5.05 (q, J=4.4 Hz, 1 H), 4.63 (dd, J=13.5, 2.7 Hz, 1 H), 4.37 (dd, J=13.5, 8.4 Hz, 1 H), 4.30 - 4.20 (m, 1 H), 3.71 (s, 2 H), 3.01 (d, J=4.4 Hz, 3 H), 2.63 - 2.30 (m, 13 H), 2.20 - 1.90 (m, 7 H); HRMS calculated

for $C_{33}H_{40}F_3N_8O_3$ $[M+H]^+$ 653.3175, found 653.3167. UHPLC purity: 94.2% (UV, 254 nm), 96.4% (ELSD).

2.10: ^{1}H NMR (600 MHz, DMSO-d_6) δ ppm 8.70 (br s, 1 H), 7.64 - 7.46 (m, 4 H), 7.42 - 7.24 (m, 6 H), 7.11 – 6.96 (m, 1 H), 6.96 - 6.77 (m, 4 H), 4.63 (s, 2 H), 3.67 (t, J=5.6 Hz, 2 H), 3.57 - 3.40 (m, 2 H), 2.45 - 2.27 (m, 6 H), 1.77 - 1.59 (m, 4 H); HRMS calculated for $C_{32}H_{33}ClN_5O_3$ $[M+H]^+$ 570.2272, found 570.2266. UHPLC purity: 95.3% (UV, 254 nm), 97.9% (ELSD)

Table 2.2. Protein and DNA sequences for specified constructs (**TAG**; GENE)

His_6–LIC+TEV-site–JNK1α1 (Uniprot ID: MK08_MOUSE)	
Amino Acid Sequence	**MHHHHHHSSGVDLGTENLYFQSN**MSRSKRDNNFYSVEIGDSTFTVLKRYQNLKPIGSGAQGIVCAAYDAILERNVAIKKLSRPFQNQTHAKRAYRELVLMKCVNHKNIIGLLNVFTPQKSLEEFQDVYIVMELMDANLCQVIQMELDHERMSYLLYQMLCGIKHLHSAGIIHRDLKPSNIVVKSDCTLKILDFGLARTAGTSFMMTPYVVTRYYRAPEVILGMGYKENVDLWSVGCIMGEMVCHKILFPGRDYIDQWNKVIEQLGTPCPEFMKKLQPTVRTYVENRPKYAGYSFEKLFPDVLFPADSEHNKLKASQARDLLSKMLVIDASKRISVDEALQHPYINVWYDPSEAEAPPPKIPDKQLDEREHTIEEWKELIYKEVMDLEERTKNGVKLLE
DNA Sequence	**ATGCACCATCATCATCATCATTCTTCTGGTGTAGATCTGGGTACCGAGAACCTGTACTTCCAATCCAAT**ATGAGCCGCAGCAAACGCGACAACAACTTCTACAGCGTGGAAATCGGCGACAGCACCTTCACCGTGCTGAAACGCTACCAGAACCTGAAACCTATCGGCTCTGGCGCCCAGGGCATCGTGTGTGCCGCCTACGACGCCATCCTGGAACGCAACGTGGCCATCAAAAAACTGAGCCGCCCTTTCCAGAACCAGACCCACGCCAAACGCGCCTACCGCGAGCTGGTGCTGATGAAATGCGTGAACCACAAAAACATCATCGGCCTGCTGAACGTGTTCACACCTCAGAAAAGCCTGGAAGAGTTCCAGGACGTCTACATCGTGATGGAACTGATGGACGCCAACCTGTGCCAGGTCATCCAGATGGAACTGGACCACGAGCGCATGAGCTACCTGCTGTACCAGATGCTGTGCGGCATCAAACATCTGCACAGCGCCGGCATCATCCACCGCGACCTGAAACCATCCAACATCGTGGTCAAAAGCGACTGCACCCTGAAAATCCTGGACTTCGGCCTGGCCCGCACCGCCGGCACCAGCTTCATGATGACCCCTTACGTGGTCACCCGCTACTATCGCGCCCCTGAAGTGATCCTGGGCATGGGCTACAAAGAAAACGTGGACCTGTGGTCCGTGGGCTGCATCATGGGCGAGATGGTCTGCCACAAAATCCTGTTCCCTGGCCGCGACTACATCGACCAGTGGAACAAAGTGATCGAGCAGCTGGGCACCCCTTGCCCTGAGTTCATGAAAAAACTGCAGCCTACCGTGCGCACCTACGTGGAAAACCGCCCTAAATACGCCGGCTACAGCTTCGAGAAACTGTTCCCTGACGTGCTGTTCCCTGCCGACAGCGAGCACAACAAACTGAAAG

	CCAGCCAGGCCCGCGACCTGCTGAGCAAAATGCTGGTCATCGACGCCAGCAAACGCAT CAGCGTGGACGAGGCCCTGCAGCACCCTTACATCAACGTGTGGTACGACCCTAGCGAG GCCGAGGCCCCTCCTCCAAAAATCCCTGACAAACAGCTGGACGAGCGCGAGCACACCA TCGAGGAATGGAAAGAGCTGATCTACAAAGAAGTGATGGACCTGGAAGAACGCACCA AAAACGGCGTGAAGCTTCTCGAGTAG
His_6–LIC+TEV-site–JNK2α1 (Uniprot ID: MK09_HUMAN)	
Amino Acid Sequence	**MHHHHHHSSGVDLGTENLYFQSN**DSQFYSVQVADSTFTVLKRYQQLKPIGSGAQGIVCAA FDTVLGINVAVKKLSRPFQNQTHAKRAYRELVLLKCVNHKNIISLLNVFTPQKTLEEFQDVYL VMELMDANLCQVIHMELDHERMSYLLYQMLCGIKHLHSAGIIHRDLKPSNIVVKSDCTLKIL DFGLARTACTNFMMTPYVVTRYYRAPEVILGMGYKENVDIWSVGCIMGELVKGCVIFQGT DHIDQWNKVIEQLGTPSAEFMKKLQPTVRNYVENRPKYPGIKFEELFPDWIFPSESERDKIKT SQARDLLSKMLVIDPDKRISVDEALRHPYITVWYDPAEAEAPPPQIYDAQLEEREHAIEEWK ELIYKEVM
DNA Sequence	**ATGCACCATCATCATCATCATTCTTCTGGTGTAGATCTGGGTACCGAGAACCTGTACTT CCAATCCAAT**GACAGCCAGTTCTACAGCGTGCAGGTCGCCGACAGCACCTTCACCGTGC TGAAACGCTACCAGCAGCTGAAACCTATCGGCTCTGGCGCCCAGGGCATCGTGTGCGCC GCCTTTGACACCGTGCTGGGCATCAACGTGGCCGTGAAAAAACTGAGCCGCCCTTTCCA GAACCAGACCCACGCCAAACGCGCCTACCGCGAGCTGGTGCTGCTGAAATGCGTGAAC CACAAAAACATCATCAGCCTGCTGAACGTGTTCACACCCCAGAAAACCCTGGAAGAGTT CCAGGACGTGTACCTGGTCATGGAACTGATGGACGCCAACCTGTGCCAGGTCATCCACA TGGAACTGGACCACGAGCGCATGAGCTACCTGCTGTACCAGATGCTGTGCGGCATCAA ACATCTGCACAGCGCCGGCATCATCCACCGCGACCTGAAACCTAGCAACATCGTGGTCA AAAGCGACTGCACCCTGAAAATCCTGGACTTCGGCCTGGCCCGCACCGCCTGCACCAAC TTCATGATGACCCCTTACGTGGTCACCCGCTACTATCGCGCCCCTGAAGTGATCCTGGGC ATGGGCTACAAAGAGAACGTCGACATTTGGAGCGTGGGCTGCATCATGGGCGAGCTGG TCAAAGGCTGCGTGATCTTCCAGGGCACCGACCACATCGACCAGTGGAACAAAGTGAT CGAGCAGCTGGGCACCCCTAGCGCCGAGTTCATGAAAAAACTGCAGCCTACCGTGCGC AACTACGTGGAAAACCGCCCTAAATACCCCGGCATCAAATTCGAGGAACTGTTCCCTGA CTGGATCTTCCCTAGCGAGAGCGAGCGCGACAAAATCAAAACCAGCCAGGCCCGCGAC CTGCTGAGCAAAATGCTGGTCATCGACCCTGACAAACGCATCAGCGTGGACGAGGCCC TGCGCCACCCTTACATCACCGTGTGGTACGACCCTGCCGAGGCCGAAGCCCCTCCACCT CAGATCTACGACGCCCAGCTGGAAGAACGCGAGCACGCCATCGAGGAATGGAAAGAG CTGATCTACAAAGAAGTGATGTGA
His_6–LIC+TEV-site–JNK3α1 (Uniprot ID: MK10_HUMAN)	
Amino Acid Sequence	**MHHHHHHSSGVDLGTENLYFQSNG**SKSKVDNQFYSVEVGDSTFTVLKRYQNLKPIGSGAQ GIVCAAYDAVLDRNVAIKKLSRPFQNQTHAKRAYRELVLMKCVNHKNIISLLNVFTPQKTLEE FQDVYLVMELMDANLCQVIQMELDHERMSYLLYQMLCGIKHLHSAGIIHRDLKPSNIVVKS

	DCTLKILDFGLARTAGTSFMMTPYVVTRYYRAPEVILGMGYKENVDIWSVGCIMGEMVRH KILFPGRDYIDQWNKVIEQLGTPCPEFMKKLQPTVRNYVENRPKYAGLTFPKLFPDSLFPADS EHNKLKASQARDLLSKMLVIDPAKRISVDDALQHPYINVWYDPAEVEAPPPQIYDKQLDERE HTIEEWKELIYKEVMNSE
DNA Sequence	**ATGCACCATCATCATCATCATTCTTCTGGTGTAGATCTGGGTACCGAGAACCTGTACTT CCAATCCAAT**GGCAGCAAAAGCAAAGTTGACAACCAGTTCTACAGTGTGGAAGTGGGA GACTCAACCTTCACAGTTCTCAAGCGCTACCAGAATCTAAAGCCTATTGGCTCTGGGGCT CAGGGCATAGTTTGTGCCGCGTATGATGCTGTCCTTGACAGAAATGTGGCCATTAAGAA GCTCAGCAGACCCTTTCAGAACCAAACACATGCCAAGAGAGCGTACCGGGAGCTGGTC CTCATGAAGTGTGTGAACCATAAAAACATTATTAGTTTATTAAATGTCTTCACACCCCAG AAAACGCTGGAGGAGTTCCAAGATGTTTACTTAGTAATGGAACTGATGGATGCCAACTT ATGTCAAGTGATTCAGATGGAATTAGACCATGAGCGAATGTCTTACCTGCTGTACCAAA TGTTGTGTGGCATTAAGCACCTCCATTCTGCTGGAATTATTCACAGGGATTTAAAACCAA GTAACATTGTAGTCAAGTCTGATTGCACATTGAAAATCCTGGACTTTGGACTGGCCAGG ACAGCAGGCACAAGCTTCATGATGACTCCATATGTGGTGACACGTTATTACAGAGCCCC TGAGGTCATCCTGGGGATGGGCTACAAGGAGAACGTGGATATATGGTCTGTGGGATGC ATTATGGGAGAAATGGTTCGCCACAAAATCCTCTTTCCAGGAAGGGACTATATTGACCA GTGGAATAAGGTAATTGAACAACTAGGAACACCATGTCCAGAATTCATGAAGAAATTGC AACCCACAGTAAGAAACTATGTGGAGAATCGGCCCAAGTATGCGGGACTCACCTTCCCC AAACTCTTCCCAGATTCCCTCTTCCCAGCGGACTCCGAGCACAATAAACTCAAAGCCAGC CAAGCCAGGGACTTGTTGTCAAAGATGCTAGTGATTGACCCAGCAAAAAGAATATCAGT GGACGACGCCTTACAGCATCCCTACATCAACGTCTGGTATGACCCAGCCGAAGTGGAG GCGCCTCCACCTCAGATATATGACAAGCAGTTGGATGAAAGAGAACACACAATTGAAG AATGGAAAGAACTTATCTACAAGGAAGTAATGAATTCAGAATGA
His_6–SUMO-MKK4β [Uniprot IDs: SMT3_YEAST (SUMO); MP2K4_HUMAN (MKK4β)]	
Amino Acid Sequence	**MGHHHHHHGHGMSDSEVNQEAKPEVKPEVKPETHINLKVSDGSSEIFFKIKKTTPLRRL MEAFAKRQGKEMDSLRFLYDGIRIQADQTPEDLDMEDNDIIEAHREQIGG**MAAPSPSGG GGSGGGSGSGTPGPVGSPAPGHPAVSSMQGKRKALKLNFANPPFKSTARFTLNPNPTGVQ NPHIERLRTHSIESSGKLKISPEQHWDFTAEDLKDLGEIGRGAYGSVNKMVHKPSGQIMAVK RIRSTVDEKEQKQLLMDLDVVMRSSDCPYIVQFYGALFREGDCWICMELMSTSFDKFYKYV YSVLDDVIPEEILGKITLATVKALNHLKENLKIIHRDIKPSNILLDRSGNIKLCDFGISGQLVDSIA KTRDAGCRPYMAPERIDPSASRQGYDVRSDVWSLGITLYELATGRFPYPKWNSVFDQLTQV VKGDPPQLSNSEEREFSPSFINFVNLCLTKDESKRPKYKELLKHPFILMYEERAVEVACYVCKIL DQMPATPSSPMYVD
DNA Sequence	**ATGGGCCATCACCATCACCATCACGGCCATGGCATGTCGGACTCAGAAGTCAATCAAG AAGCTAAGCCAGAGGTCAAGCCAGAAGTCAAGCCTGAGACTCACATCAATTTAAAGG TGTCCGATGGATCTTCAGAGATCTTCTTCAAGATCAAAAAGACCACTCCTTTAAGAAG**

	GCTGATGGAAGCGTTCGCTAAAAGACAGGGTAAGGAAATGGACTCCTTAAGATTCTT GTACGACGGTATTAGAATTCAAGCTGATCAGACCCCTGAAGATTTGGACATGGAGGA TAACGATATTATTGAGGCACACCGTGAACAGATTGGTGGCATGGCGGCTCCGAGCCCG AGCGGCGGCGGCGGCTCCGGGGGCGGCAGCGGCAGCGGCACCCCCGGCCCCGTAGG GTCCCCGGCGCCAGGCCACCCGGCCGTCAGCAGCATGCAGGGTAAACGCAAAGCACTG AAGTTGAATTTTGCAAATCCACCTTTCAAATCTACAGCAAGGTTTACTCTGAATCCCAAT CCTACAGGAGTTCAAAACCCACACATAGAGAGACTGAGAACACACAGCATTGAGTCATC AGGAAAACTGAAGATCTCCCCTGAACAACACTGGGATTTCACTGCAGAGGACTTGAAA GACCTTGGAGAAATTGGACGAGGAGCTTATGGTTCTGTCAACAAAATGGTCCACAAACC AAGTGGGCAAATAATGGCAGTTAAAAGAATTCGGTCAACAGTGGATGAAAAAGAACAA AAACAACTTCTTATGGATTTGGATGTAGTAATGCGGAGTAGTGATTGCCCATACATTGTT CAGTTTTATGGTGCACTCTTCAGAGAGGGTGACTGTTGGATCTGTATGGAACTCATGTC TACCTCGTTTGATAAGTTTTACAAATATGTATATAGTGTATTAGATGATGTTATTCCAGA AGAAATTTTAGGCAAAATCACTTTAGCAACTGTGAAAGCACTAAACCACTTAAAAGAAA ACtTGAAAATTATTCACAGAGATATCAAACCTTCCAATATTCTTCTGGACAGAAGTGGAA ATATTAAGCTCTGTGACTTCGGCATCAGTGGACAGCTTGTGGACTCTATTGCCAAGACA AGAGATGCTGGCTGTAGGCCATACATGGCACCTGAAAGAATAGACCCAAGCGCATCAC GACAAGGATATGATGTCCGCTCTGATGTCTGGAGTTTGGGGATCACATTGTATGAGTTG GCCACAGGCCGATTTCCTTATCCAAAGTGGAATAGTGTATTTGATCAACTAACACAAGTC GTGAAAGGAGATCCTCCGCAGCTGAGTAATTCTGAGGAAAGGGAATTCTCCCCGAGTTT CATCAACTTTGTCAACTTGTGCCTTACGAAGGATGAATCCAAAAGGCCAAAGTATAAAG AGCTTCTGAAACATCCCTTTATTTTGATGTATGAAGAACGTGCCGTTGAGGTCGCATGCT ATGTTTGTAAAATCCTGGATCAAATGCCAGCTACTCCCAGCTCTCCCATGTATGTCGATT GA
His_6–SUMO-MKK7β1 [Uniprot IDs: SMT3_YEAST (SUMO); MP2K7_MOUSE (MKK7β1)]	
Amino Acid Sequence	**MGHHHHHHGHGMSDSEVNQEAKPEVKPEVKPETHINLKVSDGSSEIFFKIKKTTPLRRL MEAFAKRQGKEMDSLRFLYDGIRIQADQTPEDLDMEDNDIIEAHREQIGG**AASSLEQKLS RLEAKLKQENREARRRIDLNLDISPQRPRPTLQLPLANDGGSRSPSSESSPQHPTPPTRPRH MLGLPSTLFTPRSMESIEIDQKLQEIMKQTGYLTIGGQRYQAEINDLENLGEMGSGTCGQV WKMRFRKTGHIIAVKQMRRSGNKEENKRILMDLDVVLKSHDCPYIVQCFGTFITNTDVFIA MELMGTCAEKLKKRMQGPIPERILGKMTVAIVKALYYLKEKHGVIHRDVKPSNILLDERGQI KLCDFGISGRLVDSKAKTRSAGCAAYMAPERIDPPDPTKPDYDIRADVWSLGISLVELATGQ FPYKNCKTDFEVLTKVLQEEPPLLPGHMGFSGDFQSFVKDCLTKDHRKRPKYNKLLEHSFIKH YEILEVDVASWFKDVMAKTESPRTSGVLSQHHLPFFR
DNA Sequence	**ATGGGCCATCACCATCACCATCACGGCCATGGCATGTCGGACTCAGAAGTCAATCAAG AAGCTAAGCCAGAGGTCAAGCCAGAAGTCAAGCCTGAGACTCACATCAATTTAAAGG TGTCCGATGGATCTTCAGAGATCTTCTTCAAGATCAAAAAGACCACTCCTTTAAGAAG GCTGATGGAAGCGTTCGCTAAAAGACAGGGTAAGGAAATGGACTCCTTAAGATTCTT GTACGACGGTATTAGAATTCAAGCTGATCAGACCCCTGAAGATTTGGACATGGAGGA T**AACGATATTATTGAGGCACACCGTGAACAGATTGGTGGCGCGGCGTCCTCCCTGGAGC

	AGAAGCTGTCCCGCCTGGAAGCCAAGCTGAAGCAGGAGAACCGTGAGGCCCGCAGGA GGATCGACCTCAACTTGGATATCAGCCCACAGCGGCCCAGGCCCACCCTGCAACTCCCA CTGGCCAACGATGGGGGCAGCCGCTCACCATCCTCAGAGAGCTCCCCACAGCACCCTAC ACCCCCCACCCGGCCCCGCCACATGCTGGGGCTCCCATCAACCTTGTTCACACCGCGCA GTATGGAGAGCATCGAGATTGACCAGAAGCTGCAGGAGATCATGAAGCAGACAGGGT ACCTGACTATCGGGGGCCAGCGTTATCAGGCAGAAATCAATGACTTGGAGAACTTGGG TGAGATGGGCAGTGGTACCTGTGGTCAGGTGTGGAAGATGCGGTTCCGGAAGACAGG CCACATCATTGCTGTTAAGCAAATGCGGCGCTCTGGGAACAAGGAAGAGAATAAGCGC ATTTTGATGGACCTGGATGTAGTACTCAAGAGCCATGACTGCCCTTACATCGTTCAGTGC TTTGGCACCTTCATCACCAACACAGACGTCTTTATTGCCATGGAGCTCATGGGCACATGT GCAGAGAAGCTGAAGAAACGAATGCAGGGCCCCATTCCAGAGCGAATCCTGGGCAAG ATGACTGTGGCGATTGTGAAAGCACTGTACTATCTGAAGGAGAAGCATGGCGTCATCC ATCGCGATGTCAAACCCTCCAACATCCTGCTAGATGAGCGGGGCCAGATCAAGCTCTGT GACTTTGGCATCAGTGGCCGCCTTGTTGACTCCAAAGCCAAAACACGGAGTGCTGGCTG TGCTGCCTATATGGCTCCCGAGCGCATCGACCCTCCAGATCCCACCAAGCCTGACTATGA CATCCGAGCTGATGTGTGGAGCCTGGGCATCTCACTGGTGGAGCTGGCAACAGGACAG TTCCCCTATAAGAACTGCAAGACGGACTTTGAGGTCCTCACCAAAGTCCTACAGGAAGA GCCCCCACTCCTGCCTGGTCACATGGGCTTCTCAGGGGACTTCCAGTCATTTGTCAAAGA CTGCCTTACTAAAGATCACAGGAAGAGACCAAAGTATAATAAGCTACTTGAACACAGCT TCATCAAGCACTATGAGATACTCGAGGTGGATGTCGCGTCCTGGTTTAAGGATGTCATG GCGAAGACCGAGTCCCCAAGGACTAGTGGAGTCCTGAGTCAGCACCATCTGCCCTTCTT CAGGTAG
Flag-JIP1b-His$_6$ (Uniprot ID: JIP1_MOUSE)	
Amino Acid Sequence	**MDYKDDDDK**MAERESGLGGGAASPPAASPFLGLHIASPPNFRLTHDISLEEFEDEDLSEITD ECGISLQCKDTLSLRPPRAGLLSAGSSGSAGSRLQAEMLQMDLIDAAGDTPGAEDDEEEED DELAAQRPGVGPPKAESNQDPAPRSQGQGPGTGSGDTYRPKRPTTLNLFPQVPRSQDTLN NNSLGKKHSWQDRVSRSSSPLKTGEQTPPHEHICLSDELPPQGSPVPTQDRGTSTDSPCRRS AATQMAPPSGPPATAPGGRGHSHRDRIHYQADVRLEATEEIYLTPVQRPPDPAEPTSTFMP PTESRMSVSSDPDPAAYSVTAGRPHPSISEEDEGFDCLSSPERAEPPGGGWRGSLGEPPPPP RASLSSDTSALSYDSVKYTLVVDEHAQLELVSLRPCFGDYSDESDSATVYDNCASASSPYESAI GEEYEEAPQPRPPTCLSEDSTPDEPDVHFSKKFLNVFMSGRSRSSSAESFGLFSCVINGEEHE QTHRAIFRFVPRHEDELELEVDDPLLVELQAEDYWYEAYNMRTGARGVFPAYYAIEVTKEPE HMAALAKNSDWIDQFRVKFLGSVQVPYHKGNDVLCAAMQKIATTRRLTVHFNPPSSCVLE ISVRGVKIGVKADDALEAKGNKCSHFFQLKNISFCGYHPKNNKYFGFITKHPADHRFACHVF VSEDSTKALAESVGRAFQQFYKQFVEYTCPTEDIYLE**HHHHHH**
DNA Sequence	**ATGGATTATAAGGATGACGACGATAAG**ATGGCGGAGCGAGAGAGCGGCCTGGGCGG GGGCGCCGCGTCCCCACCGGCCGCTTCCCCATTCCTGGGACTGCACATCGCGTCGCCTC CCAATTTCAGGCTCACCCATGACATCAGCCTGGAGGAGTTTGAGGATGAAGACCTTTCG GAGATCACTGACGAGTGTGGCATCAGCCTGCAGTGCAAAGACACCCTGTCTCTCCGGCC CCCGCGCGCCGGGCTGCTGTCTGCGGGTAGCAGCGGCAGCGCGGGGAGCCGGCTGCA

	GGCGGAGATGCTGCAGATGGACCTGATCGACGCGGCAGGTGACACTCCGGGCGCCGA GGACGACGAGGAGGAGGAGGACGACGAGCTCGCTGCCCAACGACCAGGAGTGGGGC CTCCCAAAGCGGAGTCCAACCAGGATCCGGCGCCTCGCAGCCAGGGCCAGGGCCCGGG CACAGGCAGCGGAGACACCTACCGACCCAAGAGGCCTACCACGCTCAACCTTTTCCCGC AGGTGCCGCGGTCTCAGGACACGCTGAATAATAACTCTTTAGGCAAAAAGCACAGTTG GCAGGACCGTGTGTCTCGATCATCCTCCCCTCTGAAGACAGGAGAACAGACGCCTCCAC ATGAACACATCTGCCTGAGTGATGAGCTGCCACCCCAGGGCAGTCCTGTTCCCACCCAG GACCGCGGCACTTCCACCGACAGCCCTTGTCGCCGAAGTGCAGCCACCCAGATGGCACC TCCAAGCGGTCCCCCTGCCACTGCGCCTGGTGGCCGGGGCCACTCCCATCGAGACCGAA TCCACTACCAGGCAGATGTGCGGCTCGAGGCGACTGAGGAGATCTACCTGACCCCAGT GCAGAGGCCCCCAGACCCTGCAGAACCCACCTCCACCTTCATGCCACCCACGGAGAGCC GGATGTCAGTTAGCTCGGATCCAGACCCTGCCGCTTACTCTGTAACTGCGGGGCGGCCA CACCCCTCCATCAGTGAAGAGGATGAGGGCTTCGACTGCCTGTCATCCCCAGAGCGAGC TGAGCCACCAGGTGGAGGGTGGCGGGGAAGCCTCGGGGAGCCACCACCGCCTCCACG GGCCTCACTGAGCTCGGACACCAGCGCACTGTCCTACGACTCGGTCAAGTACACACTGG TGGTGGATGAACATGCCCAGCTTGAGTTGGTGAGCCTGCGGCCGTGCTTTGGAGATTA CAGTGACGAAAGCGACTCTGCCACTGTCTATGACAACTGTGCCTCTGCCTCCTCGCCCTA CGAGTCAGCCATTGGTGAGGAGTATGAGGAGGCCCCTCAGCCCCGGCCTCCCACCTGC CTCTCAGAGGACTCCACCCCGGATGAGCCTGATGTCCACTTCTCTAAGAAGTTTCTGAAT GTCTTCATGAGTGGCCGCTCTCGTTCCTCCAGTGCTGAGTCCTTTGGGCTGTTCTCCTGC GTCATCAATGGGGAGGAGCATGAGCAAACCCATCGGGCTATATTCAGGTTTGTGCCTCG GCATGAAGATGAACTTGAGCTGGAAGTGGATGACCCCCTGCTGGTGGAGCTGCAGGCA GAAGACTATTGGTATGAGGCCTATAACATGCGCACCGGAGCCCGCGGGGTCTTCCCTGC CTACTATGCCATTGAGGTCACCAAGGAGCCTGAGCACATGGCAGCCCTTGCCAAAAACA GCGACTGGATTGACCAGTTCCGGGTGAAGTTCCTGGGGTCTGTCCAGGTTCCTTATCAC AAGGGCAATGATGTCCTCTGTGCTGCTATGCAAAAGATCGCCACCACCCGCCGGCTCAC CGTGCACTTTAACCCGCCCTCCAGCTGTGTCCTTGAGATCAGTGTCAGGGGTGTCAAGA TAGGCGTCAAAGCTGATGATGCTCTGGAGGCCAAGGGAAATAAATGTAGCCACTTCTTC CAGCTAAAGAACATCTCTTTCTGTGGATACCATCCAAAGAATAACAAGTACTTTGGGTTT ATCACTAAGCACCCTGCTGACCACCGGTTTGCCTGCCATGTCTTTGTGTCTGAAGATTCC ACCAAAGCCCTGGCGGAGTCTGTGGGGCGTGCATTTCAGCAGTTCTACAAGCAGTTTGT GGAGTATACCTGTCCTACAGAAGATATCTACTTGGAG**CACCACCACCACCACCAC**TGA
His_6–SUMO-JNK1α1 [Uniprot IDs: SMT3_YEAST (SUMO); MK08_MOUSE (JNK1α1)]	
Amino Acid Sequence	**MGHHHHHHGHGMSDSEVNQEAKPEVKPEVKPETHINLKVSDGSSEIFFKIKKTTPLRRL MEAFAKRQGKEMDSLRFLYDGIRIQADQTPEDLDMEDNDIIEAHREQIGG**GSRSKRDNN FYSVEIGDSTFTVLKRYQNLKPIGSGAQGIVCAAYDAILERNVAIKKLSRPFQNQTHAKRAYR ELVLMKCVNHKNIIGLLNVFTPQKSLEEFQDVYIVMELMDANLCQVIQMELDHERMSYLLY QMLCGIKHLHSAGIIHRDLKPSNIVVKSDCTLKILDFGLARTAGTSFMMTPYVVTRYYRAPEV ILGMGYKENVDLWSVGCIMGEMVCHKILFPGRDYIDQWNKVIEQLGTPCPEFMKKLQPTV RTYVENRPKYAGYSFEKLFPDVLFPADSEHNKLKASQARDLLSKMLVIDASKRISVDEALQHP YINVWYDPSEAEAPPPKIPDKQLDEREHTIEEWKELIYKEVMDLEERTKNGVKLLE

DNA Sequence	**ATGGGCCATCACCATCACCATCACGGCCATGGCATGTCGGACTCAGAAGTCAATCAAG AAGCTAAGCCAGAGGTCAAGCCAGAAGTCAAGCCTGAGACTCACATCAATTTAAAGG TGTCCGATGGATCTTCAGAGATCTTCTTCAAGATCAAAAAGACCACTCCTTTAAGAAG GCTGATGGAAGCGTTCGCTAAAAGACAGGGTAAGGAAATGGACTCCTTAAGATTCTT GTACGACGGTATTAGAATTCAAGCTGATCAGACCCCTGAAGATTTGGACATGGAGGA T**AACGATATTATTGAGGCACACCGTGAACAGATTGGTGGCggaAGCCGCAGCAAACGCG ACAACAACTTCTACAGCGTGGAAATCGGCGACAGCACCTTCACCGTGCTGAAACGCTAC CAGAACCTGAAACCTATCGGCTCTGGCGCCCAGGGCATCGTGTGTGCCGCCTACGACGC CATCCTGGAACGCAACGTGGCCATCAAAAAACTGAGCCGCCCTTTCCAGAACCAGACCC ACGCCAAACGCGCCTACCGCGAGCTGGTGCTGATGAAATGCGTGAACCACAAAAACAT CATCGGCCTGCTGAACGTGTTCACACCTCAGAAAAGCCTGGAAGAGTTCCAGGACGTCT ACATCGTGATGGAACTGATGGACGCCAACCTGTGCCAGGTCATCCAGATGGAACTGGA CCACGAGCGCATGAGCTACCTGCTGTACCAGATGCTGTGCGGCATCAAACATCTGCACA GCGCCGGCATCATCCACCGCGACCTGAAACCATCCAACATCGTGGTCAAAAGCGACTGC ACCCTGAAAATCCTGGACTTCGGCCTGGCCCGCACCGCCGGCACCAGCTTCATGATGAC CCCTTACGTGGTCACCCGCTACTATCGCGCCCCTGAAGTGATCCTGGGCATGGGCTACA AAGAAAACGTGGACCTGTGGTCCGTGGGCTGCATCATGGGCGAGATGGTCTGCCACAA AATCCTGTTCCCTGGCCGCGACTACATCGACCAGTGGAACAAAGTGATCGAGCAGCTGG GCACCCCTTGCCCTGAGTTCATGAAAAAACTGCAGCCTACCGTGCGCACCTACGTGGAA AACCGCCCTAAATACGCCGGCTACAGCTTCGAGAAACTGTTCCCTGACGTGCTGTTCCCT GCCGACAGCGAGCACAACAAACTGAAAGCCAGCCAGGCCCGCGACCTGCTGAGCAAAA TGCTGGTCATCGACGCCAGCAAACGCATCAGCGTGGACGAGGCCCTGCAGCACCCTTAC ATCAACGTGTGGTACGACCCTAGCGAGGCCGAGGCCCCTCCTCCAAAAATCCCTGACAA ACAGCTGGACGAGCGCGAGCACACCATCGAGGAATGGAAAGAGCTGATCTACAAAGA AGTGATGGACCTGGAAGAACGCACCAAAAACGGCGTGAAGCTTCTCGAGTAG**
His_6-Ulp1 (Uniprot ID: ULP1_YEAST)	
Amino Acid Sequence	**MGHHHHHHGHG**LVPELNEKDDDQVQKALASRENTQLMNRDNIEITVRDFKTLAPRRWL NDTIIEFFMKYIEKSTPNTVAFNSFFYTNLSERGYQGVRRWMKRKKTQIDKLDKIFTPINLNQ SHWALGIIDLKKKTIGYVDSLSNGPNAMSFAILTDLQKYVMEESKHTIGEDFDLIHLDCPQQP NGYDCGIYVCMNTLYGSADAPLDFDYKDAIRMRRFIAHLILTDALK
DNA Sequence	**ATGGGCCATCACCATCACCATCACGGCCATGGC**CTGGTCCCGGAACTGAACGAAAAAG ACGACGATCAAGTCCAAAAAGCACTGGCAAGCCGCGAAAATACCCAACTGATGAACCG TGACAACATTGAAATCACCGTTCGTGATTTTAAAACGCTGGCGCCGCGTCGCTGGCTGA ATGACACCATCATCGAATTTTTCATGAAATACATCGAAAAAAGCACCCCGAACACGGTG GCCTTCAATAGCTTTTTCTATACGAACCTGTCCGAACGTGGCTACCAGGGTGTTCGTCGC TGGATGAAGCGTAAGAAAACCCAAATCGATAAACTGGACAAAATTTTTACGCCGATCAA CCTGAATCAGTCTCATTGGGCGCTGGGCATTATCGATCTGAAAAAGAAAACCATTGGCT ATGTCGACAGCCTGTCTAACGGTCCGAATGCAATGTCATTTGCTATCCTGACCGATCTGC

	AAAAATACGTGATGGAAGAATCGAAACATACGATTGGCGAAGATTTCGACCTGATCCAC CTGGATTGCCCGCAGCAACCGAACGGCTATGACTGCGGTATTTACGTCTGTATGAATAC CCTGTATGGTTCCGCGGATGCCCCGCTGGATTTCGACTACAAAGATGCTATCCGTATGC GTCGTTTTATTGCCCACCTGATTCTGACCGATGCCCTGAAATAA

Chapter 3. TOOLS AND METHODOLOGY TO EXPLORE JNK INHIBITION AND JIP SCAFFOLDING

Acknowledgement: This chapter includes experiments that were published in Fang, L. *et al.* (2019) Chemoproteomic Method for Profiling Inhibitor-Bound Kinase Complexes, *J. Am. Chem. Soc 141,* 11912-11922.[25] TCO-conjugated **3.1**, **3.2**, and **3.3** (**Figure 3.5**) were reported as **1-TCO**, **3-TCO**, and **2-TCO**, respectively. Radioassays for **3.1**, **3.2**, and **3.3** against JNK2a2 were conducted by C. Lombard (**Figure 3.8**). L. Fang conducted the **1-TCO**, **2-TCO**, and **3-TCO** pull-down assays targeting recombinant JNK2a2 in HEK293 T-REx Flp-In cell lysate (**Figure 3.9**).

3.1 INTRODUCTION TO JNK ALLOSTERY AND SCAFFOLDING

In the human genome there are 538 protein kinases, a class of phosphotransferase enzymes, that all share a highly conserved, bi-lobal catalytic domain, centered around an ATP-binding cleft.[1, 2, 8] Despite catalyzing the same chemical reaction, each kinase has unique and essential functions in a cellular environment. A better understanding of the mechanisms by which such structurally homologous enzymes are able to play a wide range of roles in the cell will provide valuable insight into how complex signaling events can be mediated using relatively simple protein components.

The c-Jun N-terminal kinases (JNKs), a subfamily of the Mitogen Activated Protein Kinases (MAPKs), play vital roles in immune responses, cell migration and differentiation, and both cell survival and cell death.[32, 53, 56] JNKs interact allosterically with JNK interacting proteins (JIPs), a family of scaffolds that have been shown to potentiate JNK activation in vivo, under specific conditions.[53, 56, 66, 67] The JNK docking-domain (D-domain) of JIPs bind to the D-recruitment sites (DRSs) of JNKs, located on the kinase domain's C-terminal lobe, and induce conformational shifts in JNK ATP-binding sites, which are located ~16.5 Angstroms from the

DRS (**Figure 2.1**). Allosteric coupling is bi-directional, meaning a binding event at either the DRS or the ATP-binding cleft can alter the conformation and behavior of the other site.[8, 12, 53]

We investigated the ability of ATP-competitive inhibitors to modulate the DRSs of JNKs in Chapter 2.[10] We found that ATP-competitive inhibitors could differentially affect the ability of non-phosphorylated JNKs to bind to JIP1. We also found that inhibitors could alter the ability of MKK4β and MKK7β1, which also bind to JNK DRSs, to phosphorylate the activation loops of JNKs.

The functional role of the allosteric coupling between the ATP-binding sites and the DRSs of JNKs in cells remains unclear. ATP-competitive inhibitors that differentially modulate the abilities of JNKs to interact with JIP1 could serve as useful tools for exploring allosteric coupling. Unfortunately, most ATP-competitive inhibitors that target JNKs do not have sufficient selectivity to be used for this purpose. Targeting any single JNK isoform with an ATP-competitive inhibitor is particularly challenging because most inhibitors do not discriminate between isoforms due to their high sequence homology.[10, 23] This makes it difficult to selectively target and study individual JNK isoforms, something that is necessary if we wish to fully understand this complex kinase family. In this chapter, we explore a methodology that uses orthogonal drug-sensitized JNK mutants with orthogonal, conformation-selective inhibitor pairs to selectively investigate JNK biology in vivo.

Since it also still remains unclear how JIPs potentiate JNK activation in vivo, or if the allosteric changes JNK undergoes upon JIP binding are an important mechanism in their activation or overall regulation, this chapter also presents an approach for further characterizing JNK-JIP signaling module dynamics both in vitro and in vivo.

3.2 ATP-Competitive Inhibitors Modulate Binding of JNK Signaling Partners In Vitro

In Chapter 2, we described how ATP-competitive inhibitors can affect JNK's active site conformation and, thus, affect binding of essential signaling partners, like scaffolds and activators in vitro.[10] We wanted to understand how this would translate to cells and if we could use these tools to understand JNK regulation in vivo. However, due to the potential off-target effects that ATP-competitive inhibitors can have on various aspects of JNK biology, we reasoned that each inhibitor should be characterized as fully as possible in vitro before making strong conclusions about their effects in vivo. Thus, before using these tools in cells, we first tested their ability to modulate other aspects of JNK behavior in vitro.

3.3 JIPtide Prevents Certain ATP-Competitive Inhibitors From Binding to Active JNK1 and JNK2

In Chapter 2, we investigated how ATP-competitive inhibitors can influence the behavior of non-phosphorylated, inactive JNKs. However, prior work has shown that phosphorylation of kinases, including other MAPKs, leads to conformational changes, many of which occur at or around the ATP-binding site.[53, 68, 69] Thus, we suspected that activation of JNKs may change the behavior of how inhibitors influence the interactions between JNKs and their binding partners. While this would add another layer of complexity to an already complicated system, we reasoned that before putting inhibitors in cells, we should consider as many variables as possible. The better our understanding of all the possible ways inhibitors can influence JNK behavior, and vice versa, the easier it will be to explain the effects observed in cells. Additionally, this system has been notoriously difficult to target in disease, and will likely remain so; however, the more we are able to purposely tune JNK inhibitors to have certain effects, and not others, the more possible it seems.

Thus, before putting ATP-competitive inhibitors of JNKs in cells, we decided to probe if activating phosphorylation of JNKs affects the allostery between JNK ATP-binding sites and their DRSs. To study active JNKs, we used a Perkin Elmer Lance Ultra TR-FRET (time-resolved fluorescence resonance energy transfer) activity assay (**Figure 3.1A**). In these assays, JNK activity is determined by monitoring the phosphorylation of a fluorescently-labeled peptide of the JNK substrate, Myelin Basic Protein, termed ulight-MBPtide. JNK1α1 or JNK2α1 were first pre-activated using MKK4α that was purified in its activated form via co-expression with MAP3K1. Activated JNKs were then allowed to phosphorylate ulight-MBPtide. Relative amounts of phosphorylated ulight-MBPtide were determined using TR-FRET between ulight-MBPtide and Anti-phospho-MBPtide.

To better understand how activation would influence JNK allostery and overall behavior, we decided to test how inhibitor potency for activated JNKs change in the presence or absence of the DRS binder, JIPtide. Since allostery is bi-directional, one would expect the effects that JIPtide has on inhibitor potency to correlate with the results described in Chapter 2. In Chapter 2, we found that inhibitors that enhanced binding of non-phosphorylated JNK to JIP1 demonstrated increased affinity for JNK in the presence of a saturating concentration of JIPtide, with the opposite being true for disruptors of the JNK-JIP interaction. However, based on the fact that phosphorylation can induce conformational changes in kinases, we were curious if that would be the case, and reasoned that this would be a good model system to test the difference between phosphorylated and non-phosphorylated JNKs.

To determine whether there was a change in inhibitor affinity for free phospho-JNK or the phospho-JNK-JIPtide complex, we ran inhibitor titrations using the TR-FRET activity assay to determine inhibitor IC_{50}s against apo-JNK1/2 or JNK1/2 in complex with JIPtide (>75% JIPtide

bound JNK).[10] Before running inhibitor titrations, we first ran enzyme titrations for JNK1α1 and JNK2α1, to make sure activity was linear under our assay conditions for both apo-JNKs and JNK-JIPtide complexes (**Figure 3.1B – 3.1E**). We also titrated ATP at 15 nM JNK1α1 to determine the K_m ATP for apo-JNK1α1 and JIPtide bound JNK1α1 (single time point) (**Figure 3.1F**). We found both species had similar K_ms for ATP under our assay conditions. Finally, we confirmed that there was no detectable activity for non-phosphorylated JNK1α1, which allowed us to probe inhibitor affinity for only the population of activated JNKs (**Figure 3.1G**).

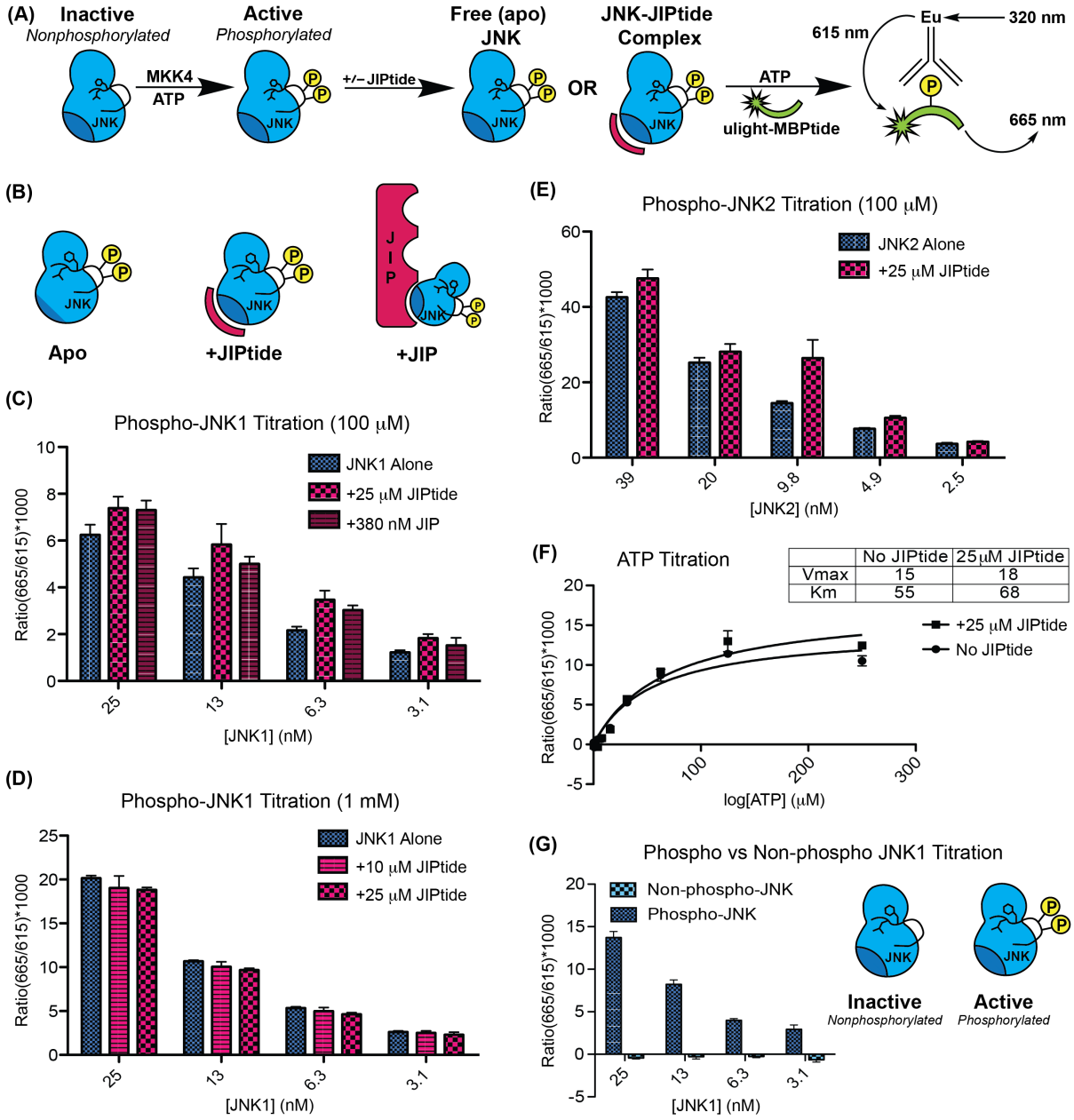

Figure 3.1. *Control experiments for JNK TR-FRET activity assays.* (A) Schematic of the assay used to measure inhibition of activated JNKs ± JIPtide. (B-E) Enzyme titrations for JNK1α1 and JNK2α1. Pre-activated JNKs were incubated with ATP for 30 min. Assays were initiated by the addition of ulight-MBPtide, incubated (4 hr), and quenched using EDTA. TR-FRET between Eu-Anti-pMBPtide (615 nm emission) and ulight-pMBPtide (665 nm emission) was used as measure of activity. (F) K_m ATP for JNK1α1 (15 nM) ± 25 μM JIPtide was determined using a single (4 hr) time point. (G) Activity for activated

JNK1α1 compared to inactive JNK1α1 (no MKK4α in pre-activation reaction). Assays were run with 100 μM ATP.

Using this assay, we then measured the affinity of the ATP-competitive inhibitors **2.1**, **2.2**, **2.4**, **2.5**, and **2.10** (**Figure 2.1** and Referenced again in **Figure 3.2**) for activated JNK1α1 and JNK2α1 in their free or JIPtide bound forms (**Table 3.1** and **Figure 3.2**). Comparisons of the IC_{50} values and IC_{50} curves for apo or JIPtide bound JNKs revealed that certain ATP-competitive inhibitors interact divergently with the phosphorylated JNK-JIPtide complex than with the non-phosphorylated JNK-JIPtide complex. JIPtide binding to phospho-JNKs appears to result in a conformational shift in the ATP-binding site that disrupts the ability of some ATP-competitive inhibitors to bind to JNKs. Both compounds **2.1** and **2.2** -which are an enhancer and disruptor of the non-phosphorylated JNK-JIPtide interaction, respectively, show reduced inhibition in the presence of JIPtide. Compound **2.5** also shows this trend. However, unlike the majority of the inhibitors that were screened, it was much more potent against JNK2α1, and JIPtide appears to more potently shift the phospho-JNK/inhibitor binding equilibrium towards an uncomplexed state. Other inhibitors, such as compounds **2.4** and **2.10** showed very little difference in affinity for activated apo-JNKs or the JNK-JIPtide complexes.

Table 3.1. IC_{50}s of inhibitors (**Figure 2.1**) for activated JNK1α1 and JNK2α1 ± JIPtide.

Compound Apo-JNK1 IC_{50} (μM) JNK1/JIPtide IC_{50} (μM)	Compound Apo-JNK2 IC_{50} (μM) JNK2/JIPtide IC_{50} (μM)	Structure
2.1 0.88 ± 0.19 12 ± 2	2.1 1.2 ± 0.3 4.8 ± 1.0	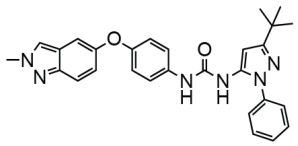
2.2 0.48 ± 0.27 >30	2.2 2.8 ± 1.1 >30	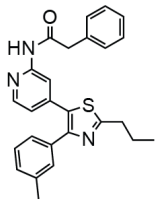
2.4 0.070 ± 0.023 0.23 ± 0.12	2.4 0.59 ± 0.15 0.87 ± 0.16	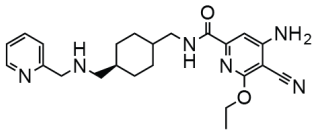
2.5 19 ± 5 >30	2.5 0.99 ± 0.33 >30	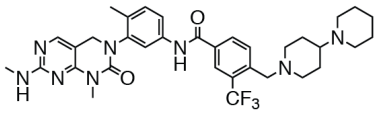
2.10 0.10 ± 0.03 0.15 ± 0.04	2.10 0.14 ± 0.03 0.27 ± 0.09	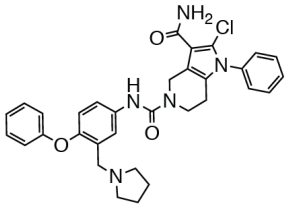

Compound	Effect on Nonphospho-JNK1/JIPtide Binding in FP Assay	Effect on Nonphospho-JNK2/JIPtide Binding in FP Assay	JNK1 IC_{50} Curve +/- JIPtide WT JIPtide No JIPtide	JNK2 IC_{50} Curve +/- JIPtide WT JIPtide No JIPtide
2.1	Enhancer	Enhancer	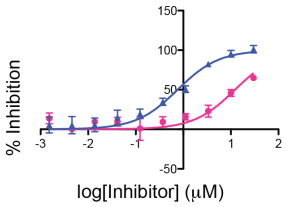	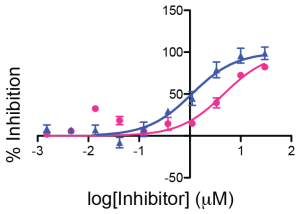
2.2	Disruptor	Disruptor	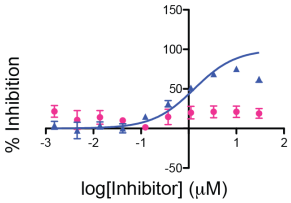	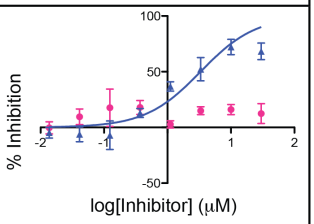
2.4	Disruptor	Enhancer	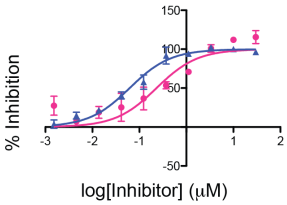	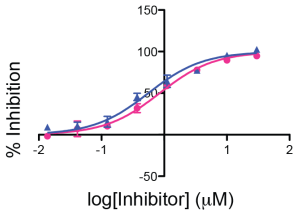
2.5	Enhancer	Disruptor	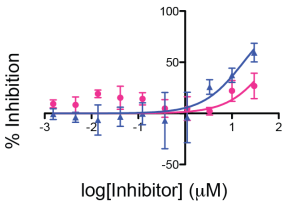	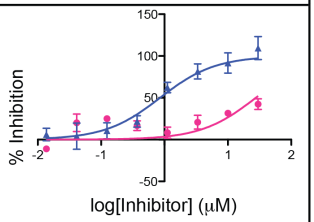
2.10	Enhancer	Enhancer	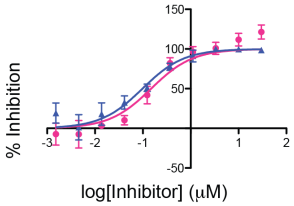	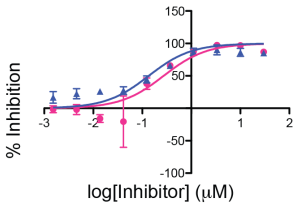

Figure 3.2 *JIPtide prevents specific ATP-competitive inhibitors from binding to active JNKs.* A TR-FRET activity assay was used to determine IC_{50}s of ATP-competitive inhibitors for phosphorylated -activated- apo-JNKs or JNK-JIPtide[10] complexes. Pre-activated JNKs (± JIPtide) were incubated with ATP and inhibitors for 30 min. Assays were initiated by the addition of the ulight-MBPtide substrate. Assays were incubated for 4 hr and quenched by the addition of EDTA. Relative activity was measured using TR-FRET between phospho-ulight-MBPtide and Eu-Anti-pMBPtide.

3.4 Full-Length JIP1b Prevents Certain ATP-Competitive Inhibitors from Binding to Active JNK1

We then sought to confirm that the results from the TR-FRET activity assay with JIPtide would be similar for full-length JIP1b. To do this, we included full-length JIP1b in the activity assay in place of JIPtide for three inhibitor concentrations in the linear range for inhibition. These experiments showed that JIP1b, like JIPtide, affected the ability of certain inhibitors (compound **2.2**) to bind to active JNKs, but not others (compound **2.10**) (**Figure 3.3**). These data suggest that the cellular state of JNKs will affect their ability to be inhibited by certain ATP-competitive inhibitors but not others. Certain inhibitors are able to bind to active JNKs regardless of their scaffolded state. However, other inhibitors will only be able to bind if the JNKs are free, and not if they are already scaffolded.

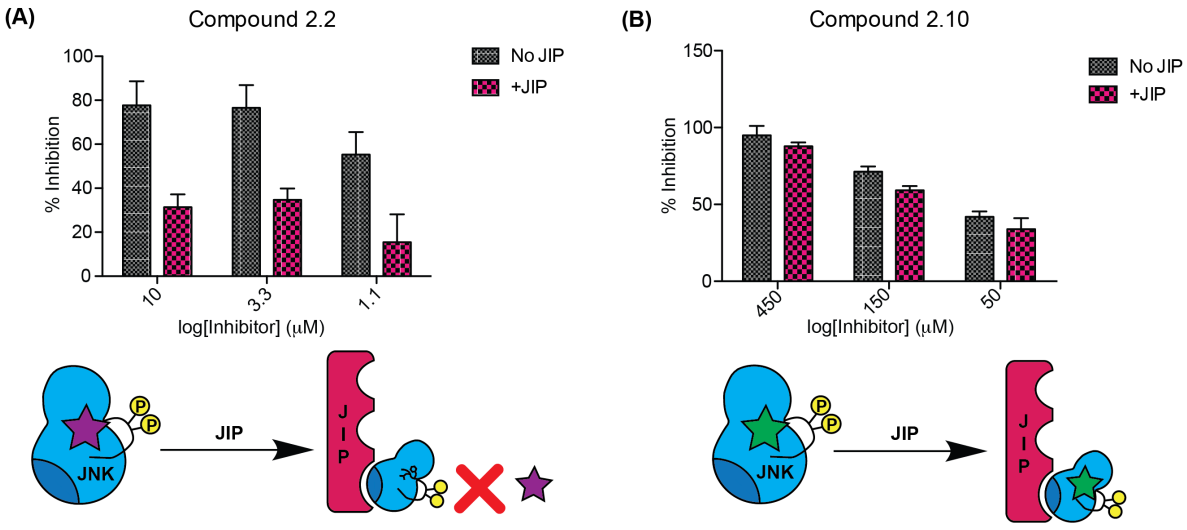

Figure 3.3. *JIP1b's effects on inhibitor binding to activated JNK1α1.* (A and B) Percent inhibition of ATP-competitive inhibitors at select inhibitor concentrations were determined for phosphorylated JNK1α1 ± using a TR-FRET activity assay. (A) Pre-activated JNK1α1 (± 380 nM JIP1b) was incubated with inhibitor **2.2** and 100 μM ATP for 30 min. Assays ran for 4 hr and were initiated by the addition of ulight-MBPtide. Assays were quenched using EDTA. Activity was measured using TR-FRET between phospho-ulight-MBPtide

and Eu-Anti-pMBPtide. (B) Inhibitor **2.10** was assayed as described in (A), except 1 mM ATP was used.

3.5 Studying the Functional Outcomes of Allosterically Modulating Each JNK Isoform in Whole Cells

Previous studies, including those in the Maly lab, have demonstrated that ATP-competitive inhibitors of protein kinases can bind to distinct active-site conformations, including the active kinase (DFG-in), or one of two inactive conformations (DFG-out or αC helix-out) (**Figure 3.4**).[14, 16] The DFG-out conformation requires a 180° rotation of the essential DFG (Asp-Phe-Gly) motif. The αC helix-out conformation results from the displacement of a glutamate that forms an essential salt bridge with a catalytic lysine in the active enzyme. These kinase conformations often have divergent effects on kinase's global conformation, thereby affecting kinase non-catalytic function, as well as the ability of the kinase to be phosphorylated or dephosphorylated by regulators.[10-16, 61, 70] These conformational shifts lead to the formation of hydrophobic pockets (blue), which can be stabilized by inhibitor ligands (**R**) that are designed to occupy these sites (**Figure 3.5**).[25] However, the biological roles of these specific conformations have not been explored in the JNK family. By stabilizing specific kinase conformations in vivo using ATP-competitive ligands, we can investigate the resultant functional outcomes in a biological context.

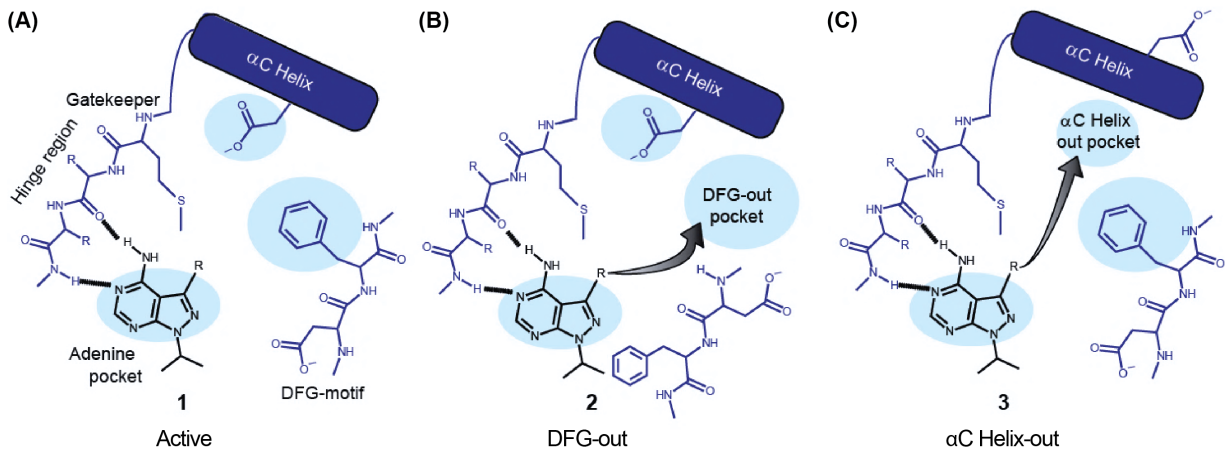

Figure 3.4. *ATP-competitive inhibitors are classified based on the kinase conformation they stabilize.* Though additional ATP-binding site conformations have recently been identified, they are generally separated into three main types (DFG-in – Type I; DFG-out – Type II; and αC helix-out – Type 1.5). (A) Structure **1** depicts a generic adenine-mimetic inhibitor scaffold in the ATP-binding site, stabilizing a kinase in its active conformation (DFG-in). (B) Structures **2** portrays an inhibitor binding to the DFG-out, inactive conformation.[9, 10] (C) The inhibitor in structure **3** is shown stabilizing another inactive conformation, αC helix-out. The conformational changes in the αC helix-out and DFG-out conformations lead to the formation of hydrophobic pockets (blue) that can be stabilized by inhibitors that contain moieties (**R**) that occupy these sites.

Due to the promiscuity of many ATP-competitive inhibitors, researchers have used drug-sensitized kinase mutants with orthogonal inhibitors to study kinase biology in vivo.[71] To achieve selective kinase inhibition in cells, scientists have created "bumped" versions of the rather promiscuous inhibitor PP1, a DFG-in (Type I) kinase inhibitor. PP1 was functionalized with a large naphthyl moiety (1NA-PP1 or 1NM-PP1), making them selective for Ala or Gly gatekeeper mutants over wild-type (WT) kinases.[62, 72] However, Ala and Gly gatekeeper kinase mutants have been shown to disturb kinase conformation and function.[4, 73]

Thus, as reported in Ahler, *et al.*, members of the Maly lab designed conformation-selective ligands that are mono-specific for kinases containing a sensitizing mutation (**Figure 3.5**).[17]

Rather than using traditionally "bumped" inhibitors, this technique uses inhibitors that are functionalized with electrophilic, Michael-type acceptors at C-6 of the pyrrolo[2,3-d]pyrimidine scaffold. This electrophile prevents these inhibitors from interacting with most wild type kinases and highly potent against sensitized, mutant kinases that contain a nucleophilic cysteine in the N-terminal lobe (β-strand 3). Almost all wild type kinases contain a valine at the site of cysteine sensitization. Electrophile-containing inhibitors stabilizing each of the three main ATP-binding site conformation were designed (DFG-in – Type I; DFG-out – Type II; and αC helix-out – Type 1.5). To engineer inhibitor-sensitized JNK1 and JNK2 variants that would interact with these ligands, their bulky methionine gatekeepers were mutated to a smaller threonine residue (M108T) in addition to the valine to cysteine mutation (V40C). A smaller gatekeeper residue was required to accommodate the large aryl groups displayed from the C-5 position of all three inhibitors.

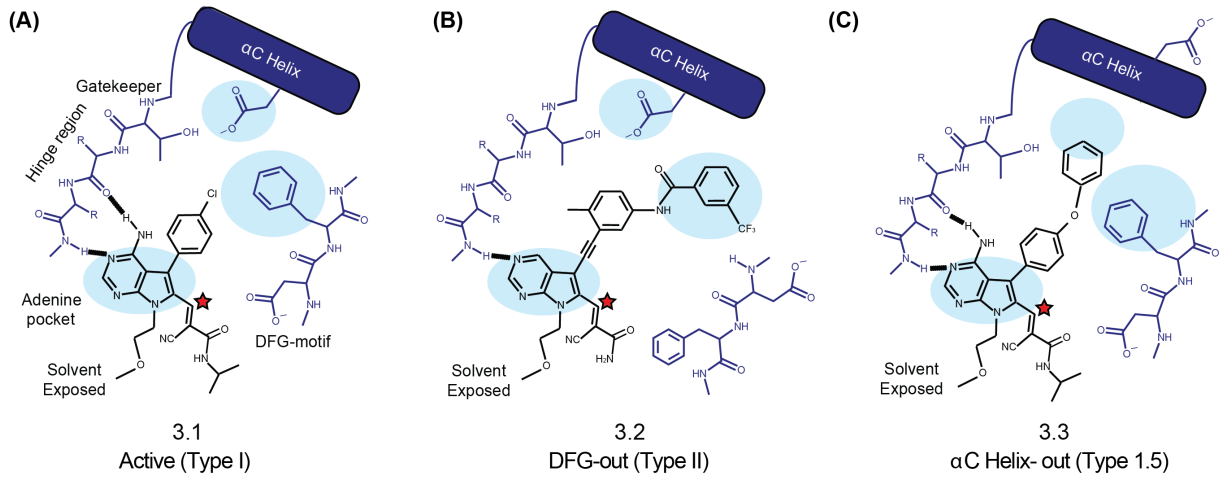

Figure 3.5. *In Ahler, et al., orthogonal, conformation-selective inhibitors of drug-sensitized kinases were designed to study the functional outcomes of conformation selective inhibitors in whole cells.*[17] Inhibitors were functionalized with electrophilic, Michael-type acceptors. Kinases that have had a conserved Val in the N-lobe mutated to a nucleophilic Cys can form reversible covalent bonds with the electrophilic inhibitors. Further selectivity for JNK1 and JNK2 was provided by mutating the bulky Met gatekeeper to a smaller Thr,

which allows binding of inhibitors that have been functionalized with a large aryl group at the C-5 position. See **Table 3.2** for sequence information, including mutation positions.

The chemical genetic tools described above allow JNK isoforms to be inhibited individually in cells by controlling which isoform contains a sensitizing mutation. This makes it possible to look for divergent behavior when either JNK1 or JNK2 is allosterically modulated. As depicted by the example in **Figure 3.6**, these inhibitors could allow an inhibited JNK isoform to act in a dominant-negative fashion, where, while their catalytic activity will be inhibited, they will still be present in the cell to displace or affect the regulation of the other isoform(s). Specifically, an allosteric disruptor and enhancer of the JNK1-JIP1 interaction could help us understand what occurs when JNK2 can and cannot interact with JIP1, respectively.

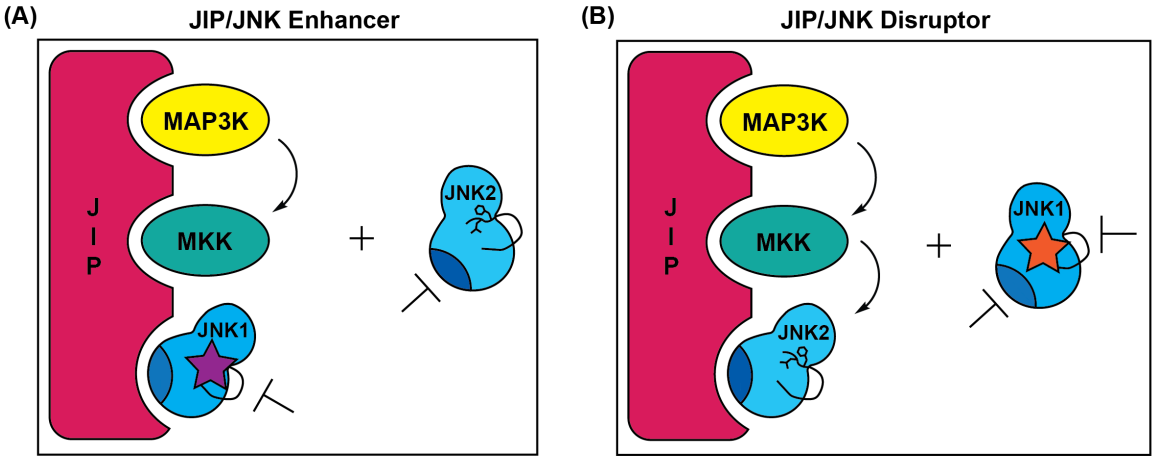

Figure 3.6. *Orthogonal, conformation-selective inhibitors of drug-sensitized JNKs can act as dominant-negatives in cells.* These inhibitor tools allow the target kinase to act as a dominant-negative in cells, where they are catalytically inactive, but are still present in the cell to affect or displace the other isoform. (A) A JNK1-JIP1 allosteric enhancer could be used in cells to understand what occurs when JNK2 cannot bind to JIP1. (B) An allosteric disruptor of the JNK1-JIP1 interaction could be used to understand what occurs when JNK2 can bind to JIP1.

Before using these inhibitors in cells, their selectivity and potency for drug-sensitized kinases versus the WT kinase was determined. To this end, we expressed and purified both WT and V40C/M108T recombinant JNK1α1 and JNK2α2. We then developed ATP-[γ^{32}P] radioassays to test the potency of the orthogonal inhibitors in vitro. In these assays, JNKs are first pre-activated using MKK4α that was purified in its activated form via co-expression with MAP3K1. We first ran enzyme titrations with our expressed proteins to determine the linear range of activity for each JNK against Myelin Basic Protein, under our assay conditions (**Figure 3.7**).

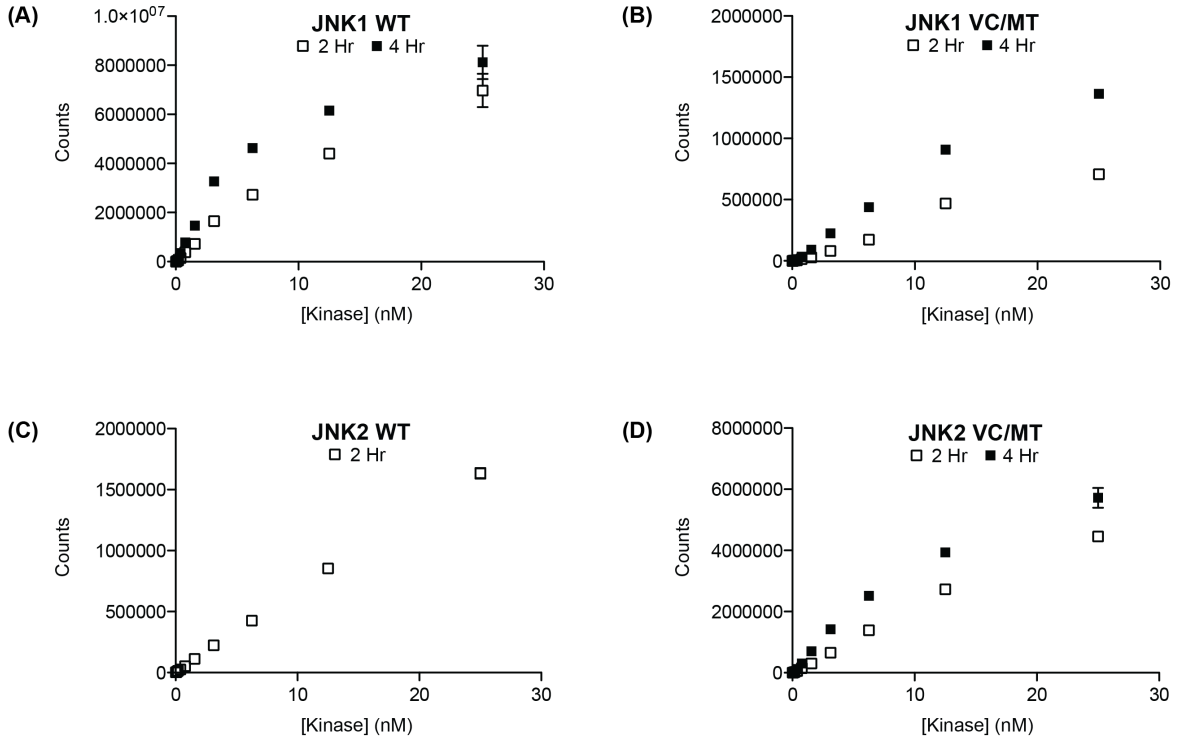

Figure 3.7. *[γ-^{32}P]ATP radioassays for recombinant JNKs, using Myelin Basic Protein as a substrate.* Enzyme titrations to determine the linear range of kinase activity for pre-activated JNKs were used to determine the JNK concentrations and incubation times used in the inhibition assays. (A) JNK1α1[WT] was linear at 3 nM (2 hr). (B) JNK1α1[V40C/M108T] was linear at 6 nM (4 hr). (C) JNK2α2[WT] was linear at 6 nM (2 hr). (D) JNK2α2[V40C/M108T] was linear at 0.5 nM (4 hr).

We then characterized the selectivity of drug-sensitized JNK mutants for our orthogonal, conformation-selective inhibitors over the wild-type kinases (data for JNK2α2 reported in Fang, *et al*.[25]). All inhibitors have IC_{50}s >30 μM for JNK1α1[WT] and IC_{50}s >10 μM for JNK2α2[WT] (**Figure 3.8**). We also determined that **3.1**, **3.2**, and **3.3** have IC_{50}s in the nM range for JNK1α1[V40C/M108T] and JNK2α2 [V40C/M108T]. Intriguingly, the DFG-out (Type II) inhibitor **3.2** was surprisingly potent against JNK2α2[V40C/M108T], with an IC_{50} of 6 ± 0 nM. The mutation of the methionine gatekeeper to a threonine likely makes it easier for both JNKs to adopt the DFG-out conformation, thereby enhancing the potency; however, it would be expected that the mutation would lead to a similar change in potency for both kinases, and thus we it seems an unlikely explanation for the preference.[74] Though we could not determine IC_{50}s for the orthogonal inhibitors against either WT JNK, we do see that even out to 30 μM of **3.2**, JNK1α1[WT] shows no significant inhibition; whereas JNK2α2[WT] shows 23 ± 9% inhibition at 10 μM **3.2**. Further, inhibition of WT JNKs showed that compound **2.5**, which is likely to stabilize a DFG-out confirmation, showed a strong preference for JNK2α1[WT] over JNK1α1[WT], with IC_{50}s of 0.99 ± 0.33 μM and 19 ± 5 μM, respectively (**Figure 2.1** and **Figure 3.2**).[10] These data indicate that there is likely a difference in allostery between JNK1 and JNK2 that makes it easier for JNK2 to adopt a DFG-out conformation. This would be interesting to further explore; especially given the advantage it could give if trying to selectively target JNK2 in disease.

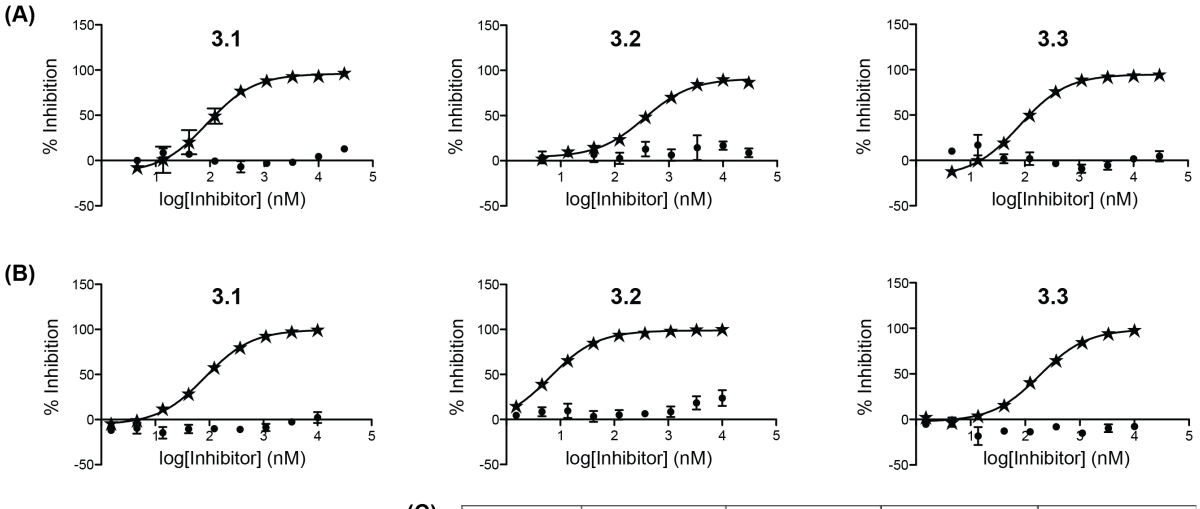

(C)

Kinase	Construct	IC50 3.1 (nM)	IC50 3.2 (nM)	IC50 3.3 (nM)
JNK1α1	V40C/M108T	84 ± 11	360 ± 45	96 ± 4
JNK1α1	WT	>30,000	>30,000	>30,000
JNK2α2	V40C/M108T	83 ± 4	6 ± 0	180 ± 14
JNK2α2	WT	>10,000	>10,000	>10,000

Figure 3.8. *[γ-^{32}P]ATP Inhibition assays for **3.1**, **3.2**, and **3.3** against recombinant JNKs, using Myelin Basic Protein as a substrate.* (A) Inhibitors were assayed against JNK1α1[V40C/M108T] (6 nM) for 4 hr and JNK1α1[WT] (3 nM) for 2 hr. (B) Inhibitors were assayed against JNK2α2[V40C/M108T] (0.5 nM) for 4 hr and JNK2α2[WT] (6 nM) for 2 hr. (C) IC_{50} values reported as mean ± SEM (n = 3).

In Fang, *et al*., the orthogonal, conformation-selective inhibitors of drug-sensitized kinases were derivatized at the solvent exposed position with a *trans*-cyclooctene (TCO) handle, which could then be used to enrich the protein targets from cell lysates via conjugation to a tetrazine bead (**Figure 3.9A**).[25] This technique allows protein complexes that are enriched or reduced by the conformation-selective ligands to then be assessed by techniques such as proteomics or western blotting. HEK293 T-REx Flp-In cell lysate, containing recombinant JNK2α2[WT] or JNK2α2[V40C/M108T] (inhibitor sensitized) was used to test the ability of the TCO-inhibitors to pull the intended target -JNK2α2[V40C/M108T]- out of cell lysate, while showing negligible interaction with the WT kinase (**Figure 3.9B**).[25]

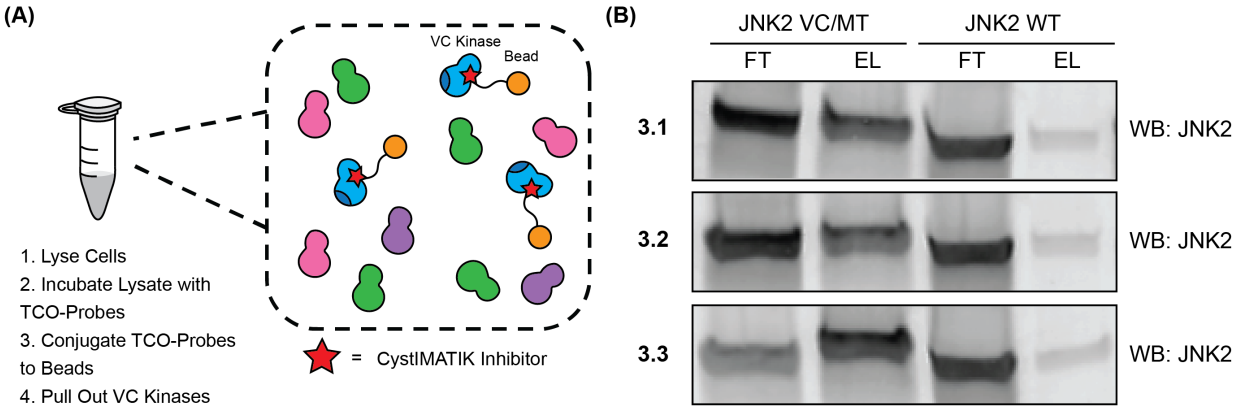

Figure 3.9. *TCO-inhibitors selectively enrich drug-sensitized JNK2α2 V40C/M108T from HEK293T T-REx cell lysates.*[25] (A) HEK293 T-REx cell lysate containing either JNK2α2[V40C/M108T] or JNK2α2[WT] were treated with 10 μM TCO-inhibitors. Lysate was then incubated with tetrazine-beads to enrich the TCO-inhibitor bound targets. The flow through (FT) was aspirated from the beads and the beads were washed. Captured proteins were eluted (EL) under reducing and denaturing conditions. (B) JNK2 was detected by WB.

HEK293 T-REx Flp-In stable cells expressing doxycycline-inducible, inhibitor-sensitized JNK1α1[V40C/M108T] or JNK2α2[V40C/M108T] were created to test orthogonal inhibitors in vivo.[25] Control lines expressing WT JNKs were also created. Before creation of the stable cell, the JNK constructs in pcDNA5 FRT/TO were validated via transient transfection (**Figure 3.10A**). HEK293 T-REx Flp-In cells stably expressing doxycycline-inducible JNK constructs were then created and confirmed by Western blotting (WB) (**Figure 3.10B**).

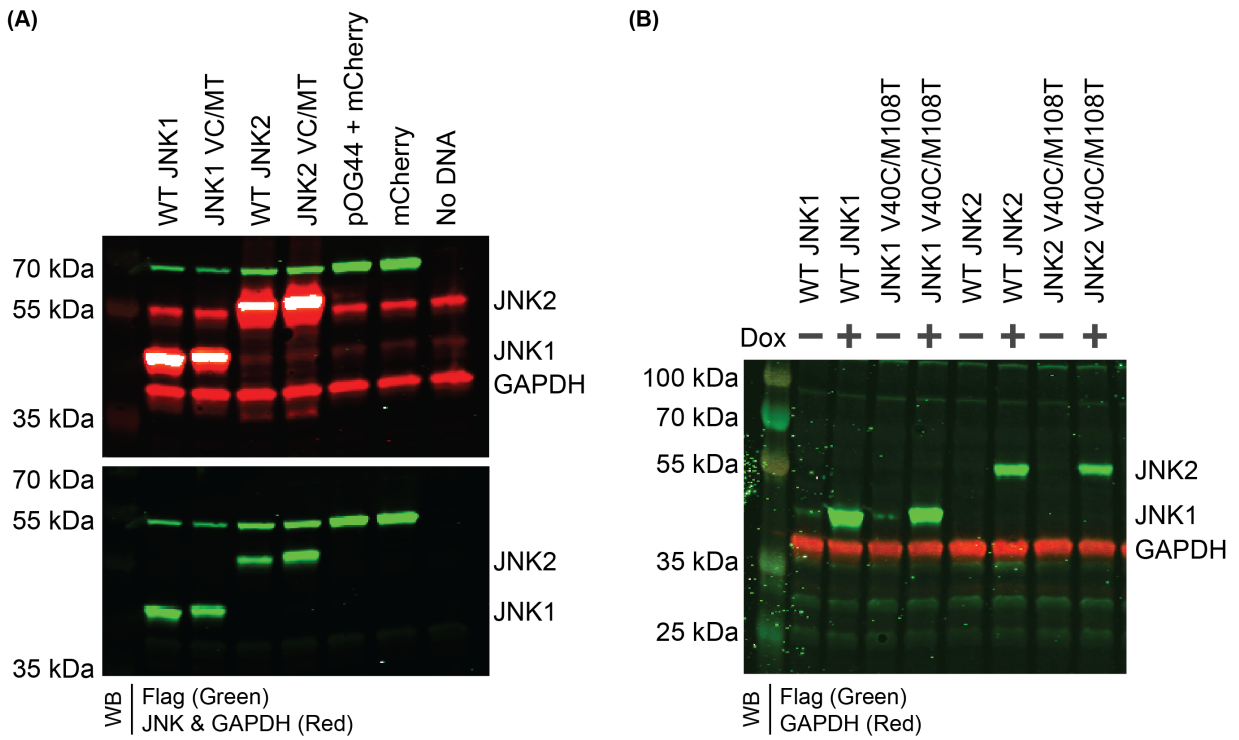

Figure 3.10. *Generation of HEK293 T-REx Flp-In cells expressing WT or V40C/M108T JNK1α1 or JNK2α2.* (A) Validation of JNK pcDNA5 FRT/TO constructs via transiently expression (+1 ug/mL doxycycline). Expression of Flag-tagged JNKs was confirmed by WB for Flag, JNK, and GAPDH. (B). HEK293 T-REx Flp-In cells stably expressing doxycycline inducible JNK constructs were confirmed by WB for Flag and GAPDH.

In the future, it would be interesting to further use these TCO-inhibitor probes to assess how JNK conformation affects its binding partners in cells. To tune effects that the inhibitors have on JNK binding partners in cells, different allosteric inhibitors of JNKs may need to be functionalized with the reversible-covalent Michael type acceptor seen in the general probes **3.1**, **3.2**, and **3.3**. Initial experiments could be completed in HEK293 cells, however, it would also be interesting to test in a cell line that has higher levels of endogenous JIP, as the inhibitor effects will likely vary across cell lines with different JIP and JNK expression profiles.

Additionally, these tools could be used in numerous ways to further study specific aspects of JNK biology, specifically their cellular localization, which has been shown to influence JNK

activation.[75] It would be exciting to use the tools in tandem with those in Chapter 4, where we present a methodology that allows modified ATP-competitive inhibitors to be tethered to localized protein domains via SNAP-tag. It would be interesting to study localized JNK -or other MAPK- biology using localized, SNAP-tethered **3.1**, **3.2**, and **3.3**. In essence, this would allow these orthogonal, conformation-selective inhibitors to be directed to specific sub-cellular locations, where effects on discrete populations of JNKs could be observed.

3.6 Using Phos-tag SDS-PAGE to Measure Activation of JNKs in Cells

JNK activation is an important readout for determining how inhibitors or other perturbations affect JNK behavior both in vitro and in vivo. In Chapter 2, we used Phos-tag SDS-PAGE to measure the activation of JNK1α1 in vitro.[10] Here, we use Phos-tag SDS-PAGE to measure JNK activation in HEK239 T-REx cells expressing doxycycline-inducible JNK1α1[V40C/M108T] or JNK2α2[V40C/M108T], following exposure to either anisomycin or TNFα (**Figure 3.11**). In future experiments using orthogonal inhibitors, the WT cell lines should be used as a control, in addition to those without stimulus.

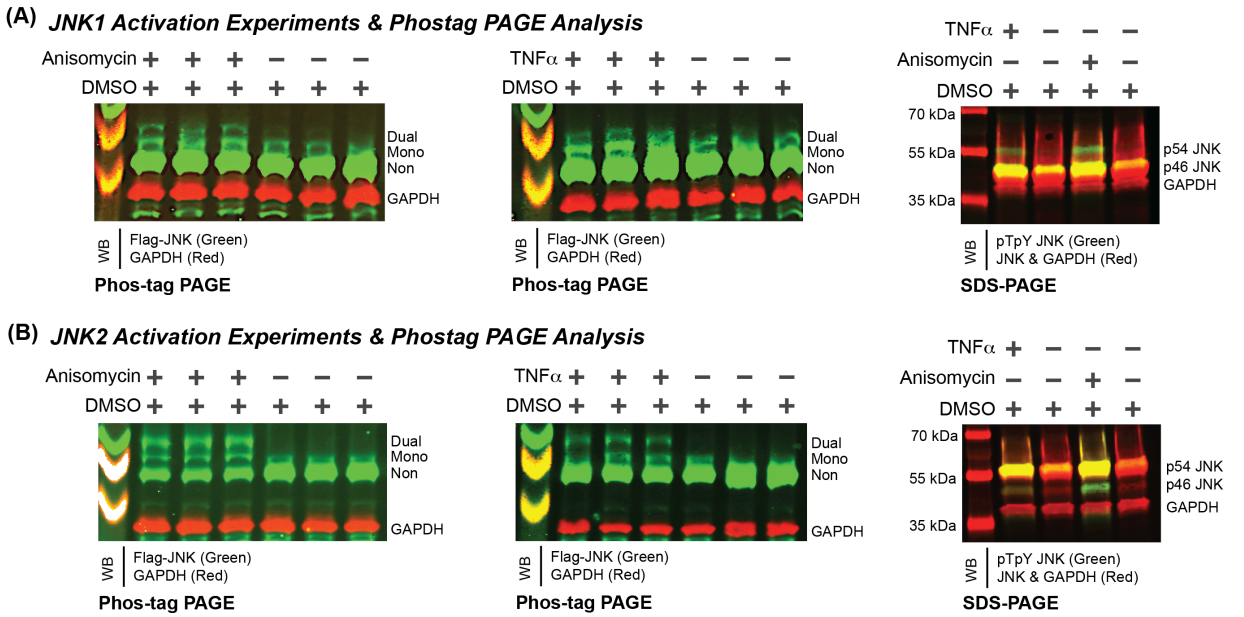

Figure 3.11. *Using Phos-tag SDS-PAGE to measure the activation of JNKs in HEK239 T-REx cells expressing Flag-JNK1α1[V40C/M108T] and Flag-JNK2α2[V40C/M108T]*. (A) JNK1α1 expressing cells were activated with anisomycin (1 hr) or TNFα (20 min). Cell lysates were run on both SDS-PAGE and Phos-tag SDS-PAGE gels and activity was measured using WB. (B) As in (A), using JNK2α2 expressing cells.

3.7 Reconstitution of JNK-JIP Signaling Modules In Vitro

The core of most JNK signaling modules, like other MAPKs (Erk and p38), consists of a MAP3K, a MAP2K (MKK), and a MAPK (JNK), where each kinase phosphorylates and activates the next, where the then activated JNK can go on to phosphorylate cellular substrates.[48] JIP scaffolds have been shown to bind all three components of the JNK activation modules, as well as enhance activation of JNKs in vivo (**Figure 3.12**). However, the mechanism by which JIPs are able to perpetuate JNK activity in unknown. It has been hypothesized for JIPs, like for other scaffolds, that they may function by "tethering" scaffolded components in close proximity or an ideal orientation for efficient activation. JIP1 has been shown to interact directly with several MAP3Ks, MKK7, and JNK1/2/3. It is important to note that JIP1, the focus of our work, does not

scaffold MKK4, thus we reasoned that their activation of JNKs may be differentially affected by this scaffold. JIP2 also interacts with MKK7, but not MKK4; however, JIP3 has been shown to scaffold both MKKs.

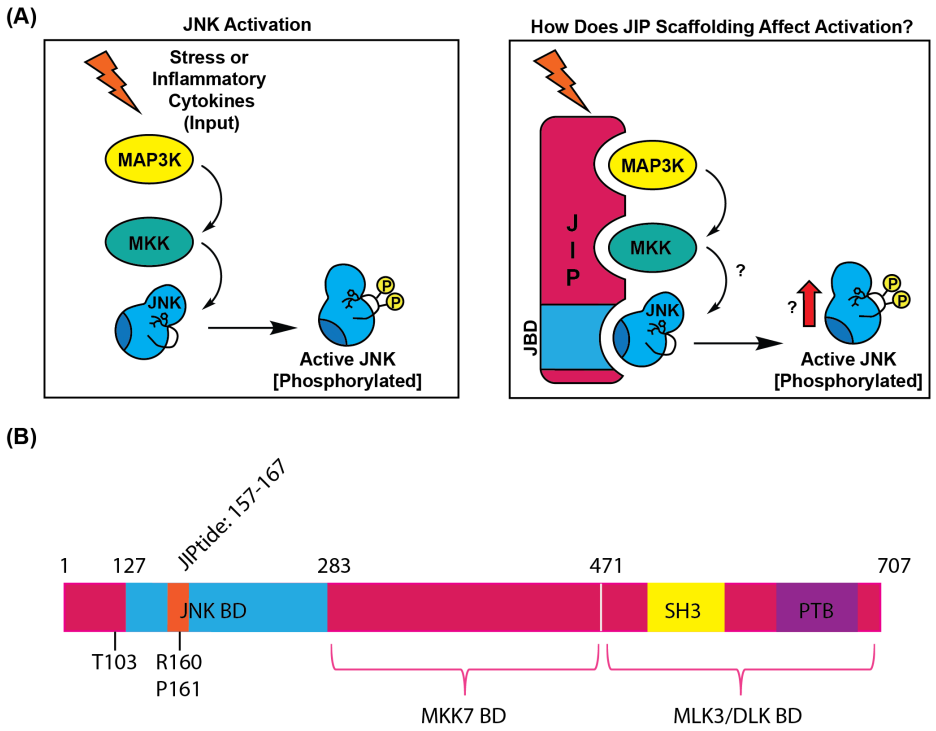

Figure 3.12. *How does JIP scaffolding affect JNK activation?* (A) JNK activation is preceded by a MAP3K activating MKK7, which can then phosphorylate JNK. JIP1 has been shown to potentiate JNK activation in vivo, though it is unclear how it does this. (B) Schematic showing JIP1b's domains.

Though JIP may potentiate JNK activation using multiple mechanisms, we were most interested in exploring JIPs role in facilitating the activation of JNKs by their upstream MKKs, MKK4 and MKK7. Published data shows that mutations in any one of MKK7's three D-domains prevented JNK-MKK7 binding by ~50-70%, and mutations in D1 and D2 prevented JNK activation.[44] Peptides containing minimal D-domains of MKK7, MKK4 and JIP1 also prevented MKK7 binding. Further, structures show the minimal JBD (D-domain) of both JIP1 and MKK7 overlapping with JNK1's DRS (PDB: JNK/JIPtide, 4E73; JNK/MKK7tide, 4UX9) (**Figure**

3.13A). These data indicate that MKK binding to JNKs' DRSs should be necessary for activation. Furthermore, JIPs and MKKs should compete for binding to JNK DRSs, as do JNK substrates.[47] We were curious to understand more about JNK-JIP1 signaling module dynamics, as competing for binding with an activator seemed inconsistent with the ability of JIP1 to potentiate JNK activation. It would seem inefficient, though not impossible, for a JNK to first bind to a JIP, dissociate, and re-bind to an MKK for phosphorylation. Therefore, we suspected that JIPs may be able to compensate for the inability of MKKs to reach the DRS of the JNKs while they are both simultaneously bound to JIP.

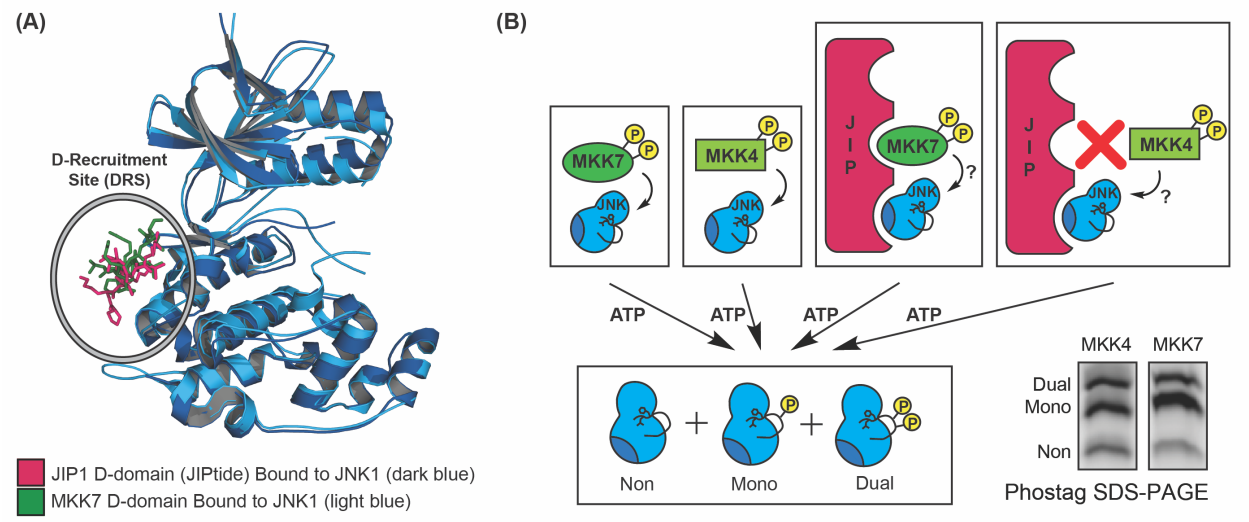

Figure 3.13. *JIPs and MKKs -Upstream activators of JNK-appear to compete for binding to JNK DRSs.* (A) JIPtide (the D-domain of JIP) and the D-domain of MKK7 both bind to JNK DRSs (B) Experimental design for testing how JIP1 binding to JNK affects MKK activation. MKK7, but not MKK4, associates with JIP1.[48]

To explore this, we designed reconstitution experiments that can measure activation of recombinant JNK1α1 by MKK4β or MKK7β1 in the presence or absence of JIP1b or a JIP1b variant (**Figure 3.13B**). We used MKKs that have been expressed in their active form by co-expression with MAP3K1, so that we could focus on perturbations to a single activation step. Following activation of the JNKs under the varying conditions, their phospho-forms were resolved

using Phos-tag SDS PAGE and relative amounts of phosphorylation were observed.

Though we later conducted experiments with full-length JIP1b, we were first curious how JIPtide itself would affect JNK activation by MKKs (**Figure 3.14A**). We activated JNK1α1 in the presence or absence of 20 μM JIPtide (>95% JIPtide-bound JNK1α1). Effects from JIPtide were observed for mono and dual phosphorylation events, under MKK concentration regimes that were linear for production of either species (**Figure 3.14B**). Under low MKK concentration regimes, the production of the mono-phosphorylated species was linear and high concentration regimes were linear in dual phosphorylation. To rule out any possible artifacts induced by a high concentration of peptide in the activation reactions, "no JIPtide" reactions contained a JIPtide variant with two point-mutations, which prevent binding to JNK.[53, 76] Our first experiments showed that JIPtide, but not mutant JIPtide, significantly inhibited both mono and dual phosphorylation of JNK1α1 by MKKs. This supports the idea that they bind competitively, and also that MKKs need to bind to JNKs' DRSs for activation.

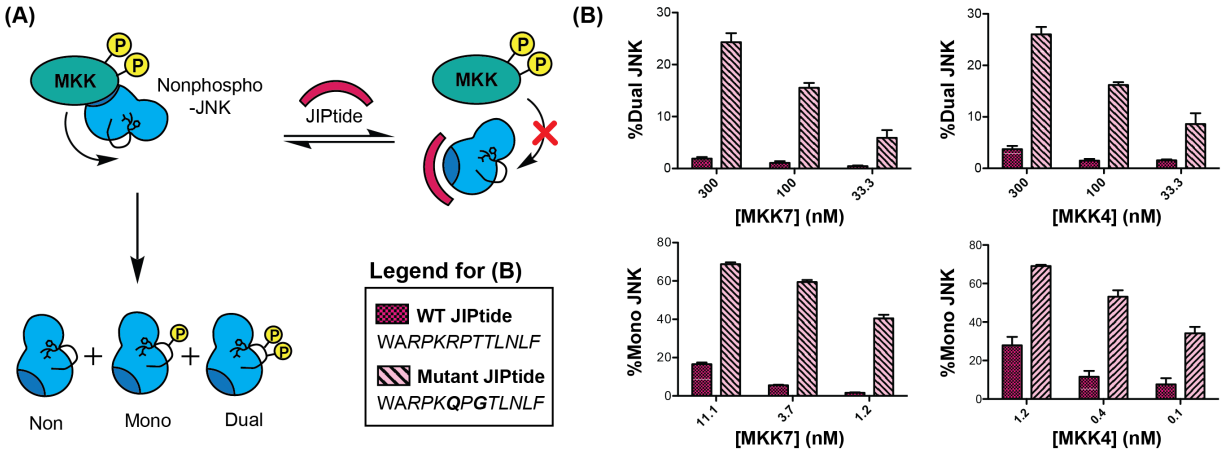

Figure 3.14. *JIPtide inhibits MKK activation of JNK1α1.* (A) Schematic showing the model of JIPtide competing with MKKs for JNK binding, and thus, preventing JNK activation. (B) JNK1α1 was activated in the presence or "absence" of JIPtide and its phosphorylation by MKK4β or MKK7β1 was measured by Phos-tag SDS-PAGE. Samples

mimicking "no JIPtide" contained a double mutant JIPtide that does not bind to JNK (K_D > 32 μM).[53, 76]

JIPtide's inhibition of both MKK7 and MKK4 activation of JNK1α1 convinced us that to fully understand the signaling dynamics of this module, we would need to reconstitute this system with full-length JIP1. Since phosphorylation is thought to be important for JIP1's regulation, we opted to express and purify full-length JIP1b and several JIP1b variants in *E. coli*, rather than in mammalian cells or *Drosophila*, allowing us to isolate non-phosphorylated constructs (**Figure 3.15**).[76]

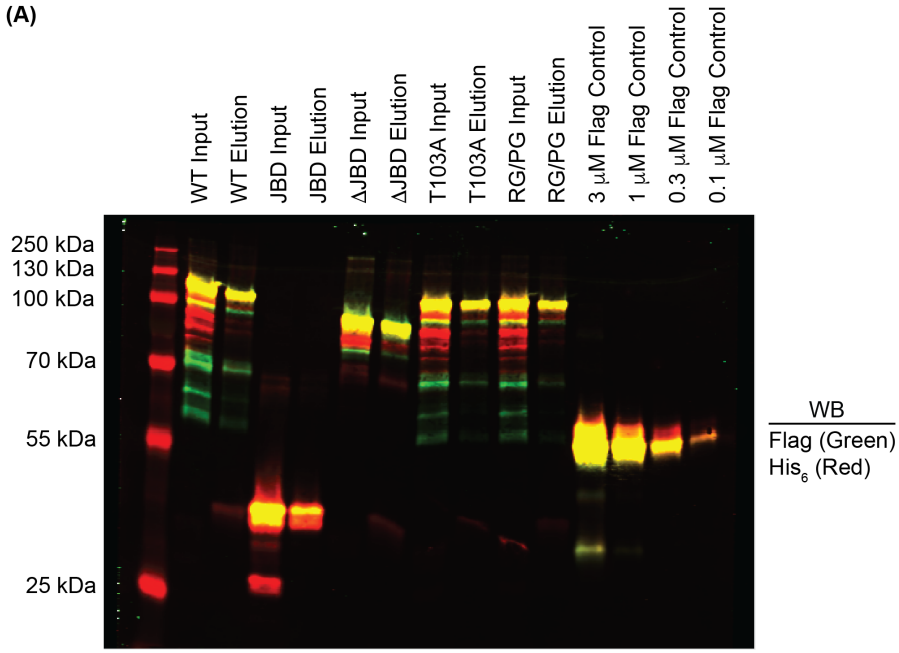

Figure 3.15. *Purification of recombinant, full-length Flag-JIP1b-His$_6$ and Flag-JIP1b-His$_6$ variants from E. coli.* (A) WB showing Ni-NTA purified recombinant Flag-JIP-His$_6$ variants (input) and the final Anti-Flag purified products (elution). Proteins were quantified using Flag-tagged standard (control) proteins, which had been previously quantified using a Bradford assay.

In our preliminary experiments with full-length JIP1b or a JIP1b variant, we again chose to use pre-activated MKKs, allowing us to focus on modulating one activation step at a time. Since activations were conducted using JIP1b constructs bound to M2 Anti-Flag magnetic beads, we used a Flag-Grb2 construct that that does not bind to JNK as a control for activation of "free" JNK. Following activations, JNK1α1 phospho-forms were resolved using Phos-tag SDS-PAGE and detected by WB. Our initial reconstitution experiments were designed with a single concentration of each module component. MKK concentrations (1 μM) in excess of JNK1α1 (200 nM) were used to minimize any dilution effects from JNK binding to JIP1b (0.6 μM) that does not contain MKK7β1. Under these conditions, we are under a dual activation regime and observe effects solely to dual phosphorylation. In the future, however, experiments in the linear range for either mono or dual phosphorylation of different amounts of JNK will likely need to be conducted in the presence of variable amounts of JIP1b or JIP1b variants. This will allow us to find concentration regimes that are able to more closely mimic the biological concentrations of these components. This will allow us to be more confident that our results are biologically relevant.

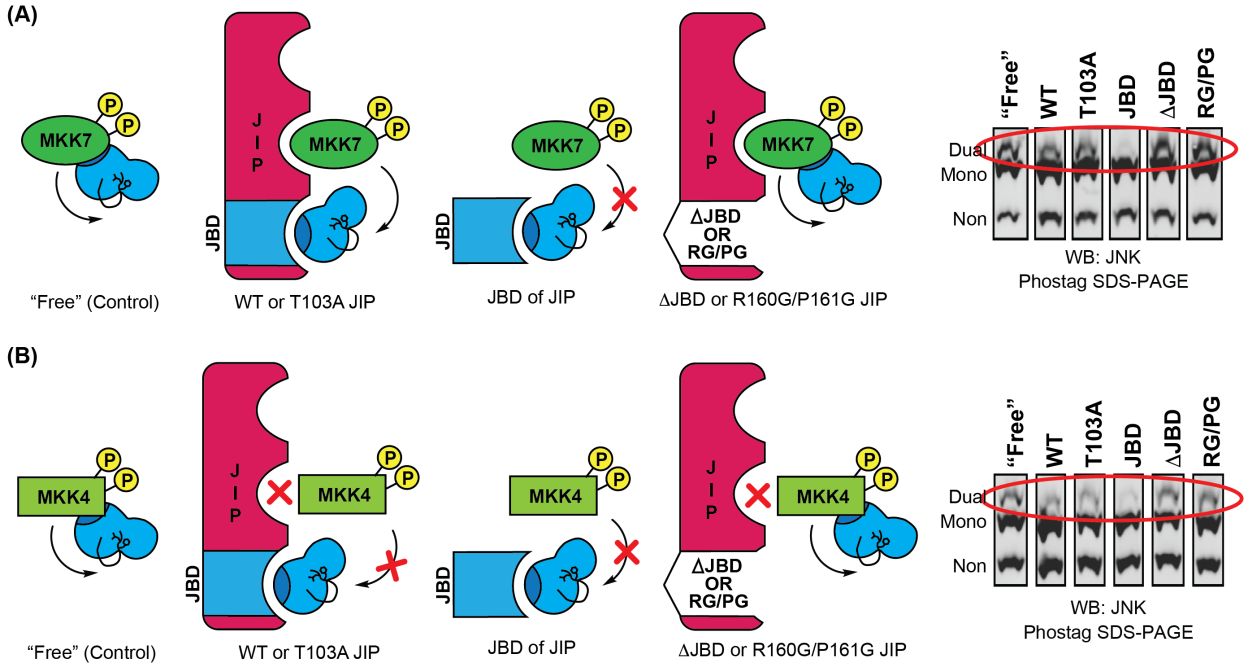

Figure 3.16 *Reconstitution experiments using pre-activated MKKs, JNK1α1, and a JIP construct.* (A) JNK1α1 (200 nM) was activated with 1 μM MKK7β1 in the presence of 0.6 μM of each Flag-JIP1b variant or Flag-Grb2 (control scaffold) bound to M2 Anti-Flag magnetic beads. All proteins were eluted using 1 mg/mL 3X flag peptide and JNK1α1 phospho-forms were separated by Phostag SDS-PAGE and detected by WB for total JNK. (B) was performed as described in (A), except JNK1α1 (200 nM) was activated with 1 μM MKK4β.

Our experiments looking at how JIP1b variants modulated dual phosphorylation of JNK1α1, showed that the JNK binding domain (JBD) of JIP1b alone inhibited both MKK4β and MKK7β1 when compared to activation in the absence of JIP1b (Grb2 control) (**Figure 3.16**). This is consistent with our data showing JIPtide also inhibits both MKKs. Both MKKs seemed to be unaffected by the JIP1b **Δ**JBD and JIP1b R160G/P161G constructs, which do not bind to JNK.[76] These data together provide further evidence that JIPs compete with MKKs for JNK binding–as predicted based on the crystal structures–and that MKKs apparently need to interact with the DRSs of JNKs to activate them. Consistently, WT JIP1b, as well as the T103A non-phosphorylatable

mutant, decreased MKK4β dual activation of JNK1α1 by ~50%–based on two replicate experiments. Intriguingly, neither WT JIP1b nor the T103A mutant had a significant impact on MKK7β1's activation of JNK1α1.

As suggested by JIPtide's inhibition of MKK4/7, MKKs need to associate with the DRSs of JNKs to phosphorylate the activation loops of JNKs. However, these data seem to indicate that full-length JIP1 has a mechanism to compensate for MKK7's inability to bind to the DRSs of JNKs when JNKs are bound to JIP1. This allows MKK7 to phosphorylate JNKs while they are both bound to the scaffold. Since JIP1 is not known to scaffold MKK4, it is logical that the full-length Jip1 is inhibitory towards MKK4's phosphorylation of JNK1α1.[48]

It would be interesting to use a combination of our reconstituted scaffolding systems and conformation-selective inhibitors to further probe whether JIP1 binding to JNKs explicitly prevents MKK4 activation, while allowing activation by MKK7. Specifically, inhibitors that affect JNK-JIP1 binding but not activation by our MKKs would be useful in this pursuit (**Figure 3.17**). If JIP1 is indeed acting to facilitate JNK activation by MKK7, while preventing activation by MKK4, we would expect that an inhibitor that enhances the JNK-JIP1 interaction would maintain or enhance MKK7's activation while further disrupting MKK4's ability to activate JNKs. However, a JNK-JIP1 disruptor would likely increase MKK4's phosphorylation of JNKs.

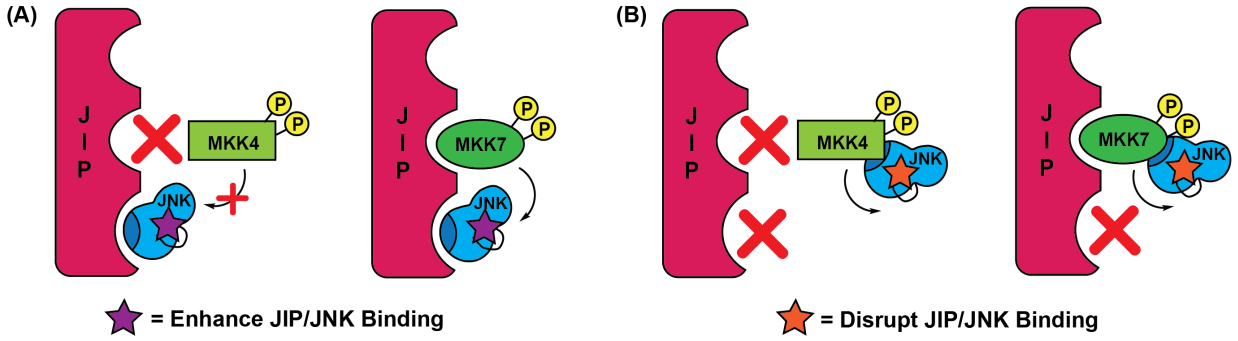

Figure 3.17. *Testing JIP1's ability to select between MKK4 and MKK7 activation of JNKs using ATP-competitive inhibitors.* (A) A molecule that solely has the effect of enhancing JNK-JIP1 binding should further prevent activation by MKK4, while enhancing or maintaining activation by MKK7. (B). A molecule that solely has the effect of disrupting JNK-JIP binding should allow both MKK4 and MKK7 to activate JNKs.

The specific reasons that it would be advantageous to have JIPs facilitate activation by one MKK over the other are not entirely clear. However, there are a number of possibilities. It seems possible that JIP could be functioning to enhance selectivity of downstream JNK activity and, thus, enable a specific output over another (**Figure 3.18**). Other scaffolds have been shown to allow similar MAPK pathway components to achieve desired outputs in response to specific, divergent inputs.[66, 77]

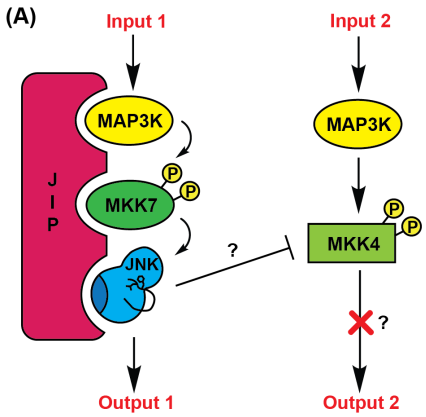

Figure 3.18. *Possible model for JIP1 regulation of JNK Signaling.* (A) JIP1 may allow MKK7 to phosphorylate the activation loops of JNKs while bound to the DRSs of JNKs, while inhibiting activation of JNKs by MKK4.

In our future studies, it would also be interesting to study T103A JIP1, a JNK phosphorylation mutant, which has been shown to only weakly potentiate JNK activation in vivo relative to WT JIP1.[76] However, within the context of our two-tiered reconstitution experiments, T103A behaved similarly to WT JIP1 (**Figure 3.16**). These data may indicate that phosphorylation of JIP1 at T103 does not affect JNK activation at the level of the MKK. Rather, it is consistent with evidence showing that this phosphorylation site is important for the release of certain MAP3Ks from JIP, such as DLK. DLK is scaffolded by JIP in an inactive state until JNK phosphorylates T103 of JIP1.[76] JNK's phosphorylation of T103 of JIP1 leads to the release of DLK, after which it can oligomerize and autophosphorylate. Due to this, the T103A JIP1 mutant is more likely to show significant differences relative WT JIP1 in three-tiered reconstitution experiments containing a MAP3K.

3.8 Determining JIP1 and JNK Concentrations in HEK293 T-REx Cells

We wanted to further explore the possible models that could be arrived at based on the in vitro JIP reconstitution experiments. A model where JIPs are functioning to enhance pathway specificity would be unreasonable if JIP concentrations are much less than the concentrations of JNKs due to the physical limitations of the components. To investigate which concentration regimes are biologically relevant, we conducted an analysis of the relative expression levels of JNK1, JNK2, and JIP1 proteins in HEK293 T-REx cells. We quantified the concentrations of JNK1, JNK2, and JIP1 in cell lysates by western blotting each pathway component, which were fitted to a standard curve of recombinant standards (**Figure 3.19**). We found that the concentration of JIP1 was ~14 nM in HEK293 T-REx cells. The p46 and p54 isoforms of JNK1 were ~78 nM and ~28 nM, respectively. JNK2 was approximated to have similar concentrations to JNK1, with ~50 nM of the p46 isoform and ~108 nM of the p54 isoform. Although these expression levels do

not specifically confirm or exclude any specific model, it is useful to know that the concentration of JIP1 in HEK293 T-REx cells is on a similar order of magnitude to both JNK1 and JNK2. It is especially striking given that HEK293 T-REx cells are expected to have low JIP1 expression levels relative to other cell lines. In the future, cell lines that have higher levels of endogenous JIP, such β-cells or neurons, should be tested.[48, 76]

The mechanism by which JIP functions, as well as the necessity for JIP activation of JNKs, could vary in different cells types. Depending on the specific cellular or sub-cellular concentrations of JIP1 and JNKs, it seems reasonable to speculate that JIP1 could essentially shield a significant amount of JNK from MKK4 in cells with higher levels of JIP1. This would allow the activation of the JIP1 scaffolded population of JNKs in response to a MKK7 activating stimuli but prevent it if MKK4 is activated. Since MKK7 is not known to have substrates other than JNK, whereas MKK4 is known to also activate the MAPK p38, it would make sense that the two pathways have a mechanism to prevent cross-talk, and that JNK would at times be shielded from MKK4.[60] Further, JIP1 is only one of many JNK scaffolds. This list also includes JIP2/3, JLP (JIP4), and WRD62, along with several others.[78] It seems possible that each is functioning to ensure the specificity of a certain population of JNKs, but further experimentation would be required to verify such a hypothesis.

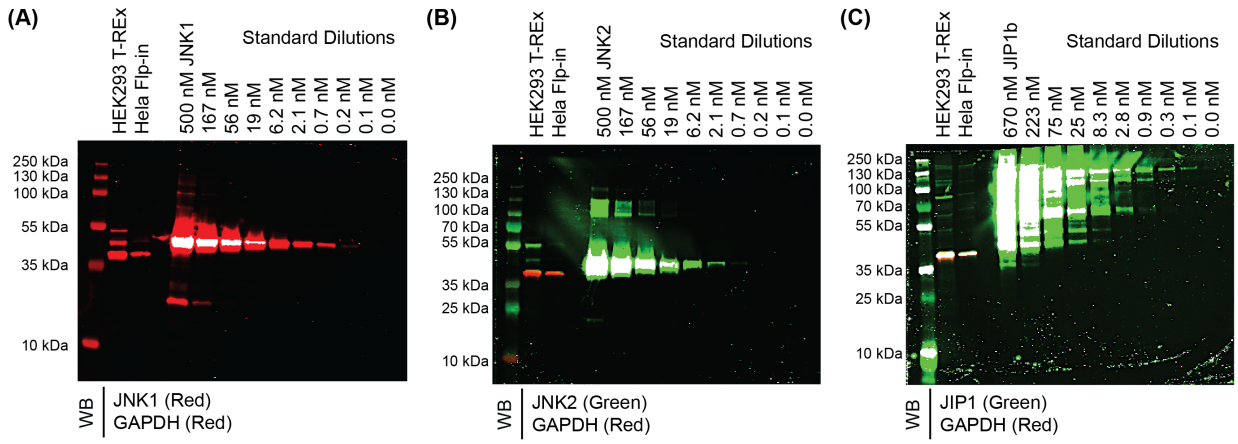

Figure 3.19. *Determination of JIP and JNK concentrations in HEK293 T-REx cells.* WB of recombinant protein standards and HEK293 T-REx cell lysate. A standard curve was made for each, which was used to approximate the concentration of the respective proteins in cells. (A) WB of recombinant JNK1α1 standards and HEK293 T-REx cell lysate. (B) WB of recombinant JNK2α2 standards and HEK293 T-REx cell lysate. (C) WB of recombinant JIP1b standards and HEK293 T-REx cell lysate.

3.9 Investigate the effects of JIP variants on JNK activation in vivo

In the future, the results from the preliminary (and any further) reconstitution experiments should be validated in cells. To this end, we created HEK293 T-REx Flp-In stable cells expressing doxycycline inducible full-length Flag-JIP1b and Flag-JIP1b variants. These cell lines will be a valuable tool for validating the in vitro reconstitutions. However, given that scaffolds are thought to have an ideal concentration regime to work under, the expression levels of JIP constructs may need to be optimized to prevent JNK module components from being significantly diluted, which would result in all JIP1b constructs appearing inhibitory. Mathematical modeling by Witzel, *et al.* suggests that the ideal scaffold concentration falls between the least and second least concentrated kinases in the module.[79]

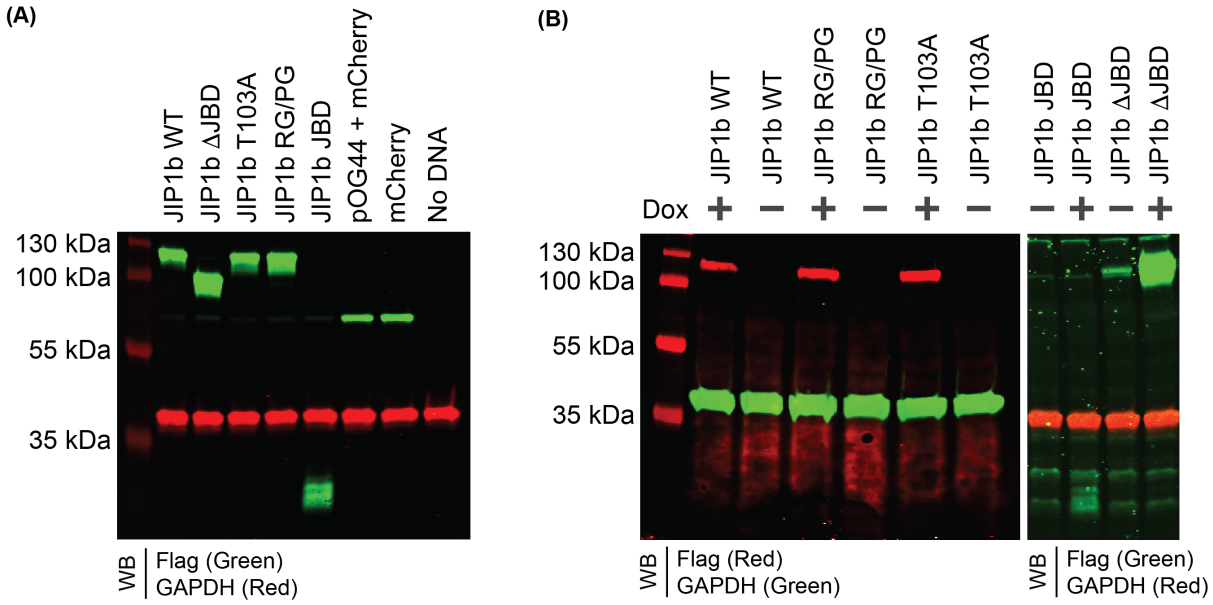

Figure 3.20. *Generation of HEK293 T-REx Flp-In cells expressing Flag-JIP1b WT or a Flag-JIP1b Variant.* (A) Validation of Flag-JIP1b constructs (+1 ug/mL doxycycline) via transient expression. Expression was measured by WB. (B). HEK293 T-REx Flp-In cells stably expressing doxycycline inducible JIP1b constructs.

3.10 Conclusions and Future Work

In Chapter 2, we found that allosteric, ATP-competitive inhibitors of the JNKs are able to differentially modulate binding of non-phosphorylated JNKs to JIPtide/JIP1b and the ability of JNKs to be activated by MKK4 or MKK7. Here, we show that activation of JNKs can further alter their allostery, where both JIPtide and JIP1b were able to prevent binding of specific inhibitors–but not others–to phosphorylated JNKs. This indicates that the scaffold state of JNKs in cells may affect the ability of activated JNKs to be targeted by certain inhibitors. Further, these data support the idea that JNKs undergo conformational changes upon phosphorylation of their activation loops. If allostery remained similar between the phosphorylated and non-phosphorylated JNKs, we would expect that enhancers of non-phospho-JNK/JIPtide interaction would bind more potently to activated JNKs in the presence of JIPtide, with the reverse being true for molecules that disrupt

the interaction. However, we did not find correlation between the effect the inhibitors had on non-phosphorylated JNKs and activated JNKs, suggesting that phosphorylation leads to conformational changes at or near the ATP-binding site, which are able to influence inhibitor binding.

In order to use ATP-competitive inhibitors as tools to study kinase biology in vivo, Ahler, *et al*. reported the design of mono-specific, conformation-selective inhibitors for kinases containing a valine to cysteine sensitizing mutation.[17] We have shown that these inhibitors have high selectivity for JNK1[V40C/M108T] and JNK2[V40C/M108T][25] over the wild-type kinases. These tools were also used to selectively enrich JNK2[V40C/M108T] from cell lysate.[25] In the future, these tools could be used to study JNK biology in the HEK293 T-REx Flp-In cells expressing either WT or V40C/M108T JNK1 or JNK2, where they essentially allow the inhibited kinase to function as a dominant-negative.

This work has also conducted preliminary experiments exploring how JIP1 scaffolding is able to affect JNK activation. Our data suggest that JIP1 scaffolding could be important in dictating which pathways are activated under certain conditions and not others, potentially providing a source of insulation that prevents inappropriate cross-talk between JNK or other MAPK pathways. It remains unclear however, how JIP1 may potentiate JNK activation in vivo, and we hope future studies can more thoroughly investigate this phenomenon, as well as the ability of JIPs to mediate signaling selectivity. Due to JNKs' participation in many critical signaling pathways, misregulation of JNKs can lead to cancer, insulin resistance, neurodegeneration and the development of several autoimmune conditions.[32] It is thus advantageous to carefully characterize the many levels of JNK regulation so that alternative methods of exerting control over misregulated JNK signaling systems can later be exploited in disease treatment.

3.11 MATERIALS AND METHODS

Cloning and mutagenesis. Bacterial expression plasmids containing genes encoding His_6-JNK1α1[WT], His_6-JNK2α1[WT], His_6-JNK2α2[WT], His_6-SUMO-MKK4β, His_6-SUMO-MKK7β1, Flag-JIP1b-His_6[WT], Flag-JIP1b-His_6[JBD] (residues 127-282), Flag-JIP1b-His_6[ΔJBD] (residues 1-126/283-707), Flag-JIP1b-His_6[T103A], Flag-JIP1b-His_6[R160G/P161G], and His_6–Ulp1 in pMCSG7 vectors were created as in Lombard *et al*., using Gibson assembly.[10, 64] Sequences for His_6-JNK1α1[WT], His_6-JNK2α1[WT], His_6-SUMO-MKK4β, His_6-SUMO-MKK7β1, Flag-JIP1b-His_6[WT] and His_6–Ulp1 were reported in Lombard *et al.* and **Table 2.2**.[10] His_6-JNK1α1[V40C/M108T] and His_6-JNK2α2[V40C/M108T] in pMCSG7 were created using Quikchange (Agilent). Mammalian expression plasmids (pcDNA5/FRT/TO) containing genes encoding Flag-JNK1α1[WT], Flag-JNK1α1[V40C/M108T], Flag-JNK2α2[WT], Flag-JNK2α2[V40C/M108T], Flag-JIP1b-His_6[WT], Flag-JIP1b-His_6[JBD] (residues 127-282), Flag-JIP1b-His_6[ΔJBD] (residues 1-126/283-707), Flag-JIP1b-His_6[T103A], and Flag-JIP1b-His_6[R160G/P161G] were created using Gibson assembly.[10, 64] All genes in pcDNA5/FRT/TO vectors contained a Kozak sequence at the start of the gene. The genes for MKK4β, MKK7β1, Flag-JNK2α2, and Flag-JIP1b[WT] were obtained as gifts from Roger Davis and were provided in pcDNA3 (Addgene plasmid #s MKK4β: 15517; MKK7β1: 14622; Flag-JNK2α2: 13755; Flag-JIP1b: 52123). His_6–GST–MAP3K1 and His_6-MKK4α were provided by Hari, *et al.* in bacterial expression vectors.[65] Uniprot IDs, DNA, and protein sequences for constructs not reported in **Table 2.2** are provided in **Table 3.2**.

Protein expression and purification. His_6-JNK1α1[WT], His_6-JNK2α1[WT], His_6-JNK2α2[WT], His_6-JNK2α2[V40C/M108T], His_6-MKK4α (active), His_6-SUMO-MKK4β (phosphorylated), His_6-SUMO-MKK7β1 (active), His_6–MAP3K1 (active), Flag-JIP1b-His_6[WT],

Flag-JIP1b-His_6[JBD], Flag-JIP1b-His_6[ΔJBD], Flag-JIP1b-His_6[T103A], Flag-JIP1b-His_6[R160G/P161G], and His_6–Ulp1 were expressed and purified as in Lombard, *et al*. JIP1b variants were purified using the JIP1b[WT] purification protocol in Lombard *et al*.[10]

Instrumentation. TR-FRET assays were conducted using 384 well plates and detected using a PerkinElmer Envision 2104 Multi-label Reader. Radioassays were imaged on a Typhoon FL 9000 (GE Healthcare). WBs were imaged on a LiCor Odyssey gel image scanner using both 680 nm and 780 nm channels.

TR-FRET based activity assays for JNK1α1 and JNK2α1 (± JIPtide or full-length JIP1b; IC_{50}s for apo-JNKs were reported in Lombard, *et al*.).[10] JNKs were activated using phospho-MKK4α. 900 nM JNK1α1 or 2.7 μM JNK2α1 were pre-activated with 150 nM MKK4α and 400 μM ATP for 1 hr, at RT, in buffer (50 mM Tris/HCl (pH 7.5), 0.01% (v/v) Tween 20, 10 mM $MgCl_2$, 2 mM DTT, 1 mM EGTA, 0.1 mg/mL BSA). Activated JNKs were tested using a Lance Ultra TR-FRET assay (Perkin Elmer). Enzyme titrations under the following assay conditions were carried out to determine the linear working range of JNK1α1 and JNK2α1 prior to running inhibition assays. To test for inhibition, serial dilutions (1:3) of compounds in DMSO (4% v/v final in assay) were prepared at a 750 μM starting concentration (diluted to 30 μM final in the assay). Compounds and ATP were pre-incubated with 15 nM JNKs (± 10 μM JIPtide for JNK1α1; ± 25 μM JIPtide for JNK2α1) in buffer (50 mM Tris/HCl (pH 7.5), 0.01% (v/v) Tween 20, 10 mM $MgCl_2$, 2 mM DTT, 1 mM EGTA, 0.1 mg/mL BSA). Inhibition of JNK1α1 by compounds **2.1**-**2.9** was measured in the presence of 100 μM ATP and inhibition by compound **2.10** was measured in the presence of 1 mM ATP. Inhibition of JNK2α1 by **2.1**-**2.10** was measured in the presence of 100 μM ATP. Inhibition of JNK1α1 by compounds **2.2** (100 μM ATP) and **2.10** (1 mM ATP) was tested ± 380 nM JIP1b. To initiate the reactions, ulight-labeled myelin basic peptide (ulight-

MBPtide) was added (300 nM for JNK1α1 and 150 nM for JNK2α1). The reaction mixtures were incubated in a volume of 15 µL per well (white, 384-well plate, 20 µL, Corning), at RT for 4 hr, then quenched with 2.5 µL 80 mM EDTA (10 mM final) in modified Lance Detect Buffer (LDB; 40 mM Tris-HCl (pH 7.5) and 100 mM NaCl). After a 5 min incubation with the quench reagents, 2.5 µL of 4 nM europium labeled Anti-phospho-MBPtide (0.5 nM final) was added in LDB (V_T = 20 µL). After a 1 hr incubation, the plates were read on an Envision Multi-label Reader. TR-FRET was determined using an excitation wavelength of 320 nm and emission wavelengths of 615 nm (Eu^{3+}) and 665 nm (ulight-MBPtide). Relative amounts of activity were calculated using the ratio of 665 nm light to 615 nm light. IC_{50} values were determined using GraphPad Prism's "One-site fit logIC_{50}" option and reported as IC_{50} ± SEM (*n=3*).

JNK1α1 and JNK2α2 radioassays. JNK2α2 inhibition assays for the reversible-covalent inhibitors (**3.1**, **3.2**, and **3.3**) were reported in Fang, *et al*. (compounds reported as **3.1** = **1**, **3.2** = **3**, **3.3** = **2**).[25] JNK1α1 inhibition assays were conducted using a method modified from the JNK2α2 assays in Fang, *et al*.[25] Briefly, 2.5 µM JNK1α1 was pre-activated with 150 nM MKK4α and 400 µM ATP for 1 hr, at RT, in assay buffer (50 mM Tris/HCl (pH 7.5), 0.01% (v/v) Tween 20, 10 mM $MgCl_2$, 0.1 mM DTT, 1 mM EGTA, 0.1 mg/mL BSA). Enzyme titrations were carried out to determine the linear working range of JNK1α1[WT] (3 nM) and JNK1α1[V40C/M108T] (6.25 nM). JNKs were incubated with inhibitors (initial concentration = 30 µM, 3-fold serial dilutions, 9 data points), 4 µM cold ATP, and 0.007 µCi/uL [γ-^{32}P]ATP for 30 mins. Myelin basic protein (MBP) was then added, at a final concentration of 0.2 mg/mL (V_T = 30.2 µL). Reactions were incubated at RT (2 hr for WT and 4 hr for V40C/M108T). 4.6 µl of the reactions were spotted onto phosphocellulose membranes (Reaction Biology), which were then washed 3X with 0.5% phosphoric acid and dried with acetone. Membranes were exposed overnight to a phosphorscreen,

which was then imaged on a Typhoon FL 9000. IC_{50} values were determined using GraphPad Prism's "One-site fit logIC_{50}" option and reported as IC_{50} ± SEM (*n=3*).

JNK2 pull-downs with CystIMATIK probes. Pull-downs with recombinant JNK2α2[WT] and JNK2α2[V40C/M108T] in HEK293 T-REx Flp-In cell lysate using CystIMATIK probes (TCO-conjugated **3.1**, **3.2**, and **3.3**), were conducted by Linglan Fang in the Maly lab, and were reported in Fang, *et al*.[25]

Activation of JNK1α1 by MKK4β/MKK7β1 +/- JIPtide. JNK1α1 activations used a method modified from Lombard, *et al*.[10] JNK1α1 activation reactions (60 µL) were carried out in buffer (50 mM Tris/HCl (pH 7.5), 0.01% (v/v) Tween 20, 10 mM $MgCl_2$, and 0.1 mg/mL BSA) and contained 200 nM JNK1α1, 400 µM ATP, 4% DMSO (v/v), 20 µM of either WT (WARPKRPTTLNLF) or Mutant JIPtide (WARPK**Q**P**G**TLNLF), and a varying concentration of either MKK4β or MKK7β1. There was a 30 min pre-incubation of JNK1α1 and JIPtide before starting the activations by addition of MKKs. The reactions proceeded for 1 hr at RT. JNK1α1 phospho-forms were separated using Phos-tag SDS-PAGE as in Lombard, *et al*.[10] and detected by WB for total JNK (Anti-JNK, Santa Cruz #sc-7345) (*n=3*).

JIP1b reconstitution experiments. Each reaction (V_T = 120 µL) contained 0.6 µM of Flag-JIP1b, a Flag-JIP1b variant, or Flag-Grb2(dead)-SNAP (control scaffold), bound to 20 µL of M2 Anti-Flag magnetic beads (Sigma). Flag-constructs were first allowed to bind to the beads at 4 °C for 1 hr, with rotation. Beads were washed 2X with 5 CV of TBS (50 mM Tris, pH 7.5; 150 mM NaCl). Activation of 200 nM JNK1α1 (in the presence of a Bead-bound Flag construct) by 1 uM of either MKK4β or MKK7β1 (1 mM ATP) was carried out in assay buffer (50 mM Tris/HCl (pH 7.5), 150 mM NaCl, 0.01% (v/v) Tween 20, 10 mM $MgCl_2$, and 0.1 mg/mL BSA). Reactions also included 1 mg/mL 3X Flag Peptide (MDYKDHDGDYKDHDIDYKDDDDK), such that both apo-JNK and

scaffold-bound JNK could be isolated from the samples immediately following a 1 hr (RT) reaction. Reactions were quenched by adding 3X loading dye (240 mM Tris-HCl (pH 6.8), 16% BME (v/v), 6% SDS (wt/v), 0.06% bromophenol blue (wt/v), and 30% glycerol (v/v)). Samples were run on both SDS-PAGE and Phos-tag SDS-PAGE gels. Phos-tag SDS-PAGE gels allowed the JNK1α1 phospho-forms to be separated as in Lombard, *et al*. and they were detected by WB for total JNK (Anti-JNK, Santa Cruz #sc-7345).[10]

Creation of stable HEK293 T-REx Flp-In cell lines. HEK293 T-REx Flp-In cells (Thermo Fisher) were used to generate cells expressing doxycycline-inducible Flag-JNK1α1[WT], Flag-JNK2α2[WT], Flag-JNK1α1[V40C/M108T], Flag-JNK2α2[V40C/M108T][25], Flag-JIP1b[WT], Flag-JIP1b[JBD], Flag-JIP1b[ΔJBD], Flag-JIP1b[T103A], or Flag-JIP1b[R160G/P161G]. Early passage cells were chosen for creation of the stables. Cells were woken up in complete media (DMEM + 10% FBS) and passaged 2-3 times, until normal growth was achieved. On day 1 of the stable generation process, 3 mL of cells were plated at a density of 2.5 * 10^5 cells/mL in 6-well plates. The next day, if cells were ~60% confluent, the cells were transfected with the Flag-tagged constructs, pOG44 (a Flp recombinase), and mCherry (a transfection control). To transfect the cells, the media was first removed and replaced (2 mL). The transfection mixtures were then prepared, each containing 250 uL serum (FBS) free DMEM, 2 ug DNA (900 ng pcDNA5-FRT-TO construct, 900 ng pOG44 vector, and 200 ng mCherry control vector), and 6 uL Turbofectin 8.0 (1 μg of DNA: 3 μL of Turbofectin). The DMEM and DNA were first mixed and then the Turbofectin was added. The mixtures were allowed to sit at RT for 15 min, after which they were added to the cells dropwise. The plates were rocked gently to mix. Cells were incubated for 24 hr before exchanging the media and incubating for another 24 hr. On day 5, cells were washed with 0.5 mL DPBS. Cells were detached with 250 uL Trypsin/EDTA and diluted with 3 mL media

before pelleting via centrifugation for 3 min (800 RPM) in a 15 mL Falcon tube. The media/Trypsin were removed, and cells were diluted in new media such that they would be ~25% confluent upon attachment. Cells were plated in 6-well plates and incubated for 24 hr. Selection was started the next day (day 6), by exchanging the media with 100 ug/mL hygromycin containing media. Cells were checked daily until detachment of control cells (no pcDNA5-FRT-TO construct) was observed (5-7 days). Hygromycin containing media was replaced every 3 days. After detachment of controls was observed, cells were switched to hygromycin free media and allowed to grow for 48 hours. A few colonies were generally observed at this point, and they were transferred to a 24-well plate in 1 mL media containing 50 ug/mL hygromycin. Once confluent, cells were passaged into a 12-well plate and then into a T75. 10% (v/v) DMSO cell stocks were made. Cells were maintained in media containing 50 ug/mL hygromycin. Expression of the inducible Flag-constructs with 1 µg/mL of doxycycline was verified using WB (Anti-Flag, CST #2368). GAPDH was used as a loading control on all blots (Anti-GAPDH, Abcam #ab8245).

Activation of HEK293T T-REx JNK Flp-in cell lines. On day 1, HEK293T T-REx Flp-In stable cells containing doxycycline-inducible Flag-JNK1α1[V40C/M108T] or Flag-JNK2α2[V40C/M108T] constructs were plated at ~2.5*10^5 cells on Poly-D-Lysine plates in complete media containing 1 ug/mL doxycycline. The next day, cells were washed 2X with DPBS and serum starved for 18 hours. After the 18 hr serum starvation, cells were ~80-90% confluent. TNFα (100 ug/mL stock, made in sterile filtered DPBS containing 1 mg/mL BSA) was added to the media (50 ng/mL final). Control wells received an equivalent volume of sterile filtered DPBS containing 1 mg/mL BSA. Wells were mixed via rocking. After 20 min, cells were placed on ice and the media was removed. Cells were washed once with ice cold DPBS and lysed on ice using lysis buffer (50 mM Tris, 150 mM NaCl, 1% IGEPAL, 1X Sigma-Aldrich Phosphatase Inhibitor

Cocktails 2/3, and 1X Pierce Protease Inhibitor). Lysate was clarified via centrifugation at 13k g for 10 min at 4 °C. Supernatant was added to 3X SDS loading dye and boiled for 5 min and 95 °C. WB of samples run on both SDS-PAGE (Biorad) and Phos-tag SDS-PAGE[10] were used to assess JNK activation. WB of samples run on standard SDS-PAGE was used to measure JNK expression (Anti-Flag, CST #2368) and activation (Anti-pTpY-JNK, CST #4668). WB for Flag-JNK expression (Anti-Flag, CST #2368) on Phos-tag SDS-PAGE separated samples was used to measure both mono and dual JNK phosphorylation. GAPDH was used as a loading control on all blots (Anti-GAPDH, Abcam #ab8245).

Determination of JIP1, JNK1, and JNK2 concentrations in HEK293 T-REx cells. WB of HEK293 T-REx cell lysate and JNK1α1, JNK2α2, and JIP1b recombinant standards allowed determination of approximate JNK1, JNK2 and JIP1 concentrations in HEK293 T-REx cells. HEK293 T-REx cells were grown in a 6-well plate to ~90-100% confluency. Cells were detached using Trypsin/EDTA and re-suspended in 2 mL of media ($1.3*10^6$ cells/mL → $2.6*10^6$ cells). Cells were lysed in 200 µL lysis buffer (50 mM Tris, 150 mM NaCl, 1% IGEPAL, 1X Sigma-Aldrich Phosphatase Inhibitor Cocktails 2/3, and 1X Pierce Protease Inhibitor) on ice. Lysate was clarified by spinning down at 13k g for 10 min at 4 ºC. Lysate was added to 3X loading dye (240 mM Tris-HCl (pH 6.8), 16% BME (v/v), 6% SDS (wt/v), 0.06% bromophenol blue (wt/v), and 30% glycerol (v/v)). 15 µL of lysate -in loading dye- was added to a 15-well SDS-PAGE gel (Biorad). Each gel -one for JNK1, one for JNK2, and one for JIP1- contained a standard dilution series of recombinant JNK1α1, JNK2α2, or JIP1b. JNK1, JNK2, or JIP1 in HEK293 T-REx cell lysate -and their recombinant standards- were detected by WB for JNK1 (Anti-JNK1, CST #3708), JNK2 (Anti-JNK2, CST #G6G8), or JIP1 (Anti-JIP1, GeneTex, Inc. #GTX100604), respectively. Signal for the recombinant proteins (in the linear range surrounding the HEK293 sample signal) was used to

create a standard curve for each protein of interest, which was then used to determine the concentration of JNK1, JNK2, and JIP1 in HEK293 T-REx cell lysate (*n=1*). The concentrations in the lysate were then used to calculate the number of moles of each protein in the total lysate volume. The volume of the HEK293 cells was estimated using a diameter of 13 μm, giving a cell volume of 1.2 pL.[80] The number of cells, along with the estimated volume of each cell, gave an estimated "total cell volume" for the sample. The total moles of protein and "total cell volume" for the sample were used to determine the approximate molarity of JNK1, JNK2, or JIP1 in HEK293 T-REx cells. Hela cells were also included on the standard blots, but concentrations of JNK1, JNK2, and JIP1 were outside the limit of detection due to low lysate concentration.

Table 3.2. Protein and DNA sequences for specified constructs (**TAG**; GENE)

His_6–LIC+TEV-site–JNK1α1[WT] (Uniprot ID: MK08_MOUSE)* **Also Reported in **Table 2.2**, duplicated for reference.[10]*	
Amino Acid Sequence	**MHHHHHHSSGVDLGTENLYFQSN**MSRSKRDNNFYSVEIGDSTFTVLKRYQNLKPIGSGAQGIVCAAYDAILERNVAIKKLSRPFQNQTHAKRAYRELVLMKCVNHKNIIGLLNVFTPQKSLEEFQDVYIVMELMDANLCQVIQMELDHERMSYLLYQMLCGIKHLHSAGIIHRDLKPSNIVVKSDCTLKILDFGLARTAGTSFMMTPYVVTRYYRAPEVILGMGYKENVDLWSVGCIMGEMVCHKILFPGRDYIDQWNKVIEQLGTPCPEFMKKLQPTVRTYVENRPKYAGYSFEKLFPDVLFPADSEHNKLKASQARDLLSKMLVIDASKRISVDEALQHPYINVWYDPSEAEAPPPKIPDKQLDEREHTIEEWKELIYKEVMDLEERTKNGVKLLE
DNA Sequence	**ATGCACCATCATCATCATCATTCTTCTGGTGTAGATCTGGGTACCGAGAACCTGTACTTCCAATCCAAT**ATGAGCCGCAGCAAACGCGACAACAACTTCTACAGCGTGGAAATCGGCGACAGCACCTTCACCGTGCTGAAACGCTACCAGAACCTGAAACCTATCGGCTCTGGCGCCCAGGGCATCGTGTGTGCCGCCTACGACGCCATCCTGGAACGCAACGTGGCCATCAAAAAACTGAGCCGCCCTTTCCAGAACCAGACCCACGCCAAACGCGCCTACCGCGAGCTGGTGCTGATGAAATGCGTGAACCACAAAAACATCATCGGCCTGCTGAACGTGTTCACACCTCAGAAAAGCCTGGAAGAGTTCCAGGACGTCTACATCGTGATGGAACTGATGGACGCCAACCTGTGCCAGGTCATCCAGATGGAACTGGACCACGAGCGCATGAGCTACCTGCTGTACCAGATGCTGTGCGGCATCAAACATCTGCACAGCGCCGGCATCATCCACCGCGACCTGAAACCATCCAACATCGTGGTCAAAAGCGACTGCACCCTGAAAATCCTGGACTTCGGCCTGGCCCGCACCGCCGGCACCAGCTTCATGATGACCCCTTACGTGGTCACCCGCTACTATCGCGCCCCTGAAGTGATCCTGGGCATGGGCTACAAAGAAAACGTGGACCTGTGGTCCGTGGGC

	TGCATCATGGGCGAGATGGTCTGCCACAAAATCCTGTTCCCTGGCCGCGACTACATCGA CCAGTGGAACAAAGTGATCGAGCAGCTGGGCACCCCTTGCCCTGAGTTCATGAAAAAA CTGCAGCCTACCGTGCGCACCTACGTGGAAAACCGCCCTAAATACGCCGGCTACAGCTT CGAGAAACTGTTCCCTGACGTGCTGTTCCCTGCCGACAGCGAGCACAACAAACTGAAAG CCAGCCAGGCCCGCGACCTGCTGAGCAAAATGCTGGTCATCGACGCCAGCAAACGCAT CAGCGTGGACGAGGCCCTGCAGCACCCTTACATCAACGTGTGGTACGACCCTAGCGAG GCCGAGGCCCCTCCTCCAAAAATCCCTGACAAACAGCTGGACGAGCGCGAGCACACCA TCGAGGAATGGAAAGAGCTGATCTACAAAGAAGTGATGGACCTGGAAGAACGCACCA AAAACGGCGTGAAGCTTCTCGAGTAG
His_6–LIC+TEV-site–JNK1α1[V40C/M108T] (Uniprot ID: MK08_MOUSE)	
Amino Acid Sequence	**MHHHHHHSSGVDLGTENLYFQSN**MSRSKRDNNFYSVEIGDSTFTVLKRYQNLKPIGSGAQ GICCAAYDAILERNVAIKKLSRPFQNQTHAKRAYRELVLMKCVNHKNIIGLLNVFTPQKSLEE FQDVYIV*T*ELMDANLCQVIQMELDHERMSYLLYQMLCGIKHLHSAGIIHRDLKPSNIVVKSD CTLKILDFGLARTAGTSFMMTPYVVTRYYRAPEVILGMGYKENVDLWSVGCIMGEMVCHKI LFPGRDYIDQWNKVIEQLGTPCPEFMKKLQPTVRTYVENRPKYAGYSFEKLFPDVLFPADSE HNKLKASQARDLLSKMLVIDASKRISVDEALQHPYINVWYDPSEAEAPPPKIPDKQLDEREH TIEEWKELIYKEVMDLEERTKNGVKLLE
DNA Sequence	**ATGCACCATCATCATCATCATTCTTCTGGTGTAGATCTGGGTACCGAGAACCTGTACTT CCAATCCAAT**ATGAGCCGCAGCAAACGCGACAACAACTTCTACAGCGTGGAAATCGGC GACAGCACCTTCACCGTGCTGAAACGCTACCAGAACCTGAAACCTATCGGCTCTGGCGC CCAGGGCATCtgcTGTGCCGCCTACGACGCCATCCTGGAACGCAACGTGGCCATCAAAA AACTGAGCCGCCCTTTCCAGAACCAGACCCACGCCAAACGCGCCTACCGCGAGCTGGTG CTGATGAAATGCGTGAACCACAAAAACATCATCGGCCTGCTGAACGTGTTCACACCTCA GAAAAGCCTGGAAGAGTTCCAGGACGTCTACATCGTG*AcG*GAACTGATGGACGCCAAC CTGTGCCAGGTCATCCAGATGGAACTGGACCACGAGCGCATGAGCTACCTGCTGTACCA GATGCTGTGCGGCATCAAACATCTGCACAGCGCCGGCATCATCCACCGCGACCTGAAAC CATCCAACATCGTGGTCAAAAGCGACTGCACCCTGAAAATCCTGGACTTCGGCCTGGCC CGCACCGCCGGCACCAGCTTCATGATGACCCCTTACGTGGTCACCCGCTACTATCGCGCC CCTGAAGTGATCCTGGGCATGGGCTACAAAGAAAACGTGGACCTGTGGTCCGTGGGCT GCATCATGGGCGAGATGGTCTGCCACAAAATCCTGTTCCCTGGCCGCGACTACATCGAC CAGTGGAACAAAGTGATCGAGCAGCTGGGCACCCCTTGCCCTGAGTTCATGAAAAAAC TGCAGCCTACCGTGCGCACCTACGTGGAAAACCGCCCTAAATACGCCGGCTACAGCTTC GAGAAACTGTTCCCTGACGTGCTGTTCCCTGCCGACAGCGAGCACAACAAACTGAAAGC CAGCCAGGCCCGCGACCTGCTGAGCAAAATGCTGGTCATCGACGCCAGCAAACGCATC AGCGTGGACGAGGCCCTGCAGCACCCTTACATCAACGTGTGGTACGACCCTAGCGAGG CCGAGGCCCCTCCTCCAAAAATCCCTGACAAACAGCTGGACGAGCGCGAGCACACCATC GAGGAATGGAAAGAGCTGATCTACAAAGAAGTGATGGACCTGGAAGAACGCACCAAA AACGGCGTGAAGCTTCTCGAGTAG

His_6–LIC+TEV-site–JNK2α2[WT] (Uniprot ID: MK09_HUMAN)	
Amino Acid Sequence	**MHHHHHHSSGVDLGTENLYFQSN**SDSKCDSQFYSVQVADSTFTVLKRYQQLKPIGSGAQG IVCAAFDTVLGINVAVKKLSRPFQNQTHAKRAYRELVLLKCVNHKNIISLLNVFTPQKTLEEFQ DVYLVMELMDANLCQVIHMELDHERMSYLLYQMLCGIKHLHSAGIIHRDLKPSNIVVKSDC TLKILDFGLARTACTNFMMTPYVVTRYYRAPEVILGMGYKENVDIWSVGCIMGELVKGCVIF QGTDHIDQWNKVIEQLGTPSAEFMKKLQPTVRNYVENRPKYPGIKFEELFPDWIFPSESERD KIKTSQARDLLSKMLVIDPDKRISVDEALRHPYITVWYDPAEAEAPPPQIYDAQLEEREHAIEE WKELIYKEVMDWEERSKNGVVKDQPSDAAVSSNATPSQSSSINDISSMSTEQTLASDTDSS LDASTGPLEGCR
DNA Sequence	**ATGCACCATCATCATCATCATTCTTCTGGTGTAGATCTGGGTACCGAGAACCTGTACTT CCAATCCAAT**AGCGACAGTAAATGTGACAGTCAGTTTTATAGTGTGCAAGTGGCAGACT CAACCTTCACTGTCCTAAAACGTTACCAGCAGCTGAAACCAATTGGCTCTGGGGCCCAA GGGATTGTTTGTGCTGCATTTGATACAGTTCTTGGGATAAaTGTTGCAGTCAAGAAACTA AGCCGTCCTTTTCAGAACCAAACTCATGCAAAAAGAGCTTATCGTGAACTTGTCCTCTTA AAATGTGTCAATCATAAAAATATAATTAGTTTGTTAAATGTGTTTACACCACAAAAAACT CTAGAAGAATTTCAAGATGTGTATTTGGTTATGGAATTAATGGATGCTAACTTATGTCAG GTTATTCACATGGAGCTGGATCATGAAAGAATGTCCTACCTTCTTTACCAGATGCTTTGT GGTATTAAACATCTGCATTCAGCTGGTATAATTCATAGAGATTTGAAGCCTAGCAACATT GTTGTGAAATCAGACTGCACCCTGAAGATCCTTGACTTTGGCCTGGCCCGGACAGCGTG CACTAACTTCATGATGACCCCTTACGTGGTGACACGGTACTACCGGGCGCCCGAAGTCA TCCTGGGTATGGGCTACAAAGAGAACGTTGATATCTGGTCAGTGGGTTGCATCATGGG AGAGCTGGTGAAAGGTTGTGTGATATTCCAAGGCACTGACCATATTGATCAGTGGAATA AAGTTATTGAGCAGCTGGGAACACCATCAGCAGAGTTCATGAAGAAACTTCAGCCAACT GTGAGGAATTATGTCGAAAACAGACCAAAGTATCCTGGAATCAAATTTGAAGAACTCTT TCCAGATTGGATATTCCCATCAGAATCTGAGCGAGACAAAATAAAAACAAGTCAAGCCA GAGATCTGTTATCAAAAATGTTAGTGATTGATCCTGACAAGCGGATCTCTGTAGACGAA GCTCTGCGTCACCCATACATCACTGTTTGGTATGACCCCGCCGAAGCAGAAGCCCCACC ACCTCAAATTTATGATGCCCAGTTGGAAGAAAGAGAACATGCAATTGAAGAATGGAAA GAGCTAATTTACAAAGAAGTCATGGATTGGGAAGAAAGAAGCAAGAATGGTGTTGTAA AAGATCAGCCTTCAGATGCAGCAGTAAGTAGCAACGCCACTCCTTCTCAGTCTTCATCGA TCAATGACATTTCATCCATGTCCACTGAGCAGACGCTGGCCTCAGACACAGACAGCAGT CTTGATGCCTCGACGGGACCCCTTGAAGGCTGTCGATGA
His_6–LIC+TEV-site–JNK2α2[V40C/M108T] (Uniprot ID: MK09_HUMAN)	
Amino Acid Sequence	**MHHHHHHSSGVDLGTENLYFQSN**SDSKCDSQFYSVQVADSTFTVLKRYQQLKPIGSGAQG I*C*CAAFDTVLGINVAVKKLSRPFQNQTHAKRAYRELVLLKCVNHKNIISLLNVFTPQKTLEEFQ DVYLV*T*ELMDANLCQVIHMELDHERMSYLLYQMLCGIKHLHSAGIIHRDLKPSNIVVKSDCT LKILDFGLARTACTNFMMTPYVVTRYYRAPEVILGMGYKENVDIWSVGCIMGELVKGCVIF QGTDHIDQWNKVIEQLGTPSAEFMKKLQPTVRNYVENRPKYPGIKFEELFPDWIFPSESERD

	KIKTSQARDLLSKMLVIDPDKRISVDEALRHPYITVWYDPAEAEAPPPQIYDAQLEEREHAIEE WKELIYKEVMDWEERSKNGVVKDQPSDAAVSSNATPSQSSSINDISSMSTEQTLASDTDSS LDASTGPLEGCR
DNA Sequence	**ATGCACCATCATCATCATCATTCTTCTGGTGTAGATCTGGGTACCGAGAACCTGTACTT CCAATCCAAT**AGCGACAGTAAATGTGACAGTCAGTTTTATAGTGTGCAAGTGGCAGACT CAACCTTCACTGTCCTAAAACGTTACCAGCAGCTGAAACCAATTGGCTCTGGGGCCCAA GGGATT*tgT*TGTGCTGCATTTGATACAGTTCTTGGGATAAaTGTTGCAGTCAAGAAACTA AGCCGTCCTTTTCAGAACCAAACTCATGCAAAAAGAGCTTATCGTGAACTTGTCCTCTTA AAATGTGTCAATCATAAAAATATAATTAGTTTGTTAAATGTGTTTACACCACAAAAAACT CTAGAAGAATTTCAAGATGTGTATTTGGTT*AcG*GAATTAATGGATGCTAACTTATGTCAG GTTATTCACATGGAGCTGGATCATGAAAGAATGTCCTACCTTCTTTACCAGATGCTTTGT GGTATTAAACATCTGCATTCAGCTGGTATAATTCATAGAGATTTGAAGCCTAGCAACATT GTTGTGAAATCAGACTGCACCCTGAAGATCCTTGACTTTGGCCTGGCCCGGACAGCGTG CACTAACTTCATGATGACCCCTTACGTGGTGACACGGTACTACCGGGCGCCCGAAGTCA TCCTGGGTATGGGCTACAAAGAGAACGTTGATATCTGGTCAGTGGGTTGCATCATGGG AGAGCTGGTGAAAGGTTGTGTGATATTCCAAGGCACTGACCATATTGATCAGTGGAATA AAGTTATTGAGCAGCTGGGAACACCATCAGCAGAGTTCATGAAGAAACTTCAGCCAACT GTGAGGAATTATGTCGAAAACAGACCAAAGTATCCTGGAATCAAATTTGAAGAACTCTT TCCAGATTGGATATTCCCATCAGAATCTGAGCGAGACAAAATAAAAACAAGTCAAGCCA GAGATCTGTTATCAAAAATGTTAGTGATTGATCCTGACAAGCGGATCTCTGTAGACGAA GCTCTGCGTCACCCATACATCACTGTTTGGTATGACCCCGCCGAAGCAGAAGCCCCACC ACCTCAAATTTATGATGCCCAGTTGGAAGAAAGAGAACATGCAATTGAAGAATGGAAA GAGCTAATTTACAAAGAAGTCATGGATTGGGAAGAAAGAAGCAAGAATGGTGTTGTAA AAGATCAGCCTTCAGATGCAGCAGTAAGTAGCAACGCCACTCCTTCTCAGTCTTCATCGA TCAATGACATTTCATCCATGTCCACTGAGCAGACGCTGGCCTCAGACACAGACAGCAGT CTTGATGCCTCGACGGGACCCCTTGAAGGCTGTCGA**TGA
Kozak **Flag–JNK1α1[WT] (Uniprot ID: MK08_MOUSE)**	
Amino Acid Sequence	**MDYKDDDDK**SRSKRDNNFYSVEIGDSTFTVLKRYQNLKPIGSGAQGIVCAAYDAILERNVAI KKLSRPFQNQTHAKRAYRELVLMKCVNHKNIIGLLNVFTPQKSLEEFQDVYIVMELMDANL CQVIQMELDHERMSYLLYQMLCGIKHLHSAGIIHRDLKPSNIVVKSDCTLKILDFGLARTAGT SFMMTPYVVTRYYRAPEVILGMGYKENVDLWSVGCIMGEMVCHKILFPGRDYIDQWNKV IEQLGTPCPEFMKKLQPTVRTYVENRPKYAGYSFEKLFPDVLFPADSEHNKLKASQARDLLSK MLVIDASKRISVDEALQHPYINVWYDPSEAEAPPPKIPDKQLDEREHTIEEWKELIYKEVMDL EERTKNGVKLLE
DNA Sequence	*gccaccatg***GATTATAAGGATGACGACGATAAG**AGCCGCAGCAAACGCGACAACAACTT CTACAGCGTGGAAATCGGCGACAGCACCTTCACCGTGCTGAAACGCTACCAGAACCTGA AACCTATCGGCTCTGGCGCCCAGGGCATCGTGTGTGCCGCCTACGACGCCATCCTGGAA

	CGCAACGTGGCCATCAAAAAACTGAGCCGCCCTTTCCAGAACCAGACCCACGCCAAACG CGCCTACCGCGAGCTGGTGCTGATGAAATGCGTGAACCACAAAAACATCATCGGCCTGC TGAACGTGTTCACACCTCAGAAAAGCCTGGAAGAGTTCCAGGACGTCTACATCGTGATG GAACTGATGGACGCCAACCTGTGCCAGGTCATCCAGATGGAACTGGACCACGAGCGCA TGAGCTACCTGCTGTACCAGATGCTGTGCGGCATCAAACATCTGCACAGCGCCGGCATC ATCCACCGCGACCTGAAACCATCCAACATCGTGGTCAAAAGCGACTGCACCCTGAAAAT CCTGGACTTCGGCCTGGCCCGCACCGCCGGCACCAGCTTCATGATGACCCCTTACGTGG TCACCCGCTACTATCGCGCCCCTGAAGTGATCCTGGGCATGGGCTACAAAGAAAACGTG GACCTGTGGTCCGTGGGCTGCATCATGGGCGAGATGGTCTGCCACAAAATCCTGTTCCC TGGCCGCGACTACATCGACCAGTGGAACAAAGTGATCGAGCAGCTGGGCACCCCTTGC CCTGAGTTCATGAAAAAACTGCAGCCTACCGTGCGCACCTACGTGGAAAACCGCCCTAA ATACGCCGGCTACAGCTTCGAGAAACTGTTCCCTGACGTGCTGTTCCCTGCCGACAGCG AGCACAACAAACTGAAAGCCAGCCAGGCCCGCGACCTGCTGAGCAAAATGCTGGTCAT CGACGCCAGCAAACGCATCAGCGTGGACGAGGCCCTGCAGCACCCTTACATCAACGTG TGGTACGACCCTAGCGAGGCCGAGGCCCCTCCTCCAAAAATCCCTGACAAACAGCTGGA CGAGCGCGAGCACACCATCGAGGAATGGAAAGAGCTGATCTACAAAGAAGTGATGGA CCTGGAAGAACGCACCAAAAACGGCGTGAAGCTTCTCGAGTAG
Kozak **Flag–JNK1α1[V40C/M108T] (Uniprot ID: MK08_MOUSE)**	
Amino Acid Sequence	**MDYKDDDDK**SRSKRDNNFYSVEIGDSTFTVLKRYQNLKPIGSGAQGI*C*CAAYDAILERNVAI KKLSRPFQNQTHAKRAYRELVLMKCVNHKNIIGLLNVFTPQKSLEEFQDVYIV*T*ELMDANLC QVIQMELDHERMSYLLYQMLCGIKHLHSAGIIHRDLKPSNIVVKSDCTLKILDFGLARTAGTS FMMTPYVVTRYYRAPEVILGMGYKENVDLWSVGCIMGEMVCHKILFPGRDYIDQWNKVI EQLGTPCPEFMKKLQPTVRTYVENRPKYAGYSFEKLFPDVLFPADSEHNKLKASQARDLLSK MLVIDASKRISVDEALQHPYINVWYDPSEAEAPPPKIPDKQLDEREHTIEEWKELIYKEVMDL EERTKNGVKLLE
DNA Sequence	*gccaccatg***GATTATAAGGATGACGACGATAAG**AGCCGCAGCAAACGCGACAACAACTT CTACAGCGTGGAAATCGGCGACAGCACCTTCACCGTGCTGAAACGCTACCAGAACCTGA AACCTATCGGCTCTGGCGCCCAGGGCATCtgcTGTGCCGCCTACGACGCCATCCTGGAAC GCAACGTGGCCATCAAAAAACTGAGCCGCCCTTTCCAGAACCAGACCCACGCCAAACGC GCCTACCGCGAGCTGGTGCTGATGAAATGCGTGAACCACAAAAACATCATCGGCCTGCT GAACGTGTTCACACCTCAGAAAAGCCTGGAAGAGTTCCAGGACGTCTACATCGTG*AcG*G AACTGATGGACGCCAACCTGTGCCAGGTCATCCAGATGGAACTGGACCACGAGCGCAT GAGCTACCTGCTGTACCAGATGCTGTGCGGCATCAAACATCTGCACAGCGCCGGCATCA TCCACCGCGACCTGAAACCATCCAACATCGTGGTCAAAAGCGACTGCACCCTGAAAATC CTGGACTTCGGCCTGGCCCGCACCGCCGGCACCAGCTTCATGATGACCCCTTACGTGGT CACCCGCTACTATCGCGCCCCTGAAGTGATCCTGGGCATGGGCTACAAAGAAAACGTG GACCTGTGGTCCGTGGGCTGCATCATGGGCGAGATGGTCTGCCACAAAATCCTGTTCCC TGGCCGCGACTACATCGACCAGTGGAACAAAGTGATCGAGCAGCTGGGCACCCCTTGC CCTGAGTTCATGAAAAAACTGCAGCCTACCGTGCGCACCTACGTGGAAAACCGCCCTAA

	ATACGCCGGCTACAGCTTCGAGAAACTGTTCCCTGACGTGCTGTTCCCTGCCGACAGCG AGCACAACAAACTGAAAGCCAGCCAGGCCCGCGACCTGCTGAGCAAAATGCTGGTCAT CGACGCCAGCAAACGCATCAGCGTGGACGAGGCCCTGCAGCACCCTTACATCAACGTG TGGTACGACCCTAGCGAGGCCGAGGCCCCTCCTCCAAAAATCCCTGACAAACAGCTGGA CGAGCGCGAGCACACCATCGAGGAATGGAAAGAGCTGATCTACAAAGAAGTGATGGA CCTGGAAGAACGCACCAAAAACGGCGTGAAGCTTCTCGAGTAG
Kozak **Flag–JNK2α2[WT] (Uniprot ID: MK09_HUMAN)**	
Amino Acid Sequence	**MDYKDDDDK**SDSKCDSQFYSVQVADSTFTVLKRYQQLKPIGSGAQGIVCAAFDTVLGINVA VKKLSRPFQNQTHAKRAYRELVLLKCVNHKNIISLLNVFTPQKTLEEFQDVYLVMELMDANL CQVIHMELDHERMSYLLYQMLCGIKHLHSAGIIHRDLKPSNIVVKSDCTLKILDFGLARTACT NFMMTPYVVTRYYRAPEVILGMGYKENVDIWSVGCIMGELVKGCVIFQGTDHIDQWNKVI EQLGTPSAEFMKKLQPTVRNYVENRPKYPGIKFEELFPDWIFPSESERDKIKTSQARDLLSKM LVIDPDKRISVDEALRHPYITVWYDPAEAEAPPPQIYDAQLEEREHAIEEWKELIYKEVMDW EERSKNGVVKDQPSDAAVSSNATPSQSSSINDISSMSTEQTLASDTDSSLDASTGPLEGCR
DNA Sequence	*gccaccatg***GATTATAAGGATGACGACGATAAG**AGCGACAGTAAATGTGACAGTCAGTT TTATAGTGTGCAAGTGGCAGACTCAACCTTCACTGTCCTAAAACGTTACCAGCAGCTGA AACCAATTGGCTCTGGGGCCCAAGGGATTGTTTGTGCTGCATTTGATACAGTTCTTGGG ATAAaTGTTGCAGTCAAGAAACTAAGCCGTCCTTTTCAGAACCAAACTCATGCAAAAAG AGCTTATCGTGAACTTGTCCTCTTAAAATGTGTCAATCATAAAAATATAATTAGTTTGTTA AATGTGTTTACACCACAAAAAACTCTAGAAGAATTTCAAGATGTGTATTTGGTTATGGA ATTAATGGATGCTAACTTATGTCAGGTTATTCACATGGAGCTGGATCATGAAAGAATGT CCTACCTTCTTTACCAGATGCTTTGTGGTATTAAACATCTGCATTCAGCTGGTATAATTCA TAGAGATTTGAAGCCTAGCAACATTGTTGTGAAATCAGACTGCACCCTGAAGATCCTTG ACTTTGGCCTGGCCCGGACAGCGTGCACTAACTTCATGATGACCCCTTACGTGGTGACA CGGTACTACCGGGCGCCCGAAGTCATCCTGGGTATGGGCTACAAAGAGAACGTTGATA TCTGGTCAGTGGGTTGCATCATGGGAGAGCTGGTGAAAGGTTGTGTGATATTCCAAGG CACTGACCATATTGATCAGTGGAATAAAGTTATTGAGCAGCTGGGAACACCATCAGCAG AGTTCATGAAGAAACTTCAGCCAACTGTGAGGAATTATGTCGAAAACAGACCAAAGTAT CCTGGAATCAAATTTGAAGAACTCTTTCCAGATTGGATATTCCCATCAGAATCTGAGCGA GACAAAATAAAAACAAGTCAAGCCAGAGATCTGTTATCAAAAATGTTAGTGATTGATCC TGACAAGCGGATCTCTGTAGACGAAGCTCTGCGTCACCCATACATCACTGTTTGGTATG ACCCCGCCGAAGCAGAAGCCCCACCACCTCAAATTTATGATGCCCAGTTGGAAGAAAGA GAACATGCAATTGAAGAATGGAAAGAGCTAATTTACAAAGAAGTCATGGATTGGGAAG AAAGAAGCAAGAATGGTGTTGTAAAAGATCAGCCTTCAGATGCAGCAGTAAGTAGCAA CGCCACTCCTTCTCAGTCTTCATCGATCAATGACATTTCATCCATGTCCACTGAGCAGAC GCTGGCCTCAGACACAGACAGCAGTCTTGATGCCTCGACGGGACCCCTTGAAGGCTGTC GATGA

Kozak **Flag–JNK2α2[V40C/M108T] (Uniprot ID: MK09_HUMAN)**	
Amino Acid Sequence	**MDYKDDDDK**SDSKCDSQFYSVQVADSTFTVLKRYQQLKPIGSGAQGI*C*CAAFDTVLGINVA VKKLSRPFQNQTHAKRAYRELVLLKCVNHKNIISLLNVFTPQKTLEEFQDVYLV*T*ELMDANLC QVIHMELDHERMSYLLYQMLCGIKHLHSAGIIHRDLKPSNIVVKSDCTLKILDFGLARTACTN FMMTPYVVTRYYRAPEVILGMGYKENVDIWSVGCIMGELVKGCVIFQGTDHIDQWNKVIE QLGTPSAEFMKKLQPTVRNYVENRPKYPGIKFEELFPDWIFPSESERDKIKTSQARDLLSKML VIDPDKRISVDEALRHPYITVWYDPAEAEAPPPQIYDAQLEEREHAIEEWKELIYKEVMDWE ERSKNGVVKDQPSDAAVSSNATPSQSSSINDISSMSTEQTLASDTDSSLDASTGPLEGCR
DNA Sequence	*gccaccatg***GATTATAAGGATGACGACGATAAG**AGCGACAGTAAATGTGACAGTCAGTT TTATAGTGTGCAAGTGGCAGACTCAACCTTCACTGTCCTAAAACGTTACCAGCAGCTGA AACCAATTGGCTCTGGGGCCCAAGGGATT*tgT*TGTGCTGCATTTGATACAGTTCTTGGGA TAAaTGTTGCAGTCAAGAAACTAAGCCGTCCTTTTCAGAACCAAACTCATGCAAAAAGA GCTTATCGTGAACTTGTCCTCTTAAAATGTGTCAATCATAAAAATATAATTAGTTTGTTAA ATGTGTTTACACCACAAAAAACTCTAGAAGAATTTCAAGATGTGTATTTGGTT*AcG*GAAT TAATGGATGCTAACTTATGTCAGGTTATTCACATGGAGCTGGATCATGAAAGAATGTCC TACCTTCTTTACCAGATGCTTTGTGGTATTAAACATCTGCATTCAGCTGGTATAATTCATA GAGATTTGAAGCCTAGCAACATTGTTGTGAAATCAGACTGCACCCTGAAGATCCTTGAC TTTGGCCTGGCCCGGACAGCGTGCACTAACTTCATGATGACCCCTTACGTGGTGACACG GTACTACCGGGCGCCCGAAGTCATCCTGGGTATGGGCTACAAAGAGAACGTTGATATCT GGTCAGTGGGTTGCATCATGGGAGAGCTGGTGAAAGGTTGTGTGATATTCCAAGGCAC TGACCATATTGATCAGTGGAATAAAGTTATTGAGCAGCTGGGAACACCATCAGCAGAGT TCATGAAGAAACTTCAGCCAACTGTGAGGAATTATGTCGAAAACAGACCAAAGTATCCT GGAATCAAATTTGAAGAACTCTTTCCAGATTGGATATTCCCATCAGAATCTGAGCGAGA CAAAATAAAAACAAGTCAAGCCAGAGATCTGTTATCAAAAATGTTAGTGATTGATCCTG ACAAGCGGATCTCTGTAGACGAAGCTCTGCGTCACCCATACATCACTGTTTGGTATGAC CCCGCCGAAGCAGAAGCCCCACCACCTCAAATTTATGATGCCCAGTTGGAAGAAAGAG AACATGCAATTGAAGAATGGAAAGAGCTAATTTACAAAGAAGTCATGGATTGGGAAGA AAGAAGCAAGAATGGTGTTGTAAAAGATCAGCCTTCAGATGCAGCAGTAAGTAGCAAC GCCACTCCTTCTCAGTCTTCATCGATCAATGACATTTCATCCATGTCCACTGAGCAGACG CTGGCCTCAGACACAGACAGCAGTCTTGATGCCTCGACGGGACCCCTTGAAGGCTGTCG ATGA
Flag-JIP1b[WT]-His$_6$ (Uniprot ID: JIP1_MOUSE)* **Also Reported in **Table 2.2**, duplicated for reference.[10]*	
Amino Acid Sequence	**MDYKDDDDK**MAERESGLGGGAASPPAASPFLGLHIASPPNFRLTHDISLEEFEDEDLSEITD ECGISLQCKDTLSLRPPRAGLLSAGSSGSAGSRLQAEMLQMDLIDAAGDTPGAEDDEEEED DELAAQRPGVGPPKAESNQDPAPRSQGQGPGTGSGDTYRPKRPTTLNLFPQVPRSQDTLN NNSLGKKHSWQDRVSRSSSPLKTGEQTPPHEHICLSDELPPQGSPVPTQDRGTSTDSPCRRS AATQMAPPSGPPATAPGGRGHSHRDRIHYQADVRLEATEEIYLTPVQRPPDPAEPTSTFMP

	PTESRMSVSSDPDPAAYSVTAGRPHPSISEEDEGFDCLSSPERAEPPGGGWRGSLGEPPPPP RASLSSDTSALSYDSVKYTLVVDEHAQLELVSLRPCFGDYSDESDSATVYDNCASASSPYESAI GEEYEEAPQPRPPTCLSEDSTPDEPDVHFSKKFLNVFMSGRSRSSSAESFGLFSCVINGEEHE QTHRAIFRFVPRHEDELELEVDDPLLVELQAEDYWYEAYNMRTGARGVFPAYYAIEVTKEPE HMAALAKNSDWIDQFRVKFLGSVQVPYHKGNDVLCAAMQKIATTRRLTVHFNPPSSCVLE ISVRGVKIGVKADDALEAKGNKCSHFFQLKNISFCGYHPKNNKYFGFITKHPADHRFACHVF VSEDSTKALAESVGRAFQQFYKQFVEYTCPTEDIYLE**HHHHHH**
DNA Sequence	**ATGGATTATAAGGATGACGACGATAAG**ATGGCGGAGCGAGAGAGCGGCCTGGGCGG GGGCGCCGCGTCCCCACCGGCCGCTTCCCCATTCCTGGGACTGCACATCGCGTCGCCTC CCAATTTCAGGCTCACCCATGACATCAGCCTGGAGGAGTTTGAGGATGAAGACCTTTCG GAGATCACTGACGAGTGTGGCATCAGCCTGCAGTGCAAAGACACCCTGTCTCTCCGGCC CCCGCGCGCCGGGCTGCTGTCTGCGGGTAGCAGCGGCAGCGCGGGGAGCCGGCTGCA GGCGGAGATGCTGCAGATGGACCTGATCGACGCGGCAGGTGACACTCCGGGCGCCGA GGACGACGAGGAGGAGGAGGACGACGAGCTCGCTGCCCAACGACCAGGAGTGGGGC CTCCCAAAGCGGAGTCCAACCAGGATCCGGCGCCTCGCAGCCAGGGCCAGGGCCCGGG CACAGGCAGCGGAGACACCTACCGACCCAAGAGGCCTACCACGCTCAACCTTTTCCCGC AGGTGCCGCGGTCTCAGGACACGCTGAATAATAACTCTTTAGGCAAAAAGCACAGTTG GCAGGACCGTGTGTCTCGATCATCCTCCCCTCTGAAGACAGGAGAACAGACGCCTCCAC ATGAACACATCTGCCTGAGTGATGAGCTGCCACCCCAGGGCAGTCCTGTTCCCACCCAG GACCGCGGCACTTCCACCGACAGCCCTTGTCGCCGAAGTGCAGCCACCCAGATGGCACC TCCAAGCGGTCCCCCTGCCACTGCGCCTGGTGGCCGGGGCCACTCCCATCGAGACCGAA TCCACTACCAGGCAGATGTGCGGCTCGAGGCGACTGAGGAGATCTACCTGACCCCAGT GCAGAGGCCCCCAGACCCTGCAGAACCCACCTCCACCTTCATGCCACCCACGGAGAGCC GGATGTCAGTTAGCTCGGATCCAGACCCTGCCGCTTACTCTGTAACTGCGGGGCGGCCA CACCCCTCCATCAGTGAAGAGGATGAGGGCTTCGACTGCCTGTCATCCCCAGAGCGAGC TGAGCCACCAGGTGGAGGGTGGCGGGGAAGCCTCGGGGAGCCACCACCGCCTCCACG GGCCTCACTGAGCTCGGACACCAGCGCACTGTCCTACGACTCGGTCAAGTACACACTGG TGGTGGATGAACATGCCCAGCTTGAGTTGGTGAGCCTGCGGCCGTGCTTTGGAGATTA CAGTGACGAAAGCGACTCTGCCACTGTCTATGACAACTGTGCCTCTGCCTCCTCGCCCTA CGAGTCAGCCATTGGTGAGGAGTATGAGGAGGCCCCTCAGCCCCGGCCTCCCACCTGC CTCTCAGAGGACTCCACCCCGGATGAGCCTGATGTCCACTTCTCTAAGAAGTTTCTGAAT GTCTTCATGAGTGGCCGCTCTCGTTCCTCCAGTGCTGAGTCCTTTGGGCTGTTCTCCTGC GTCATCAATGGGGAGGAGCATGAGCAAACCCATCGGGCTATATTCAGGTTTGTGCCTCG GCATGAAGATGAACTTGAGCTGGAAGTGGATGACCCCCTGCTGGTGGAGCTGCAGGCA GAAGACTATTGGTATGAGGCCTATAACATGCGCACCGGAGCCCGCGGGGTCTTCCCTGC CTACTATGCCATTGAGGTCACCAAGGAGCCTGAGCACATGGCAGCCCTTGCCAAAAACA GCGACTGGATTGACCAGTTCCGGGTGAAGTTCCTGGGGTCTGTCCAGGTTCCTTATCAC AAGGGCAATGATGTCCTCTGTGCTGCTATGCAAAAGATCGCCACCACCCGCCGGCTCAC CGTGCACTTTAACCCGCCCTCCAGCTGTGTCCTTGAGATCAGTGTCAGGGGTGTCAAGA TAGGCGTCAAAGCTGATGATGCTCTGGAGGCCAAGGGAAATAAATGTAGCCACTTCTTC CAGCTAAAGAACATCTCTTTCTGTGGATACCATCCAAAGAATAACAAGTACTTTGGGTTT ATCACTAAGCACCCTGCTGACCACCGGTTTGCCTGCCATGTCTTTGTGTCTGAAGATTCC

	ACCAAAGCCCTGGCGGAGTCTGTGGGGCGTGCATTTCAGCAGTTCTACAAGCAGTTTGT GGAGTATACCTGTCCTACAGAAGATATCTACTTGGAG**CACCACCACCACCACCAC**TGA
Flag-JIP1b[JBD]-His_6 (Uniprot ID: JIP1_MOUSE) - residues 127-282	
Amino Acid Sequence	**MDYKDDDDK**PKAESNQDPAPRSQGQGPGTGSGDTYRPKRPTTLNLFPQVPRSQDTLNN NSLGKKHSWQDRVSRSSSPLKTGEQTPPHEHICLSDELPPQGSPVPTQDRGTSTDSPCRRSA ATQMAPPSGPPATAPGGRGHSHRDRIHYQADVRLEATEEIYLTPV**HHHHHH**
DNA Sequence	**ATGGATTATAAGGATGACGACGATAAG**CCCAAAGCGGAGTCCAACCAGGATCCGGCG CCTCGCAGCCAGGGCCAGGGCCCGGGCACAGGCAGCGGAGACACCTACCGACCCAAG AGGCCTACCACGCTCAACCTTTTCCCGCAGGTGCCGCGGTCTCAGGACACGCTGAATAA TAACTCTTTAGGCAAAAAGCACAGTTGGCAGGACCGTGTGTCTCGATCATCCTCCCCTCT GAAGACAGGAGAACAGACGCCTCCACATGAACACATCTGCCTGAGTGATGAGCTGCCA CCCCAGGGCAGTCCTGTTCCCACCCAGGACCGCGGCACTTCCACCGACAGCCCTTGTCG CCGAAGTGCAGCCACCCAGATGGCACCTCCAAGCGGTCCCCCTGCCACTGCGCCTGGTG GCCGGGGCCACTCCCATCGAGACCGAATCCACTACCAGGCAGATGTGCGGCTCGAGGC GACTGAGGAGATCTACCTGACCCCAGTG**CACCACCACCACCACCAC**TGA
Flag-JIP1b[ΔJBD]-His_6 (Uniprot ID: JIP1_MOUSE) - residues 1-126/283-707	
Amino Acid Sequence	**MDYKDDDDK**MAERESGLGGGAASPPAASPFLGLHIASPPNFRLTHDISLEEFEDEDLSEITD ECGISLQCKDTLSLRPPRAGLLSAGSSGSAGSRLQAEMLQMDLIDAAGDTPGAEDDEEEED DELAAQRPGVGPQRPPDPAEPTSTFMPPTESRMSVSSDPDPAAYSVTAGRPHPSISEEDEG FDCLSSPERAEPPGGGWRGSLGEPPPPPRASLSSDTSALSYDSVKYTLVVDEHAQLELVSLRP CFGDYSDESDSATVYDNCASASSPYESAIGEEYEEAPQPRPPTCLSEDSTPDEPDVHFSKKFL NVFMSGRSRSSSAESFGLFSCVINGEEHEQTHRAIFRFVPRHEDELELEVDDPLLVELQAEDY WYEAYNMRTGARGVFPAYYAIEVTKEPEHMAALAKNSDWIDQFRVKFLGSVQVPYHKGN DVLCAAMQKIATTRRLTVHFNPPSSCVLEISVRGVKIGVKADDALEAKGNKCSHFFQLKNISF CGYHPKNNKYFGFITKHPADHRFACHVFVSEDSTKALAESVGRAFQQFYKQFVEYTCPTEDI YLE**HHHHHH**
DNA Sequence	ATGGATTATAAGGATGACGACGATAAGATGGCGGAGCGAGAGAGCGGCCTGGGCGGG GGCGCCGCGTCCCCACCGGCCGCTTCCCCATTCCTGGGACTGCACATCGCGTCGCCTCC CAATTTCAGGCTCACCCATGACATCAGCCTGGAGGAGTTTGAGGATGAAGACCTTTCGG AGATCACTGACGAGTGTGGCATCAGCCTGCAGTGCAAAGACACCCTGTCTCTCCGGCCC CCGCGCGCCGGGCTGCTGTCTGCGGGTAGCAGCGGCAGCGCGGGGAGCCGGCTGCAG GCGGAGATGCTGCAGATGGACCTGATCGACGCGGCAGGTGACACTCCGGGCGCCGAG GACGACGAGGAGGAGGAGGACGACGAGCTCGCTGCCCAACGACCAGGAGTGGGGCCT CAGAGGCCCCCAGACCCTGCAGAACCCACCTCCACCTTCATGCCACCCACGGAGAGCCG GATGTCAGTTAGCTCGGATCCAGACCCTGCCGCTTACTCTGTAACTGCGGGGCGGCCAC

	ACCCCTCCATCAGTGAAGAGGATGAGGGCTTCGACTGCCTGTCATCCCCAGAGCGAGCT GAGCCACCAGGTGGAGGGTGGCGGGGAAGCCTCGGGGAGCCACCACCGCCTCCACGG GCCTCACTGAGCTCGGACACCAGCGCACTGTCCTACGACTCGGTCAAGTACACACTGGT GGTGGATGAACATGCCCAGCTTGAGTTGGTGAGCCTGCGGCCGTGCTTTGGAGATTAC AGTGACGAAAGCGACTCTGCCACTGTCTATGACAACTGTGCCTCTGCCTCCTCGCCCTAC GAGTCAGCCATTGGTGAGGAGTATGAGGAGGCCCCTCAGCCCCGGCCTCCCACCTGCCT CTCAGAGGACTCCACCCCGGATGAGCCTGATGTCCACTTCTCTAAGAAGTTTCTGAATGT CTTCATGAGTGGCCGCTCTCGTTCCTCCAGTGCTGAGTCCTTTGGGCTGTTCTCCTGCGT CATCAATGGGGAGGAGCATGAGCAAACCCATCGGGCTATATTCAGGTTTGTGCCTCGG CATGAAGATGAACTTGAGCTGGAAGTGGATGACCCCCTGCTGGTGGAGCTGCAGGCAG AAGACTATTGGTATGAGGCCTATAACATGCGCACCGGAGCCCGCGGGGTCTTCCCTGCC TACTATGCCATTGAGGTCACCAAGGAGCCTGAGCACATGGCAGCCCTTGCCAAAAACAG CGACTGGATTGACCAGTTCCGGGTGAAGTTCCTGGGGTCTGTCCAGGTTCCTTATCACA AGGGCAATGATGTCCTCTGTGCTGCTATGCAAAAGATCGCCACCACCCGCCGGCTCACC GTGCACTTTAACCCGCCCTCCAGCTGTGTCCTTGAGATCAGTGTCAGGGGTGTCAAGAT AGGCGTCAAAGCTGATGATGCTCTGGAGGCCAAGGGAAATAAATGTAGCCACTTCTTCC AGCTAAAGAACATCTCTTTCTGTGGATACCATCCAAAGAATAACAAGTACTTTGGGTTTA TCACTAAGCACCCTGCTGACCACCGGTTTGCCTGCCATGTCTTTGTGTCTGAAGATTCCA CCAAAGCCCTGGCGGAGTCTGTGGGGCGTGCATTTCAGCAGTTCTACAAGCAGTTTGTG GAGTATACCTGTCCTACAGAAGATATCTACTTGGAGCACCACCACCACCACCACTGA
Flag-JIP1b[T103A]-His_6 (Uniprot ID: JIP1_MOUSE)	
Amino Acid Sequence	**MDYKDDDDK**MAERESGLGGGAASPPAASPFLGLHIASPPNFRLTHDISLEEFEDEDLSEITD ECGISLQCKDTLSLRPPRAGLLSAGSSGSAGSRLQAEMLQMDLIDAAGD*A*PGAEDDEEEED DELAAQRPGVGPPKAESNQDPAPRSQGQGPGTGSGDTYRPKRPTTLNLFPQVPRSQDTLN NNSLGKKHSWQDRVSRSSSPLKTGEQTPPHEHICLSDELPPQGSPVPTQDRGTSTDSPCRRS AATQMAPPSGPPATAPGGRGHSHRDRIHYQADVRLEATEEIYLTPVQRPPDPAEPTSTFMP PTESRMSVSSDPDPAAYSVTAGRPHPSISEEDEGFDCLSSPERAEPPGGGWRGSLGEPPPPP RASLSSDTSALSYDSVKYTLVVDEHAQLELVSLRPCFGDYSDESDSATVYDNCASASSPYESAI GEEYEEAPQPRPPTCLSEDSTPDEPDVHFSKKFLNVFMSGRSRSSSAESFGLFSCVINGEEHE QTHRAIFRFVPRHEDELELEVDDPLLVELQAEDYWYEAYNMRTGARGVFPAYYAIEVTKEPE HMAALAKNSDWIDQFRVKFLGSVQVPYHKGNDVLCAAMQKIATTRRLTVHFNPPSSCVLE ISVRGVKIGVKADDALEAKGNKCSHFFQLKNISFCGYHPKNNKYFGFITKHPADHRFACHVF VSEDSTKALAESVGRAFQQFYKQFVEYTCPTEDIYLE**HHHHHH**
DNA Sequence	**ATGGATTATAAGGATGACGACGATAAG**ATGGCGGAGCGAGAGAGCGGCCTGGGCGG GGGCGCCGCGTCCCCACCGGCCGCTTCCCCATTCCTGGGACTGCACATCGCGTCGCCTC CCAATTTCAGGCTCACCCATGACATCAGCCTGGAGGAGTTTGAGGATGAAGACCTTTCG GAGATCACTGACGAGTGTGGCATCAGCCTGCAGTGCAAAGACACCCTGTCTCTCCGGCC CCCGCGCGCCGGGCTGCTGTCTGCGGGTAGCAGCGGCAGCGCGGGGAGCCGGCTGCA GGCGGAGATGCTGCAGATGGACCTGATCGACGCGGCAGGTGAC*gCT*CCGGGCGCCGA

	GGACGACGAGGAGGAGGAGGACGACGAGCTCGCTGCCCAACGACCAGGAGTGGGGC CTCCCAAAGCGGAGTCCAACCAGGATCCGGCGCCTCGCAGCCAGGGCCAGGGCCCGGG CACAGGCAGCGGAGACACCTACCGACCCAAGAGGCCTACCACGCTCAACCTTTTCCCGC AGGTGCCGCGGTCTCAGGACACGCTGAATAATAACTCTTTAGGCAAAAAGCACAGTTG GCAGGACCGTGTGTCTCGATCATCCTCCCCTCTGAAGACAGGAGAACAGACGCCTCCAC ATGAACACATCTGCCTGAGTGATGAGCTGCCACCCCAGGGCAGTCCTGTTCCCACCCAG GACCGCGGCACTTCCACCGACAGCCCTTGTCGCCGAAGTGCAGCCACCCAGATGGCACC TCCAAGCGGTCCCCCTGCCACTGCGCCTGGTGGCCGGGGCCACTCCCATCGAGACCGAA TCCACTACCAGGCAGATGTGCGGCTCGAGGCGACTGAGGAGATCTACCTGACCCCAGT GCAGAGGCCCCCAGACCCTGCAGAACCCACCTCCACCTTCATGCCACCCACGGAGAGCC GGATGTCAGTTAGCTCGGATCCAGACCCTGCCGCTTACTCTGTAACTGCGGGGCGGCCA CACCCCTCCATCAGTGAAGAGGATGAGGGCTTCGACTGCCTGTCATCCCCAGAGCGAGC TGAGCCACCAGGTGGAGGGTGGCGGGGAAGCCTCGGGGAGCCACCACCGCCTCCACG GGCCTCACTGAGCTCGGACACCAGCGCACTGTCCTACGACTCGGTCAAGTACACACTGG TGGTGGATGAACATGCCCAGCTTGAGTTGGTGAGCCTGCGGCCGTGCTTTGGAGATTA CAGTGACGAAAGCGACTCTGCCACTGTCTATGACAACTGTGCCTCTGCCTCCTCGCCCTA CGAGTCAGCCATTGGTGAGGAGTATGAGGAGGCCCCTCAGCCCCGGCCTCCCACCTGC CTCTCAGAGGACTCCACCCCGGATGAGCCTGATGTCCACTTCTCTAAGAAGTTTCTGAAT GTCTTCATGAGTGGCCGCTCTCGTTCCTCCAGTGCTGAGTCCTTTGGGCTGTTCTCCTGC GTCATCAATGGGGAGGAGCATGAGCAAACCCATCGGGCTATATTCAGGTTTGTGCCTCG GCATGAAGATGAACTTGAGCTGGAAGTGGATGACCCCCTGCTGGTGGAGCTGCAGGCA GAAGACTATTGGTATGAGGCCTATAACATGCGCACCGGAGCCCGCGGGGTCTTCCCTGC CTACTATGCCATTGAGGTCACCAAGGAGCCTGAGCACATGGCAGCCCTTGCCAAAAACA GCGACTGGATTGACCAGTTCCGGGTGAAGTTCCTGGGGTCTGTCCAGGTTCCTTATCAC AAGGGCAATGATGTCCTCTGTGCTGCTATGCAAAAGATCGCCACCACCCGCCGGCTCAC CGTGCACTTTAACCCGCCCTCCAGCTGTGTCCTTGAGATCAGTGTCAGGGGTGTCAAGA TAGGCGTCAAAGCTGATGATGCTCTGGAGGCCAAGGGAAATAAATGTAGCCACTTCTTC CAGCTAAAGAACATCTCTTTCTGTGGATACCATCCAAAGAATAACAAGTACTTTGGGTTT ATCACTAAGCACCCTGCTGACCACCGGTTTGCCTGCCATGTCTTTGTGTCTGAAGATTCC ACCAAAGCCCTGGCGGAGTCTGTGGGGCGTGCATTTCAGCAGTTCTACAAGCAGTTTGT GGAGTATACCTGTCCTACAGAAGATATCTACTTGGAG**CACCACCACCACCACCAC**TGA
Flag-JIP1b[R160G/P161G]-His$_6$ (Uniprot ID: JIP1_MOUSE)	
Amino Acid Sequence	**MDYKDDDDK**MAERESGLGGGAASPPAASPFLGLHIASPPNFRLTHDISLEEFEDEDLSEITD ECGISLQCKDTLSLRPPRAGLLSAGSSGSAGSRLQAEMLQMDLIDAAGDTPGAEDDEEEED DELAAQRPGVGPPKAESNQDPAPRSQGQGPGTGSGDTYRPK*GG*TTLNLFPQVPRSQDTL NNNSLGKKHSWQDRVSRSSSPLKTGEQTPPHEHICLSDELPPQGSPVPTQDRGTSTDSPCR RSAATQMAPPSGPPATAPGGRGHSHRDRIHYQADVRLEATEEIYLTPVQRPPDPAEPTSTF MPPTESRMSVSSDPDPAAYSVTAGRPHPSISEEDEGFDCLSSPERAEPPGGGWRGSLGEPP PPPRASLSSDTSALSYDSVKYTLVVDEHAQLELVSLRPCFGDYSDESDSATVYDNCASASSPY ESAIGEEYEEAPQPRPPTCLSEDSTPDEPDVHFSKKFLNVFMSGRSRSSSAESFGLFSCVINGE EHEQTHRAIFRFVPRHEDELELEVDDPLLVELQAEDYWYEAYNMRTGARGVFPAYYAIEVTK

	EPEHMAALAKNSDWIDQFRVKFLGSVQVPYHKGNDVLCAAMQKIATTRRLTVHFNPPSSC VLEISVRGVKIGVKADDALEAKGNKCSHFFQLKNISFCGYHPKNNKYFGFITKHPADHRFAC HVFVSEDSTKALAESVGRAFQQFYKQFVEYTCPTEDIYLE**HHHHHH**
DNA Sequence	**ATGGATTATAAGGATGACGACGATAAG**ATGGCGGAGCGAGAGAGCGGCCTGGGCGG GGGCGCCGCGTCCCCACCGGCCGCTTCCCCATTCCTGGGACTGCACATCGCGTCGCCTC CCAATTTCAGGCTCACCCATGACATCAGCCTGGAGGAGTTTGAGGATGAAGACCTTTCG GAGATCACTGACGAGTGTGGCATCAGCCTGCAGTGCAAAGACACCCTGTCTCTCCGGCC CCCGCGCGCCGGGCTGCTGTCTGCGGGTAGCAGCGGCAGCGCGGGGAGCCGGCTGCA GGCGGAGATGCTGCAGATGGACCTGATCGACGCGGCAGGTGACACTCCGGGCGCCGA GGACGACGAGGAGGAGGAGGACGACGAGCTCGCTGCCCAACGACCAGGAGTGGGGC CTCCCAAAGCGGAGTCCAACCAGGATCCGGCGCCTCGCAGCCAGGGCCAGGGCCCGGG CACAGGCAGCGGAGACACCTACCGACCCAAG*gGaggT*ACCACGCTCAACCTTTTCCCGC AGGTGCCGCGGTCTCAGGACACGCTGAATAATAACTCTTTAGGCAAAAAGCACAGTTG GCAGGACCGTGTGTCTCGATCATCCTCCCCTCTGAAGACAGGAGAACAGACGCCTCCAC ATGAACACATCTGCCTGAGTGATGAGCTGCCACCCCAGGGCAGTCCTGTTCCCACCCAG GACCGCGGCACTTCCACCGACAGCCCTTGTCGCCGAAGTGCAGCCACCCAGATGGCACC TCCAAGCGGTCCCCCTGCCACTGCGCCTGGTGGCCGGGGCCACTCCCATCGAGACCGAA TCCACTACCAGGCAGATGTGCGGCTCGAGGCGACTGAGGAGATCTACCTGACCCCAGT GCAGAGGCCCCCAGACCCTGCAGAACCCACCTCCACCTTCATGCCACCCACGGAGAGCC GGATGTCAGTTAGCTCGGATCCAGACCCTGCCGCTTACTCTGTAACTGCGGGGCGGCCA CACCCCTCCATCAGTGAAGAGGATGAGGGCTTCGACTGCCTGTCATCCCCAGAGCGAGC TGAGCCACCAGGTGGAGGGTGGCGGGGAAGCCTCGGGGAGCCACCACCGCCTCCACG GGCCTCACTGAGCTCGGACACCAGCGCACTGTCCTACGACTCGGTCAAGTACACACTGG TGGTGGATGAACATGCCCAGCTTGAGTTGGTGAGCCTGCGGCCGTGCTTTGGAGATTA CAGTGACGAAAGCGACTCTGCCACTGTCTATGACAACTGTGCCTCTGCCTCCTCGCCCTA CGAGTCAGCCATTGGTGAGGAGTATGAGGAGGCCCCTCAGCCCCGGCCTCCCACCTGC CTCTCAGAGGACTCCACCCCGGATGAGCCTGATGTCCACTTCTCTAAGAAGTTTCTGAAT GTCTTCATGAGTGGCCGCTCTCGTTCCTCCAGTGCTGAGTCCTTTGGGCTGTTCTCCTGC GTCATCAATGGGGAGGAGCATGAGCAAACCCATCGGGCTATATTCAGGTTTGTGCCTCG GCATGAAGATGAACTTGAGCTGGAAGTGGATGACCCCCTGCTGGTGGAGCTGCAGGCA GAAGACTATTGGTATGAGGCCTATAACATGCGCACCGGAGCCCGCGGGGTCTTCCCTGC CTACTATGCCATTGAGGTCACCAAGGAGCCTGAGCACATGGCAGCCCTTGCCAAAAACA GCGACTGGATTGACCAGTTCCGGGTGAAGTTCCTGGGGTCTGTCCAGGTTCCTTATCAC AAGGGCAATGATGTCCTCTGTGCTGCTATGCAAAAGATCGCCACCACCCGCCGGCTCAC CGTGCACTTTAACCCGCCCTCCAGCTGTGTCCTTGAGATCAGTGTCAGGGGTGTCAAGA TAGGCGTCAAAGCTGATGATGCTCTGGAGGCCAAGGGAAATAAATGTAGCCACTTCTTC CAGCTAAAGAACATCTCTTTCTGTGGATACCATCCAAAGAATAACAAGTACTTTGGGTTT ATCACTAAGCACCCTGCTGACCACCGGTTTGCCTGCCATGTCTTTGTGTCTGAAGATTCC ACCAAAGCCCTGGCGGAGTCTGTGGGGCGTGCATTTCAGCAGTTCTACAAGCAGTTTGT GGAGTATACCTGTCCTACAGAAGATATCTACTTGGAG**CACCACCACCACCACCAC**TGA

Chapter 4. LOCALIZED KINASE INHIBITION

Acknowledgement: Paula Bucko in John Scott's[2] lab conducted the experiments in mammalian cells showing the utility of the localized inhibitor-based tools (data not shown). The manuscript containing these experiments has been submitted for publication. These experiments will also be published in the dissertation of Paula Bucko. Carrie Gower, previously in the Maly Lab, was instrumental in the design of the CLP-linked inhibitors.

4.1 INTRODUCTION

At its surface, signal transduction seems misleadingly simple. An extracellular signal will bind to an extracellular receptor, which "tells" the cell to induce a number of intracellular changes, in order to produce a specific phenotypic output. Protein kinases often play essential roles in facilitating the transformations that are necessary for a cell to achieve the correct output in response to specific stimuli.[2] However, many of the 538 known human kinases have dozens of cellular substrates and the phosphorylation of those substrates can produce variable outputs.[3, 8, 81] It readily becomes apparent that kinase regulation must be incredibly complicated to allow the phosphorylation of certain substrates and not others at the correct place and time to produce the desired output.

The use of kinase inhibitors as chemical tools to tease apart complex aspects of protein kinase regulation has been broadly employed in the last couple of decades.[7, 10, 11, 13, 61, 82] The ways kinase inhibitors can be used as tools to understand kinase biology vary greatly. It is well known in biological fields that the use of non-catalytically active enzyme mutants, or even complete removal of proteins from cells, can help us understand the native role of those proteins.[2, 83, 84] We

[2] UW pharmacology department

can similarly use ATP-competitive inhibitors, which also block the activity of the kinase, while also offering control of other aspects of kinase regulation, such as the kinase conformation.[7, 85] However, since many kinases have multiple roles throughout the cell, and their roles in certain locations can be distinct, using chemical or genetic tools to study kinase biology can be challenging.[86]

One reason for this is that most of these chemical and genetic tools are applied globally, meaning they alter a specific kinase throughout the entire cell, and conclusions are generally made based on global inhibition or modulation of the pathway. We often rely on phenotypic outputs or measures of global enzyme activity (like western blotting of total cell lysate) to understand the effects our tools are having. It is often difficult to relate the phenotypic output–or changes to global activity–to an effect these perturbations have on a localized population of enzymes. Yet, understanding the role of localized kinase activity is vital to grasping how single kinases are able to achieve a high diversity in their signaling outputs.[86] Thus, we sought to develop a set of tools and methodology that would allow the study of localized kinase biology. We wanted to target ATP-competitive inhibitor tool compounds to a local enzyme population and observe the resulting output (**Figure 4.1**).

Researchers have increasingly used small protein tags, such as SNAP, CLIP, and Halo to covalently modify proteins with reporter molecules in cells over the last decade.[87-93] To direct modified kinase inhibitors to specific sub-cellular locations, we fused SNAP-tag to localization domains. We then made SNAP-linkable kinase inhibitors that could be directed to the SNAP-fusion proteins. In mammalian cells, the SNAP-tagged fusions were labeled with kinase inhibitors, and the free inhibitors were then washed away, which allowed us to increase the spatial resolution of the inhibitor-based tools. As a proof of concept, we chose to explore localized inhibition of two

mitotic kinases, Plk1 and Aurora A, which have multiple roles in mitosis at different cellular locations.[94-108] These model systems were used to determine if we could observe a significant, measurable change to the phenotypic output with our localized inhibitors, such that this methodology could be made more broadly applicable to other systems.

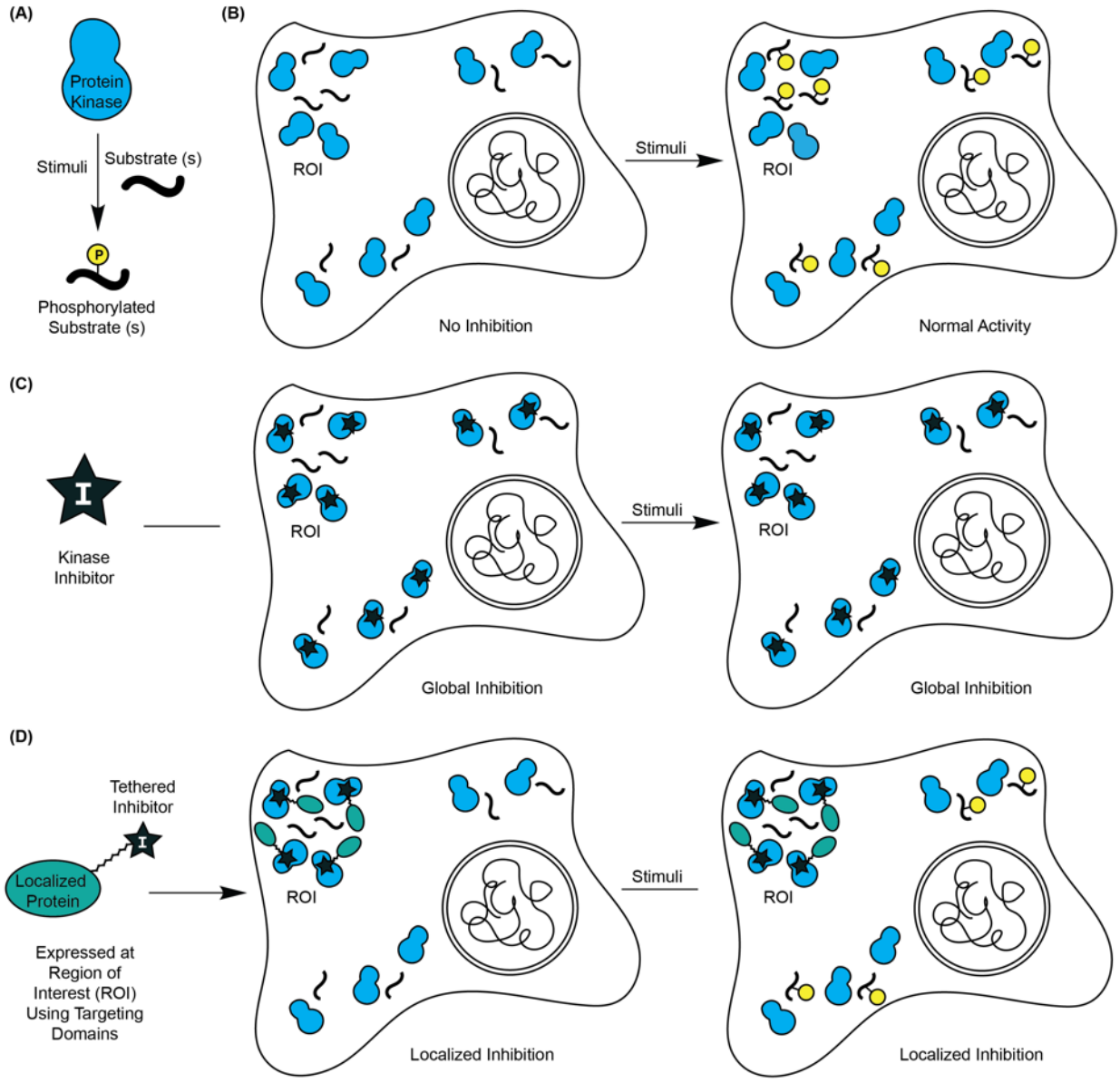

Figure 4.1. *Directing ATP-competitive inhibitors to specific areas of the cell to study localized kinase biology.* (A and B) Schematic showing normal kinase activity. (C) Schematic showing an example of global kinase inhibition. (D) Schematic showing an example of local kinase inhibition.

4.2 Using SNAP-tag to Covalently Modify Fusion Proteins in Vitro or In Vivo

SNAP-tag is a modified O^6-alkylguanine-DNA alkyltransferase (AGT), a DNA repair enzyme, that has been engineered to prevent recognition of its native substrate and instead, rapidly and irreversibly self-label with O^6-benzylguanine (BG) or O^4-benzyl-2-chloro-6-aminopyrimidine (CLP) in cells (**Figure 4.2**).[87-91] SNAP-tag can be used to label fusion proteins both in vitro and in vivo with BG- or CLP-labeled small molecules. By expressing SNAP-tag fused to localization domains in cells, we can direct kinase inhibitors to specific sub-cellular locations. After an initial labeling period, any free inhibitor can be washed from cells and the effects from the localized inhibition can be observed.

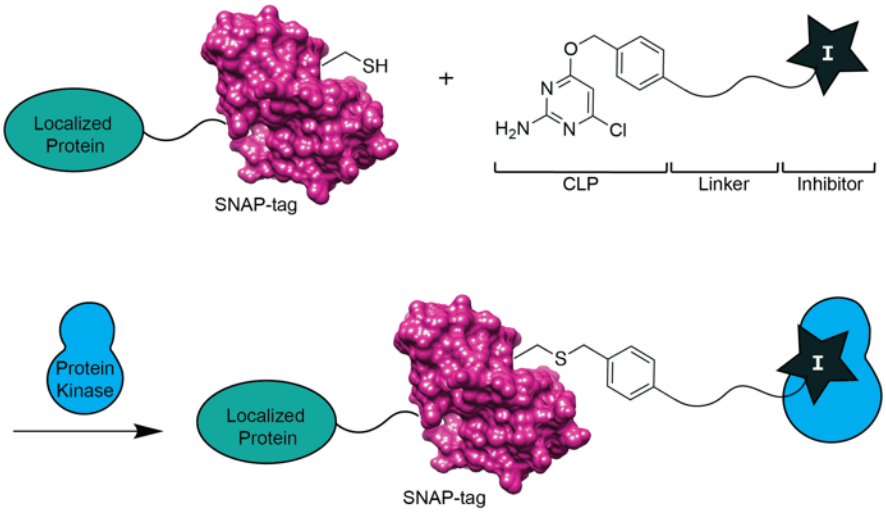

Figure 4.2. *We envisioned using SNAP-tag to covalently modify localized proteins with kinase inhibitors.* SNAP-tag is a modified O^6-alkylguanine-DNA alkyltransferase (AGT). AGT's native substrate is O^6-alkylguanine.[88-91, 93] SNAP-tag has been engineered to recognize O^4-benzyl-2-chloro-6-aminopyrimidine (CLP) in vitro or in vivo (SNAP-tag crystal structure PDB ID: 3KZZ).[93]

4.3 Design of SNAP-Tethered Inhibitors

We then made SNAP-linkable Plk1/Aurora A inhibitors. Each SNAP-linkable inhibitor was envisioned to contain a selective kinase inhibitor and a covalent SNAP-tag modifier, separated by a flexible PEG linker (**Figure 4.2**). When choosing kinase inhibitors, it was necessary to identify those that contained functional groups that would allow for modification at a position pointing away from the active site (ideally an amine or carboxylic acid). It was also necessary that those functional groups did not make any significant contacts with the kinase or that these modifications would not alter the existing contacts.

For Plk1 inhibition, we chose to use BI2536, which has an IC_{50} of 8 nM. A structure of Plk1 in complex with BI2536 shows the piperidine ring pointing away from the active site (**Figure 4.3**).[109, 110] To simplify the synthesis, a modified BI2536 with a carboxylic acid off the phenyl ring was purchased. Though the amide of BI2536 makes two hydrogen bond contacts with the active site of Plk1, the carboxylic acid of the BI2536 precursor will later undergo coupling to a PEG linker containing an amine, thus maintaining the amide hydrogen bonding in the active site of Plk1.

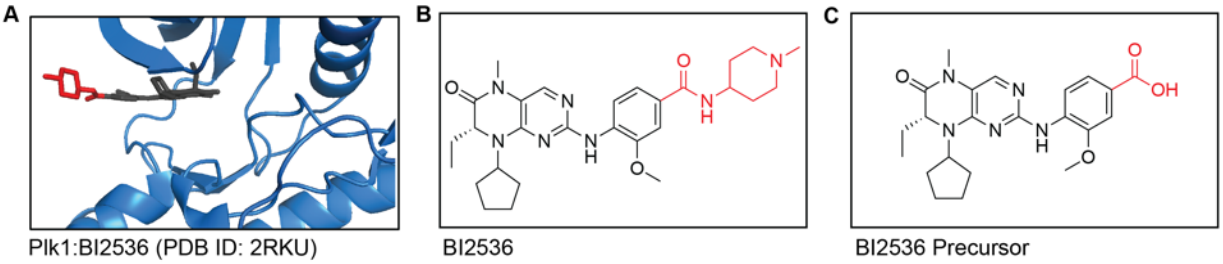

Figure 4.3. *Choosing a Plk1 inhibitor to modify for localized inhibition studies.* (A) Crystal structure of BI2356 in the active site of Plk1 (PDB ID: 2RKU) showing the piperidine ring pointing away from the active site. (B) Structure of BI2536. (C) The BI2536 precursor (Chem Scene) contains a carboxylic acid at the position modified by the piperidine. This allows coupling to the amine containing linker, while still maintaining the hydrogen bond contacts that the BI2536 amide makes with the active site.

In order to covalently label the SNAP fusion constructs with inhibitors in cells, we needed to modify them with a cell-permeable SNAP substrate. Chloropyrimidine (CLP) was chosen based on its ability rapidly label SNAP-tag both in vitro and in vivo.[93] We used a flexible PEG linker between CLP and the inhibitor to allow the SNAP-displayed inhibitors to reach the kinase active site while displayed on SNAP. We used a linker with two PEG repeats in our studies, but a longer linker may be needed for the inhibitor to reach the active site of some targets. The PEG linker was purchased with functional groups that were compatible for coupling to the CLP and inhibitor moieties. The CLP was modified to display an amine as described in Hill, *et al.* (**4.1a**; CLP-Amine) for coupling to a carboxylic acid on the linker **4.1b** (**Scheme 4.1**).[111] The BI2536 precursor (**Figure 4.3C**) contained a carboxylic acid functional group at the desired point of modification, so a linker with an amine at the other end was chosen for coupling. To prevent the linker from self-coupling during the initial reaction with CLP-amine, the amine was Boc-protected. Following coupling of the linker to the CLP-amine to yield **4.1c**, the Boc protected linker was deprotected with TFA to yield the free amine **4.1d**.

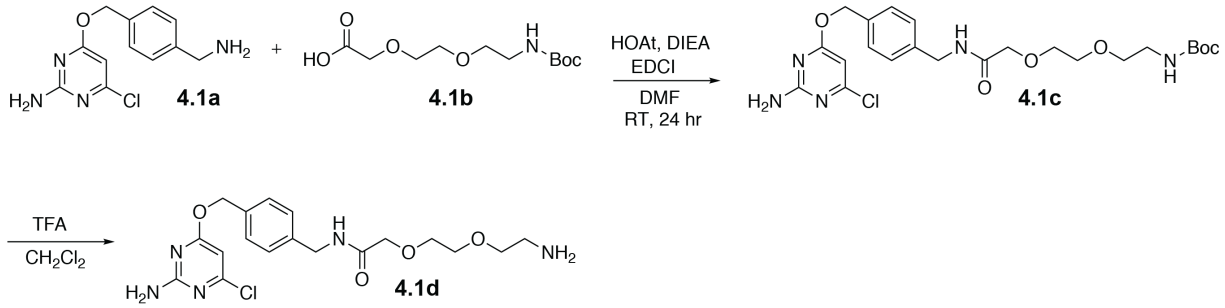

Scheme 4.1. Coupling of **4.1a** (CLP-amine) to the carboxyl end of the PEG linker (**4.1b**). Following coupling of the linker with CLP-amine, Boc-protected **4.1c** was deprotected using TFA to yield the free amine (**4.1d**).

For formation of the final SNAP-tetherable Plk1 inhibitor (**4.2b;** BI2536-CLP), the free amine of CLP-linker (**4.1d**) was coupled to the carboxylic acid of the BI2536 precursor **2.4a** (**Scheme 4.2**). **4.2b** was purified by HPLC and the identity was verified with MS.

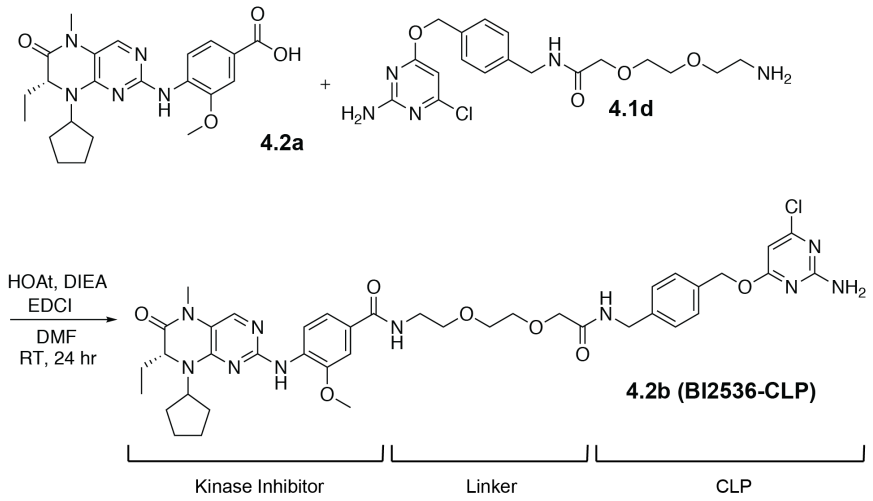

Scheme 4.2. Coupling of CLP-Linker (**4.1d**) to the BI2536 precursor (**4.2a**). The BI2536-CLP product (**4.2b**) was purified by HPLC and the identity was verified with MS. $[M+H]^+$ = 817.7 *m/z*.

For Aurora A inhibition, we chose to use the isoform selective inhibitor MLN8237. MLN8237 has an IC_{50} value for Aurora A of 1 nM and an IC_{50} for Aurora B of 1.5 μM.[112] A crystal structure of Aurora A in complex with MLN8054, which is structurally similar to MLN8237 and expected to bind in a similar manner, demonstrates that the carboxyl group points away from the active site of the kinase (**Figure 4.4**).[113] MLN8237 was selected over MLN8054 due to its higher potency (Aurora A IC_{50} for MLN8054 = 31 nM).[112] While the carbonyl of MLN8237 makes a hydrogen bond to Aurora A in the crystal structure, coupling of the linker to the carboxylic acid is not expected to significantly impact its potency.

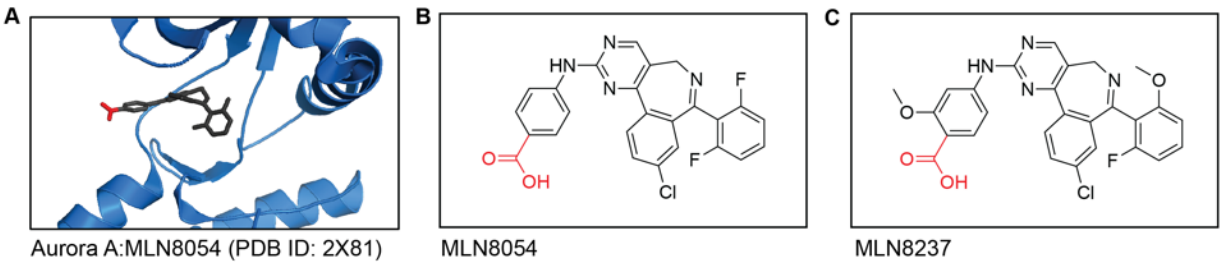

Figure 4.4. *Choosing an Aurora A inhibitor to modify for localized inhibition studies.* (A) Crystal structure showing MLN8054 in the active site of Aurora A (PDB ID: 2X81), demonstrating that the carboxylic acid group points away from the active site. (B) Structure of MLN8054. (C) Structure of MLN8237. The carboxylic acid of MLN8237 allows for coupling to an amine containing linker, while still maintaining the hydrogen bond contact the carbonyl of MNL8237 amide makes with the active site.

The carboxylic acid of MLN8237 (**4.3a**) was coupled to the CLP-Linker **4.1d** (**Scheme 4.3**) to obtain the localizable inhibitor construct (**4.3b**; MLN8237-CLP) for Aurora A. **4.3b** was purified by HPLC and the identity was verified with MS.

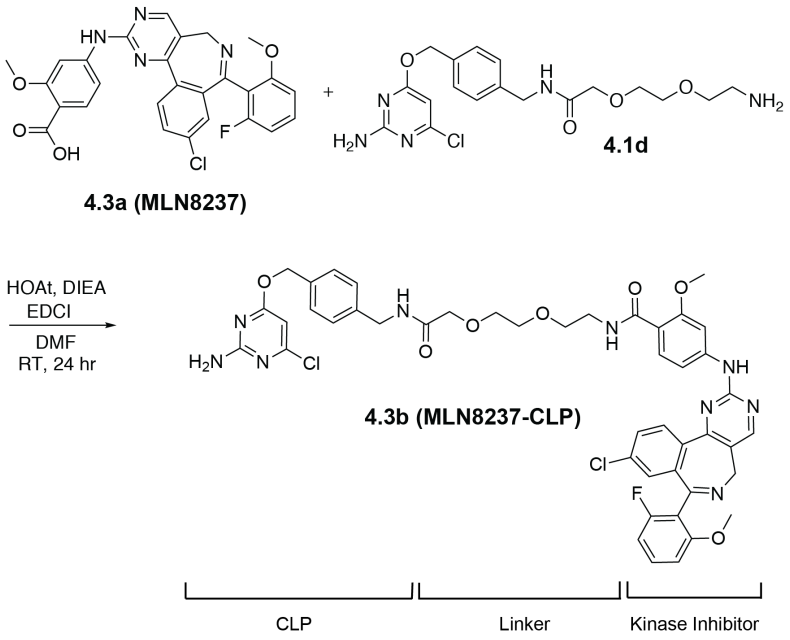

Scheme 4.3. Coupling of CLP-Linker (**4.1d**) to MLN8237 (**4.3a**). The MLN8237-CLP (**4.3b**) product was purified by HPLC and the identity was verified with MS. $[M+H]^+$ = 911.0 *m/z*.

While both MLN8237 and the BI2536 precursor had carboxylic acid functional groups at the site of linker modification, this method could be adjusted for inhibitors with different functional groups pointing out of their active sites. It would be necessary that functionalization of the inhibitor (or a close derivative) is possible and that a linker with compatible chemistry can be identified or synthesized. The resulting molecule would also need to maintain any contacts the inhibitor makes with the kinase. Localized kinase probes that necessitate the removal or alteration of the functional groups making contact with the active site would be predicted to lose potency and/or selectivity for their intended target.

4.4 Determining Potency of SNAP-Tethered Inhibitors

Before performing cellular studies, we validated that the SNAP-linked inhibitors are still able to inhibit Plk1 and Aurora A while displayed from SNAP. To test this, we first expressed and purified recombinant SNAP-tag. The SNAP-inhibitor conjugates were isolated by in vitro labeling of SNAP using CLP-linked inhibitors. The SNAP-inhibitor conjugates were then further purified using size exclusion chromatography, to remove free inhibitor prior to their use in activity assays. The amount of SNAP labeling was determined using native protein mass spectrometry. This allowed us to calculate the concentration of labeled SNAP in solution, using the ratio of labeled to unlabeled SNAP-tag and the concentration of SNAP protein.

To determine the potency of the CLP-Linker-Inhibitors and SNAP-Linker-Inhibitors, we used [γ-^{32}P]ATP radioactivity assays. We first ran enzyme titrations to determine the linear range of activity for Plk1 and Aurora A in our assays (**Figures 4.5 & 4.6**). In the Plk1 assays, Casein was used as a substrate and the Aurora A assays used Myelin Basic Protein.

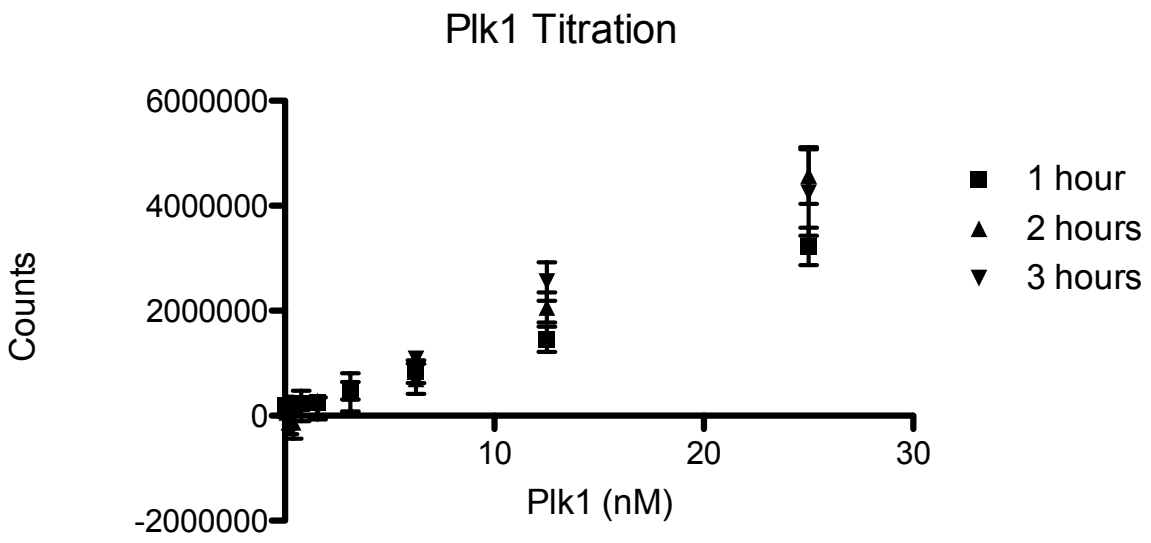

Figure 4.5. *[γ-^{32}P]ATP Radioassay for Plk1.* Enzyme titration using Casein as a substrate. 10 nM Plk1 and a 1 hr incubation were used in the inhibition assays.

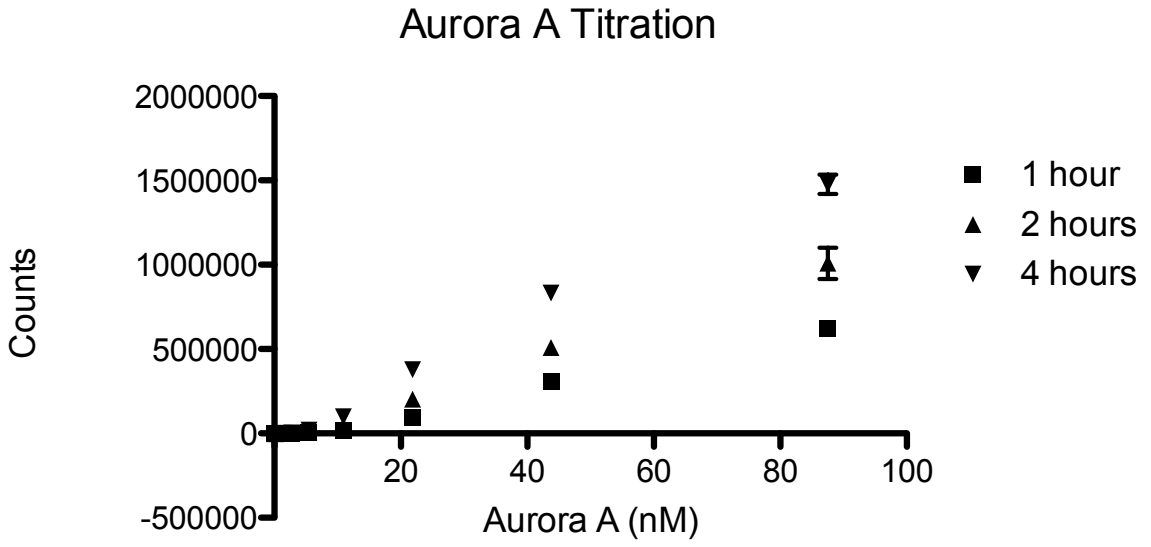

Figure 4.6. *[γ-^{32}P]ATP Radioassay for Aurora A.* Enzyme titration using Myelin Basic Protein as a substrate. 15 nM Aurora A and 4 hr incubation were used in the inhibition assays.

The IC_{50}s for CLP-BI2536 and SNAP-BI2536 for Plk1 were 49 ± 26 nM and 650 ± 80, respectively (**Figure 4.7**). The IC_{50}s for CLP-MLN8237 and SNAP-MLN8237 for Aurora A are <9.5 nM and <11 nM, respectively (**Figure 4.8**).

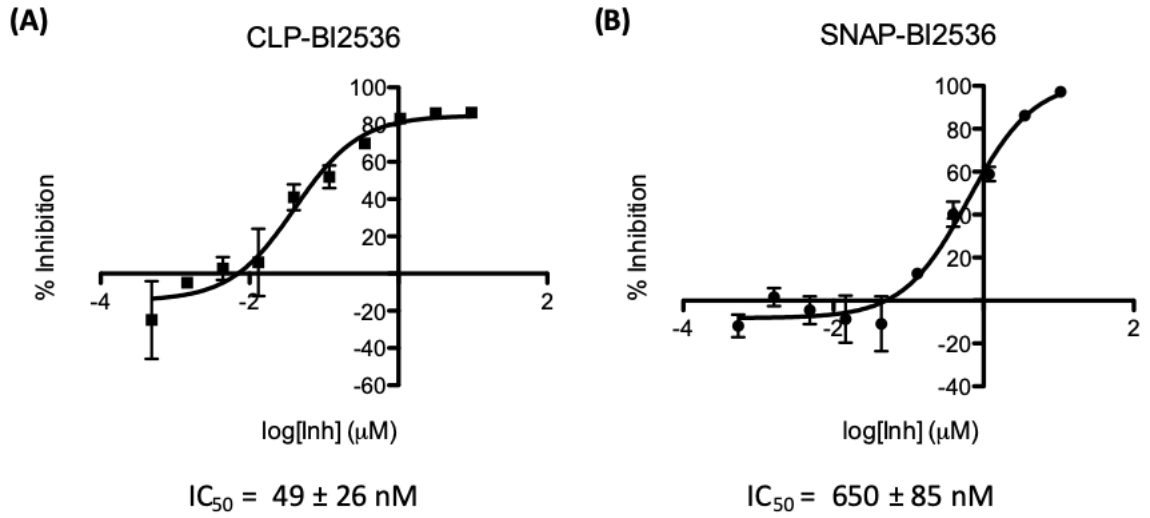

Figure 4.7. *[γ-^{32}P]ATP Inhibition assays for CLP-Linker-Inhibitors and CLP-Linker-SNAP constructs against Plk1, using Casein as a substrate.* 10 nM Plk1 and a 1 hr incubation were used in the inhibition assays. (A) Plk1 inhibition assay to determine potency of CLP-BI2536. (B) Plk1 inhibition assay to determine potency of SNAP-BI2536.

Figure 4.8. *[γ-^{32}P]ATP Inhibition assays for CLP-Linker-Inhibitors and CLP-Linker-*

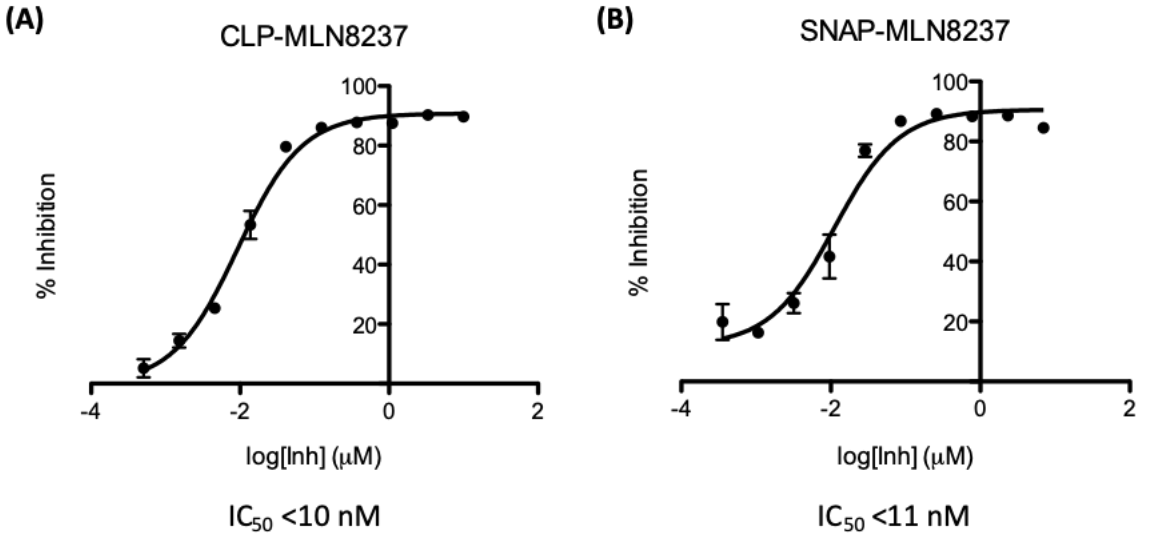

SNAP constructs against Aurora A, using Myelin Basic Protein as a substrate. 15 nM Aurora A and a 4 hr incubation were used in the assays. (A) Aurora A inhibition assay to determine potency of CLP-MLN8237. (B) Aurora A inhibition assay to determine potency of SNAP-MLN8237.

4.5 Directing PLK1 & Aurora A Inhibitors to the Centrosomes Using SNAP-PACT Fusions

This research sought to develop a method to achieve localized kinase inhibition of two mitotic kinases, Aurora A and Plk1. Since both kinases are active in the centrosomes of the cell and those roles are thought to be essential to chromosome segregation and mitosis, we first sought to target inhibitors specifically to that location.[94, 98, 100-102, 107, 108] To direct inhibitors to centrosomes, we created fusion proteins between SNAP and a domain termed PACT. PACT is a centrosomal targeting domain, first discovered by its presence in AKAP450 and pericentrin.[114] We reasoned that we could label SNAP-PACT fusion proteins with ATP-competitive inhibitors (or DMSO alone), and then observe the changes to the phenotypic output (**Figure 4.9**). Though the labeling efficiency of SNAP-tag can reach ~90% in cells, to further increase the local concentration of SNAP-tag and, thus, the inhibitor we fused the PACT domain to two N-terminal SNAP-tags, such that the overall constructs took the form of SNAP-SNAP-PACT.[115] Experiments conducted by Paula Bucko in the Scott lab show that the SNAP-SNAP-PACT constructs are localized to the centrosomes.

One significant challenge we faced when labeling the SNAP-SNAP-PACT constructs in cells, is that to introduce inhibitors locally, we must first introduce them to the cells globally. Without an appropriate control, it would still be difficult to determine if the resulting output is due to initial global inhibition or local inhibition remaining after the global washout. To differentiate local versus global inhibition, we opted to conduct parallel experiments using cell lines expressing SNAP-dead (a SNAP mutant that cannot be labeled with inhibitors) fusion proteins, which would serve as a global inhibitor background control.

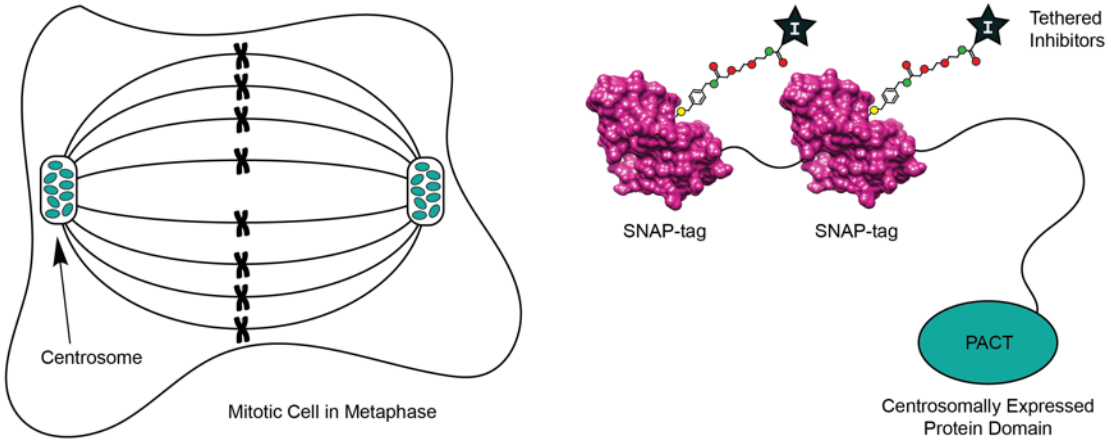

Figure 4.9 *Localizing inhibitors to the centrosomes using SNAP-SNAP-PACT.* (SNAP-tag crystal structure PDB ID: 3KZZ).

4.6 Labeling SNAP in Cells Using CLP-Linker-Inhibitors

To make sure the CLP-inhibitors were cell permeable and determine how much SNAP-tag was labeled by inhibitors in mammalian cells, we conducted labeling experiments in cells expressing SNAP-SNAP-PACT (pulse chase)[87] with varying concentrations of inhibitors & varying labeling times (**Figure 4.10**). After exposure of cells to CLP-inhibitors or DMSO, cells were washed to remove any inhibitor that is not conjugated to SNAP-SNAP-PACT. TMR-CLP was then introduced, which labeled any SNAP-SNAP-PACT that was not conjugated to a CLP-inhibitor. To determine how much of the SNAP-SNAP-PACT was labeled, the cells were lysed, and the lysate was run on an SDS-PAGE gel. The TMR-labeled SNAP is observed using direct fluorescence of the TMR, and total protein is quantitated using western blotting for SNAP. The cells that were exposed to DMSO only (no inhibitor) serve as a standard for 0% inhibitor labeling, where the TMR fluorescence is set to 100%. Cells that contained SNAP-dead were treated as a 100% inhibitor blocked control, where TMR fluorescence would be set to 0%. Experiments conducted by Paula Bucko in the Scott lab show that exposure of cells to both CLP-Linker-

Inhibitors reduced TMR fluorescence in comparison to DMSO controls, thus showing that they are cell permeable and react with the SNAP-fusion proteins. Further TMR/Inhibitor labeling experiments showed that both the active and dead SNAP-SNAP-fusions are expressed at the centrosomes and that there is exclusive labeling of the SNAP-active fusion proteins in cells, as expected.

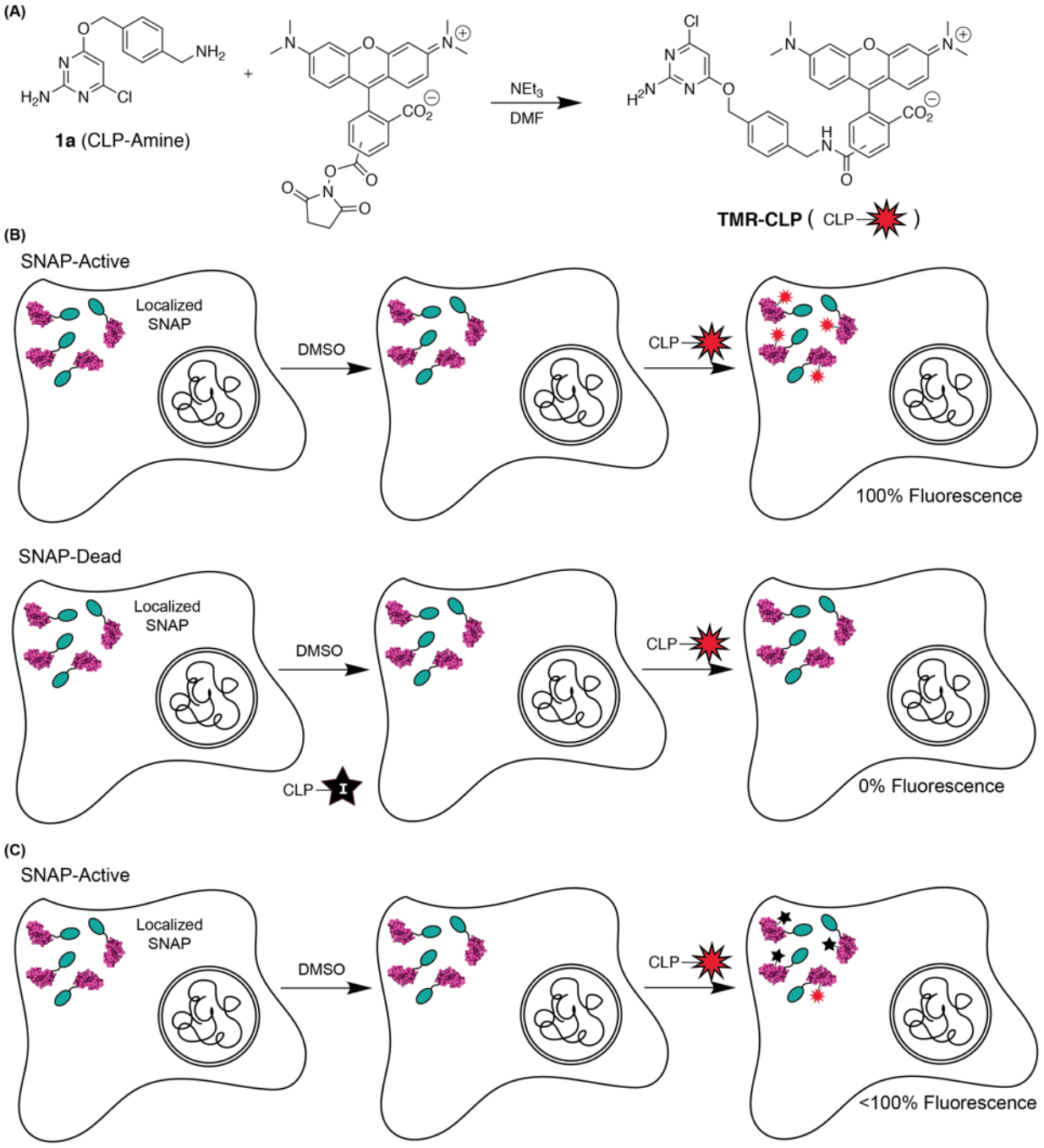

Figure 4.10. *Using pulse-chase experiments to test cell permeability and SNAP-labeling efficiency in cells.* (A) Preparation of TMR-CLP, via coupling of CLP-amine to 5(6)-carboxytetramethylrhodamine N-succinimidyl ester. (B) SNAP-active and SNAP-dead cells were exposed to DMSO (no inhibitor), followed by TMR-CLP. The SNAP-active cells served as a 100% fluorescence control (no inhibitor labeling) and the SNAP-dead cells served as a 0% fluorescence control (100% inhibitor labeling). Following labeling,

cells were lysed, and the lysate was resolved via SDS-PAGE. TMR signal from labeled SNAP-tag was measured via fluorescence and was scaled to the quantity of SNAP protein in the lysate as determined by western blotting. (C) Inhibitors were tested for the ability to modify SNAP-fusions in cells. A reduction in fluorescence is expected if inhibitors have labeled SNAP-tag and prevent TMR-CLP labeling.

4.7 Conclusions & Summary of Unpublished Work

ATP-competitive inhibitors of kinases are commonly used to understand specific aspects of kinase biology and can be used in a similar way as kinase dead mutants or kinase knockouts. However, ATP-competitive inhibitors of kinases offer several advantages to alternative approaches. These advantages often become clear when it is realized that kinase allostery plays a large role in their regulation due to reasons other than catalysis.[7] ATP-competitive inhibitors can be used to rationally modulate kinase global conformation to achieve differential outputs.[7] Kinase-dead mutants can have unpredictable effects on kinase allostery, and kinase knockouts, which not only remove the catalytic function of the kinase, but also all other functions, often offer less control than ATP-competitive inhibitors.[116] However, a limitation of kinase inhibitors, like mutants and knockouts, is that they affect all populations of the target kinase in a cell. That means that all of these approaches may be unable to fully explore the distinct roles kinases have in different locations in the cell. Here, we describe methodology for the inhibition of kinases at specific locations in the cell. We sought to achieve heightened spatial resolution of ATP-competitive inhibitors of kinases. As a proof of concept, we chose to design SNAP-tetherable inhibitors for Plk1 and Aurora A, which could then be directed to specific regions of cells expressing localized protein domains fused to SNAP-tag.

The cell-based experiments, which demonstrate the utility of these novel tools at the centrosomes and other sub-cellular locations , have been conducted by P. Bucko in the Scott lab.

Since both kinases are thought to have localized activity in the centrosomes of cells, these studies sought to direct SNAP-linkable Aurora A and Plk1 inhibitors specifically to that location, using SNAP-SNAP-PACT fusions. P. Bucko showed that the inhibitors are cell permeable, label the SNAP-tag fusion proteins in the expected region of the cell, can be used to achieve local inhibition of both Aurora A and Plk1 at the centrosomes, and produce a measurable phenotypic output. This work will be published in a manuscript that is currently in preparation, as well as in the dissertation of P. Bucko. This technique should be adaptable for many protein kinases, as well as other enzymes that are thought to have specific local activity. This technique only mandates that one can identify a small molecule inhibitor that maintains selectivity and potency towards a kinase target when modified with a SNAP-tetherable moiety via a linker molecule.

4.8 Materials and Methods

CLP-Linker Synthesis. 4.1a (CLP-Amine) was generated as described in Hill, *et al.* (2012).[111] 1 Eq **4.1a** and 1.1 Eq of **4.1b** (ChemScene) were dissolved in DMF at RT, at a concentration of 0.2 M with respect to **4.1a**. The reaction was placed on ice. While stirring, 1.3 Eq HOAt (1-Hydroxy-7-azabenzotriazole) and 3 Eq DIEA (N,N-Diisopropylethylamine) were added. After 5 minutes on ice, 1.3 Eq of EDCI (1-Ethyl-3-(3-dimethylaminopropyl)carbodiimide) was added. The reaction was allowed to stir for 24 hr (letting the ice melt and the reaction slowly come to RT). Reaction was dissolved in ethyl acetate, washed with $NaHCO_3$ and brine, and dried with Na_2SO_4. Remaining solvent and DMF were removed via rotovaping and lyophilization. The Boc-protected product (**4.1c**) was deprotected with 30% TFA in DCM (0.2 M **4.1c** final). Solid **4.1c** was dissolved in CH_2Cl_2 and cooled on ice. TFA was added dropwise until it reached 30% v/v. Reaction was stirred for 1 hr at RT. Toluene was added (to help remove TFA) and the reaction was rotovapped to near

dryness. Reaction was dissolved in ethyl acetate, washed with K_2CO_3, dried Na_2SO_4 and dried via rotovapping and lyophilization. Identity at each step was verified with MS.

BI2536 Functionalization Protocol (+CLP-Linker). 1 Eq **4.1d** and 1.1 Eq of the **4.2a** (ChemScene) were dissolved in DMF at RT (0.2 M **4.1d**). The reaction was placed on ice. While stirring, 1.3 Eq HOAt and 3 Eq DIEA were added. After 5 min on ice, 1.3 Eq of EDCI was added. The reaction was allowed to stir for 24 hr (letting the ice melt and the reaction slowly come to RT). DMF was removed and **4.2b** (BI2536-CLP) was purified by HPLC. Identity was verified with MS. $[M+H]^+ = 817.7$ *m/z*.

MLN8237 Functionalization Protocol (+CLP-Linker). 1 Eq **4.1d** and 1.1 Eq of **4.3a** were dissolved in DMF at RT (0.2 M **4.1d**). The reaction was placed on ice. While stirring, 2 Eq of HOAt and 3 Eq of DIEA were added. After 5 min on ice, 1.2 Eq of EDCI was added. The reaction was allowed to stir for 24 hr (letting the ice melt and the reaction slowly come to RT). DMF was removed and **4.3b** (MLN8237-CLP) was purified with HPLC. Identity was verified with MS. $[M+H]^+ = 911.0$ *m/z.*

TMR-Star Preparation. 1 Eq **4.1d** (0.2 M) and 1 Eq 5(6)-carboxytetramethylrhodamine N-succinimidyl ester (Thermo Fisher) were dissolved in DMF at RT. While stirring, 3 Eq of DIEA was added. The reaction was allowed to stir for 24 hr. DMF was removed and product was purified with HPLC. Identity was verified with MS. $[M+H]^+ = 676.2$ *m/z.* TMR-Star was prepared by Sujata Chakraborty in the Maly lab.

Protein Expression and Purification. His_6-SNAP-tag in an Ampicillin resistant plasmid was expressed in Escherichia coli BL21(DE3) cells using a method modified from Lombard, et al (2018).[10] The evening prior to expression, 5 mL LB Miller broth, containing 50 µg/mL Ampicillin, was inoculated with transformed cells, and they were grown at 37 °C overnight. The following

day, the starter culture was used to seed 250 mL LB Miller broth in a 500 mL baffle flask. Cells were grown to OD_{600} 0.3 and the temperature was then reduced to 20 °C. Cells were allowed to grow to OD_{600} 0.8, and they were then induced with 500 μM isopropyl β-D-thiogalactopyranoside. Induced cells were incubated at 20 °C overnight. All purification steps were carried out at 4 °C. Cells were spun down at 6500 g, suspended in 10 mL of wash/lysis buffer [50 mM HEPES (pH 7.5), 300 mM NaCl, 20 mM imidazole, and 1 mM phenylmethanesulfonyl fluoride], and lysed via sonication. The lysate was centrifuged at 10000 g for 20 min, and the supernatant was allowed to batch bind with 0.7 mL of Ni-NTA (Ni^{2+}-nitrilotriacetate) for 60 min. The resin was collected by centrifugation at 500g for 5 min and washed with 10 mL of wash/lysis buffer. The wash step was repeated three times. The Ni-NTA/His_6-SNAP-tag was added to a BioRad purification column, and washing was continued until the wash showed no remaining protein by Bradford. The protein was eluted using ~ 5 mL of elution buffer [50 mM HEPES (pH 7.5), 300 mM NaCl, 200 mM imidazole]. The eluate was dialyzed against 50 mM HEPES (pH 7.5), 200 mM NaCl, 5% glycerol, and 1 mM fresh dithiothreitol (DTT). Protein was aliquoted, flash-frozen in liquid N_2, and stored at − 80 ° C.

SNAP Labeling Experiments. 50 μM SNAP-tag was incubated with 75 μM CLP-linker-inhibitors (or DMSO alone for control reactions) [2.5% (v/v) final DMSO concentration] in buffer [20 mM Tris-Cl (pH 8), 200 mM NaCl, 1 mM DTT (added fresh)] at 26 °C for 1.5 hours. The reactions were purified using Zeba columns and exchanged into a MS compatible buffer (50 mM NH_4HCO_3, 0.2% HCO_2H). Ratios of unlabeled to labeled protein were determined using Native MS (Thermo Scientific LTQ Orbitrap XL/Bruker Esquire LC-Ion Trap).

Plk1 Inhibition Assays Using Casein as a Substrate. The kinase activity of Plk1 (SignalChem) was profiled using Casein as the substrate (0.2 mg/mL). Reactions contained 25 mM MOPS, pH

7.2; 12.5 mM β-glycerol-phosphate; 25 mM $MgCl_2$; 2 mM EGTA; 2 mM Na_3VO_4; 2 mM BME; and 0.05 mg/mL BSA. Serial dilutions (1:3) of 25X compounds in DMSO [4% (v/v) final concentration in the assay] were used. For SNAP-inhibitor titrations, serial dilutions (1:3) were made in assay buffer, and an equivalent amount of DMSO [4% (v/v) final concentration in the assay] was later added to each well. Reciprocally, in assays where 25X inhibitor was added in DMSO, assay buffer was first added to each well (equivalent to the volume of SNAP-inhibitor in buffer). The last two wells in each row served as control reactions (+Kinase/No Inhibitor; and No Kinase/No Inhibitor) and received DMSO or buffer in place of inhibitor or kinase, respectively. After addition and mixing of the above components, kinase stock dilutions (10-15 nM final) were added to each well (except for the last well in each row, which served as the No Kinase/No Inhibitor control). Next, [γ-^{32}P]ATP (final assay concentration: 0.012 μCi/μl) and unlabeled-ATP (final assay concentration: 40 μM) were added to the reactions. Plk1 was preincubated with ATP-competitive inhibitors and [γ-^{32}P]ATP/ unlabeled-ATP for 30 min. To initiate the reactions, Casein was added. The reactions were incubated for 1 hr at RT. Assays were quenched by spotting 4.6 μL of each reaction mixture onto phosphocellulose membranes (Reaction Biology). The membranes were subjected to three sequential washes in 0.5% phosphoric acid for 10 min, dried, and exposed overnight to a phosphor screen (GE Healthcare). Blots were scanned using a phosphor scanner (GE Typhoon FLA 9000). Raw data was processed with the GraphPad Prism software package (V5.0a) using the One site - Fit logIC_{50} function for curve fitting. Spots were quantified using ImageQuant. The kinase activity was first determined to be linear at 10 nM Plk1 under assay conditions, before conducting inhibitor titrations.

Aurora A Inhibition Assays Using Myelin Basic Protein as a Substrate. The kinase activity of Aurora A (Invitrogen) was profiled using myelin basic protein (MBP) as the substrate (0.2

mg/mL). Reactions contained 30 mM HEPES, pH 7.5; 10 mM $MgCl_2$; 0.6 mM EGTA; 2 mM Na_3VO_4; 2 mM BME; and 0.05 mg/mL BSA. Serial dilutions (1:3) of 25X compounds in DMSO [4% (v/v) final concentration in the assay] were used. For SNAP-inhibitor titrations, serial dilutions (1:3) were made in assay buffer, and an equivalent amount of DMSO [4% (v/v) final concentration in the assay] was later added to each well. Reciprocally, in assays where 25X inhibitor was added in DMSO, assay buffer was first added to each well (equivalent to the volume of SNAP-inhibitor in buffer). The last two wells in each row served as control reactions (+Kinase/No Inhibitor; and No Kinase/No Inhibitor) and received DMSO or buffer in place of inhibitor or kinase, respectively. After addition and mixing of the above components, kinase stock dilutions (15 nM final) were added to each well (except for the last well in each row, which served as the No Kinase/No Inhibitor control). To initiate the reactions, [γ-^{32}P]ATP (final assay concentration: 0.006 μCi/μl) was added to the reactions. The reactions were incubated for 4 hr at RT. Assays were quenched by spotting 4.6 μL of each reaction mixture onto phosphocellulose membranes (Reaction Biology). The membranes were subjected to three sequential washes in 0.5% phosphoric acid for 10 min, dried, and exposed overnight to a phosphor screen (GE Healthcare). Blots were scanned using a phosphor scanner (GE Typhoon FLA 9000). Raw data was processed with the GraphPad Prism software package (V5.0a) using the One site - Fit log IC_{50} function for curve fitting. Spots were quantified using ImageQuant. The kinase activity was first determined to be linear at 15 nM Aurora A, before conducting inhibitor titrations.

BIBLIOGRAPHY

[1] Fabbro, D., Cowan-Jacob, S. W., and Moebitz, H. (2015) Ten things you should know about protein kinases: IUPHAR Review 14, *Br. J. Pharmacol. 172*, 2675-2700.

[2] Manning, G., Whyte, D. B., Martinez, R., Hunter, T., and Sudarsanam, S. (2002) The Protein Kinase Complement of the Human Genome, *Science 298*, 1912-1916, 1933-1934.

[3] Cohen, P. (2002) Timeline: Protein kinases - the major drug targets of the twenty-first century?, *Nat. Rev. Drug Discovery 1*, 309-315.

[4] Bain, J., Plater, L., Elliott, M., Shpiro, N., Hastie, C. J., McLauchlan, H., Klevernic, I., Arthur, J. S. C., Alessi, D. R., and Cohen, P. (2007) The selectivity of protein kinase inhibitors: a further update, *Biochem. J. 408*, 297-315.

[5] Bhullar, K. S., Lagaron, N. O., McGowan, E. M., Parmar, I., Jha, A., Hubbard, B. P., and Rupasinghe, H. P. V. (2018) Kinase-targeted cancer therapies: progress, challenges and future directions, Mol. *Cancer 17*, 48/41-48/20.

[6] Knight, Z. A., and Shokat, K. M. (2005) Features of Selective Kinase Inhibitors, *Chem. Biol. 12*, 621-637.

[7] Kung, J. E., and Jura, N. (2016) Structural basis for the non-catalytic functions of protein kinases, *Structure 24*, 7-24.

[8] Taylor, S. S., Ilouz, R., Zhang, P., and Kornev, A. P. (2012) Assembly of allosteric macromolecular switches: lessons from PKA, *Nat. Rev. Mol. Cell Biol. 13*, 646-658.

[9] Lavoie, H., Li, J. J., Thevakumaran, N., Therrien, M., and Sicheri, F. (2014) Dimerization-induced allostery in protein kinase regulation, *Trends Biochem. Sci. 39*, 475-486.

[10] Lombard, C. K., Davis, A. L., Inukai, T., and Maly, D. J. (2018) Allosteric Modulation of JNK Docking Site Interactions with ATP-Competitive Inhibitors, *Biochemistry 57*, 5897-5909.

[11] Feldman, H. C., Tong, M., Wang, L., Meza-Acevedo, R., Gobillot, T. A., Lebedev, I., Gliedt, M. J., Hari, S. B., Mitra, A. K., Backes, B. J., Papa, F. R., Seeliger, M. A., and Maly, D. J. (2016) Structural and functional analysis of the allosteric inhibition of IRE1α with ATP-competitive ligands, *ACS Chem. Biol. 11*, 2195-2205.

[12] Hari, S. B., Merritt, E. A., and Maly, D. J. (2014) Conformation-Selective ATP-Competitive Inhibitors Control Regulatory Interactions and Noncatalytic Functions of Mitogen-Activated Protein Kinases, *Chem. Biol. 21*, 628-635.

[13] Hari, S. B., Perera, B. G. K., Ranjitkar, P., Seeliger, M. A., and Maly, D. J. (2013) Conformation-Selective Inhibitors Reveal Differences in the Activation and Phosphate-Binding Loops of the Tyrosine Kinases Abl and Src, *ACS Chem. Biol. 8*, 2734-2743.

[14] Leonard, S. E., Register, A. C., Krishnamurty, R., Brighty, G. J., and Maly, D. J. (2014) Divergent Modulation of Src-Family Kinase Regulatory Interactions with ATP-Competitive Inhibitors, *ACS Chem. Biol. 9*, 1894-1905.

[15] Register, A. C., Leonard, S. E., and Maly, D. J. (2014) SH2-Catalytic Domain Linker Heterogeneity Influences Allosteric Coupling across the SFK Family, *Biochemistry 53*, 6910-6923.

[16] Wang, L., Perera, B. G. K., Hari, S. B., Bhhatarai, B., Backes, B. J., Seeliger, M. A., Schuerer, S. C., Oakes, S. A., Papa, F. R., and Maly, D. J. (2012) Divergent allosteric control of the IRE1α endoribonuclease using kinase inhibitors, Nat. *Chem. Biol. 8*, 982-989.

[17] Ahler, E., Register, A. C., Chakraborty, S., Fang, L., Dieter, E. M., Sitko, K. A., Vidadala, R. S. R., Trevillian, B. M., Golkowski, M., Gelman, H., Stephany, J. J., Rubin, A. F., Merritt, E. A., Fowler, D. M., and Maly, D. J. (2019) A Combined Approach Reveals a Regulatory Mechanism Coupling Src's Kinase Activity, Localization, and Phosphotransferase-Independent Functions, *Mol. Cell 74*, 393-408.

[18] Tournier, C., Hess, P., Yang, D. D., Xu, J., Turner, T. K., Nimnual, A., Bar-Sagi, D., Jones, S. N., Flavell, R. A., and Davis, R. J. (2000) Requirement of JNK for stress-induced activation of the cytochrome c-mediated death pathway, *Science 288*, 870-874.

[19] Tournier, C. (2013) The 2 faces of JNK signaling in cancer, *Genes Cancer 4*, 397-400.

[20] Yu, C., Minemoto, Y., Zhang, J., Liu, J., Tang, F., Bui, T. N., Xiang, J., and Lin, A. (2004) JNK suppresses apoptosis via phosphorylation of the proapoptotic Bcl-2 family protein BAD, *Mol. Cell 13*, 329-340.

[21] Ma, X., Wang, H., Ji, J., Xu, W., Sun, Y., Li, W., Zhang, X., Chen, J., and Xue, L. (2017) Hippo signaling promotes JNK-dependent cell migration, *Proc. Natl. Acad. Sci. U. S. A. 114*, 1934-1939.

[22] Das, M., Jiang, F., Sluss, H. K., Zhang, C., Shokat, K. M., Flavell, R. A., and Davis, R. J. (2007) Suppression of p53-dependent senescence by the JNK signal transduction pathway, *Proc. Natl. Acad. Sci. U. S. A. 104*, 15759-15764.

[23] Bennett, B. L., Sasaki, D. T., Murray, B. W., O'Leary, E. C., Sakata, S. T., Xu, W., Leisten, J. C., Motiwala, A., Pierce, S., Satoh, Y., Bhagwat, S. S., Manning, A. M., and Anderson, D. W. (2001) SP600125, an anthrapyrazolone inhibitor of Jun N-terminal kinase, *Proc. Natl. Acad. Sci. U. S. A. 98*, 13681-13686.

[24] Dominguez, C., Powers, D. A., and Tamayo, N. (2005) p38 MAP kinase inhibitors: Many are made, but few are chosen, *Curr. Opin. Drug Discovery Dev. 8*, 421-430.

[25] Fang, L., Chakraborty, S., Dieter, E. M., Potter, Z. E., Lombard, C. K., and Maly, D. J. (2019) Chemoproteomic Method for Profiling Inhibitor-Bound Kinase Complexes, *J. Am. Chem. Soc. 141*, 11912-11922.

[26] Zeke, A., Remenyi, A., Misheva, M., and Bogoyevitch, M. A. (2016) JNK Signaling: Regulation and Functions Based on Complex Protein-Protein Partnerships, *Microbiol Mol Biol Rev 80*, 793-835.

[27] Gupta, S., Barret, T., Whitmarsh, A. J., Cavanagh, J., Sluss, H. K., Derijard, B., and Davis, R. J. (1996) Selective interaction of JNK protein kinase isoforms with transcription factors, *EMBO J. 15*, 2760-2770.

[28] Kallunki, T., Su, B., Tsigelny, I., Sluss, H. K., Derijard, B., Moore, G., Davis, R., and Karin, M. (1994) JNK2 contains a specificity-determining region responsible for efficient c-Jun binding and phosphorylation, *Genes Dev. 8*, 2996-3007.

[29] Xie, X., Gu, Y., Fox, T., Coll, J. T., Fleming, M. A., Markland, W., Caron, P. R., Wilson, K. P., and Su, M. S. S. (1998) Crystal structure of JNK3: a kinase implicated in neuronal apoptosis, *Structure 6*, 983-991.

[30] Heo, Y.-S., Kim, S.-K., Seo, C. I., Kim, Y. K., Sung, B.-J., Lee, H. S., Lee, J. I., Park, S.-Y., Kim, J. H., Hwang, K. Y., Hyun, Y.-L., Jeon, Y. H., Ro, S., Cho, J. M., Lee, T. G., and Yang, C.-H. (2004) Structural basis for the selective inhibition of JNK1 by the scaffolding protein JIP1 and SP600125, *EMBO J. 23*, 2185-2195.

[31] Davis, R. J. (2000) Signal transduction by the JNK group of MAP kinases, *Cell 103*, 239-252.

[32] Bogoyevitch, M. A., and Kobe, B. (2006) Uses for JNK: the many and varied substrates of the c-Jun N-terminal kinases, *Microbiol. Mol. Biol. Rev. 70*, 1061-1095.

[33] Lawler, S., Fleming, Y., Goedert, M., and Cohen, P. (1998) Synergistic activation of SAPK1/JNK1 by two MAP kinase kinases in vitro, *Curr. Biol. 8*, 1387-1390.

[34] Lisnock, J., Griffin, P., Calaycay, J., Frantz, B., Parsons, J., O'Keefe, S. J., and LoGrasso, P. (2000) Activation of JNK3α1 Requires both MKK4 and MKK7: Kinetic Characterization of in Vitro Phosphorylated JNK3α1, *Biochemistry 3*9, 3141-3148.

[35] Khatlani, T. S., Wislez, M., Sun, M., Srinivas, H., Iwanaga, K., Ma, L., Hanna, A. E., Liu, D., Girard, L., Kim, Y. H., Pollack, J. R., Minna, J. D., Wistuba, I. I., and Kurie, J. M. (2007) c-Jun N-terminal kinase is activated in non-small-cell lung cancer and promotes neoplastic transformation in human bronchial epithelial cells, *Oncogene 26*, 2658-2666.

[36] Aguirre, V., Uchida, T., Yenush, L., Davis, R., and White, M. F. (2000) The c-Jun NH(2)-terminal kinase promotes insulin resistance during association with insulin receptor substrate-1 and phosphorylation of Ser(307), *J. Biol. Chem. 275*, 9047-9054.

[37] Lee, Y. H., Giraud, J., Davis, R. J., and White, M. F. (2003) c-Jun N-terminal kinase (JNK) mediates feedback inhibition of insulin signaling cascade, *J. Biol. Chem. 278*, 2896-2902.

[38] Tran, E. H., Azuma, Y.-T., Chen, M., Weston, C., Davis, R. J., and Flavell, R. A. (2006) Inactivation of JNK1 enhances innate IL-10 production and dampens autoimmune inflammation in the brain, *Proc. Natl. Acad. Sci. U. S. A. 103*, 13451-13456.

[39] Shin, T., Ahn, M., Jung, K., Heo, S., Kim, D., Jee, Y., Lim, Y.-K., and Yeo, E.-J. (2003) Activation of mitogen-activated protein kinases in experimental autoimmune encephalomyelitis, *J. Neuroimmunol. 140*, 118-125.

[40] Tsuiki, H., Tnani, M., Okamoto, I., Kenyon, L. C., Emlet, D. R., Holgado-Madruga, M., Lanham, I. S., Joynes, C. J., Vo, K. T., and Wong, A. J. (2003) Constitutively active forms of c-Jun NH2-terminal kinase are expressed in primary glial tumors, *Cancer Res. 63*, 250-255.

[41] Pal, M., Febbraio, M. A., and Lancaster, G. I. (2016) The roles of c-Jun NH2-terminal kinases (JNKs) in obesity and insulin resistance, *J. Physiol. 594*, 267-279.

[42] Cui, J., Han, S.-Y., Wang, C., Su, W., Harshyne, L., Holgado-Madruga, M., and Wong, A. J. (2006) c-Jun NH2-Terminal Kinase 2α2 Promotes the Tumorigenicity of Human Glioblastoma Cells, *Cancer Res. 66*, 10024-10031.

[43] Mooney, L. M., and Whitmarsh, A. J. (2004) Docking Interactions in the c-Jun N-terminal Kinase Pathway, *J. Biol. Chem. 279*, 11843-11852.

[44] Ho, D. T., Bardwell, A. J., Grewal, S., Iverson, C., and Bardwell, L. (2006) Interacting JNK-docking Sites in MKK7 Promote Binding and Activation of JNK Mitogen-activated Protein Kinases, *J. Biol. Chem. 281*, 13169-13179.

[45] Sharrocks, A. D., Yang, S. H., and Galanis, A. (2000) Docking domains and substrate-specificity determination for MAP kinases, *Trends Biochem. Sci. 25*, 448-453.

[46] Bardwell, A. J., Flatauer, L. J., Matsukuma, K., Thorner, J., and Bardwell, L. (2001) A conserved docking site in MEKs mediates high-affinity binding to MAP kinases and cooperates with a scaffold protein to enhance signal transmission, *J. Biol. Chem. 276*, 10374-10386.

[47] Bardwell, A. J., Frankson, E., and Bardwell, L. (2009) Selectivity of Docking Sites in MAPK Kinases, *J. Biol. Chem. 284*, 13165-13173.

[48] Raman, M., Chen, W., and Cobb, M. H. (2007) Differential regulation and properties of MAPKs, *Oncogene 26*, 3100-3112.

[49] Whitmarsh, A. J. (2006) The JIP family of MAPK scaffold proteins, *Biochem. Soc. Trans. 34*, 828-832.

[50] Whitmarsh, A. J., Cavanagh, J., Tournier, C., Yasuda, J., and Davis, R. J. (1998) A mammalian scaffold complex that selectively mediates MAP kinase activation, *Science 281*, 1671-1674.

[51] Barr, R. K., Hopkins, R. M., Watt, P. M., and Bogoyevitch, M. A. (2004) Reverse Two-hybrid Screening Identifies Residues of JNK Required for Interaction with the Kinase Interaction Motif of JNK-interacting Protein-1, *J. Biol. Chem. 279*, 43178-43189.

[52] Barr, R. K., Kendrick, T. S., and Bogoyevitch, M. A. (2002) Identification of the critical features of a small peptide inhibitor of JNK activity, *J. Biol. Chem. 277*, 10987-10997.

[53] Laughlin, J. D., Nwachukwu, J. C., Figuera-Losada, M., Cherry, L., Nettles, K. W., and LoGrasso, P. V. (2012) Structural mechanisms of allostery and autoinhibition in JNK family kinases, *Structure 20*, 2174-2184.

[54] Ember, B., Kamenecka, T., and LoGrasso, P. (2008) Kinetic mechanism and inhibitor characterization for c-jun-N-terminal kinase 3alpha1, *Biochemistry 47*, 3076-3084.

[55] Ember, B., and LoGrasso, P. (2008) Mechanistic characterization for c-jun-N-Terminal Kinase 1α1, Arch. Biochem. *Biophys. 477*, 324-329.

[56] Chen, T., Kablaoui, N., Little, J., Timofeevski, S., Tschantz, W. R., Chen, P., Feng, J., Charlton, M., Stanton, R., and Bauer, P. (2009) Identification of small-molecule inhibitors of the JIP-JNK interaction, *Biochem. J. 420*, 283-294.

[57] Kinoshita, E., Kinoshita-Kikuta, E., Takiyama, K., and Koike, T. (2006) Phosphate-binding tag, a new tool to visualize phosphorylated proteins, *Mol. Cell. Proteomics 5*, 749-757.

[58] Kinoshita-Kikuta, E., Aoki, Y., Kinoshita, E., and Koike, T. (2007) Label-free kinase profiling using phosphate affinity polyacrylamide gel electrophoresis, *Mol. Cell. Proteomics 6*, 356-366.

[59] Theile, C. S., Witte, M. D., Blom, A. E. M., Kundrat, L., Ploegh, H. L., and Guimaraes, C. P. (2013) Site-specific N-terminal labeling of proteins using sortase-mediated reactions, *Nat. Protoc. 8*, 1800-1807, 1808 pp.

[60] Brancho, D., Tanaka, N., Jaeschke, A., Ventura, J.-J., Kelkar, N., Tanaka, Y., Kyuuma, M., Takeshita, T., Flavell, R. A., and Davis, R. J. (2003) Mechanism of p38 MAP kinase activation in vivo, *Genes Dev. 17*, 1969-1978.

[61] Krishnamurty, R., Brigham, J. L., Leonard, S. E., Ranjitkar, P., Larson, E. T., Dale, E. J., Merritt, E. A., and Maly, D. J. (2013) Active site profiling reveals coupling between domains in SRC-family kinases, *Nat. Chem. Biol. 9*, 43-50.

[62] Dar, A. C., and Shokat, K. M. (2011) The evolution of protein kinase inhibitors from antagonists to agonists of cellular signaling, *Annu. Rev. Biochem. 80*, 769-795.

[63] Karoulia, Z., Wu, Y., Ahmed, T. A., Xin, Q., Bollard, J., Krepler, C., Wu, X., Zhang, C., Bollag, G., Herlyn, M., Fagin, J. A., Lujambio, A., Gavathiotis, E., and Poulikakos, P. I. (2016) An Integrated Model of RAF Inhibitor Action Predicts Inhibitor Activity against Oncogenic BRAF Signaling, *Cancer Cell 30*, 485-498.

[64] Gibson, D. G., Young, L., Chuang, R.-Y., Venter, J. C., Hutchison, C. A., and Smith, H. O. (2009) Enzymatic assembly of DNA molecules up to several hundred kilobases, *Nat. Methods 6*, 343-345.

[65] Hari, S. B., Merritt, E. A., and Maly, D. J. (2013) Sequence Determinants of a Specific Inactive Protein Kinase Conformation, *Chem. Biol. 20*, 806-815.

[66] Good, M. C., Zalatan, J. G., and Lim, W. A. (2011) Scaffold proteins: Hubs for controlling the flow of cellular information, *Science 332*, 680-686.

[67] Bogoyevitch, M. A., Ngoei, K. R. W., Zhao, T. T., Yeap, Y. Y. C., and Ng, D. C. H. (2010) c-Jun N-terminal kinase (JNK) signaling: Recent advances and challenges, Biochim. Biophys. Acta, *Proteins Proteomics 1804*, 463-475.

[68] Prowse, C. N., and Lew, J. (2001) Mechanism of activation of ERK2 by dual phosphorylation, *J. Biol. Chem. 276*, 99-103.

[69] Nguyen, T., Ruan, Z., Oruganty, K., and Kannan, N. (2015) Co-conserved MAPK features couple D-domain docking groove to distal allosteric sites via the C-terminal flanking tail, *PLoS One 10*, e0119636/0119631-e0119636/0119621.

[70] Ghosh, R., Wang, L., Wang, E. S., Perera, B. G. K., Igbaria, A., Morita, S., Prado, K., Thamsen, M., Caswell, D., Macias, H., Weiberth, K. F., Gliedt, M. J., Alavi, M. V., Hari, S. B., Mitra, A. K., Bhhatarai, B., Schurer, S. C., Snapp, E. L., Gould, D. B., German, M. S., Backes, B. J., Maly, D. J., Oakes, S. A., and Papa, F. R. (2014) Allosteric Inhibition of the IRE1α RNase Preserves Cell Viability and Function during Endoplasmic Reticulum Stress, *Cell 158*, 534-548.

[71] Papa, F. R., Zhang, C., Shokat, K., and Walter, P. (2003) Bypassing a kinase activity with an ATP-competitive drug, *Science 302*, 1533-1537.

[72] Ventura, J.-J., Hubner, A., Zhang, C., Flavell, R. A., Shokat, K. M., and Davis, R. J. (2006) Chemical genetic analysis of the time course of signal transduction by JNK, Mol. *Cell 21*, 701-710.

[73] Cipak, L., Zhang, C., Kovacikova, I., Rumpf, C., Miadokova, E., Shokat, K. M., and Gregan, J. (2011) Generation of a set of conditional analog-sensitive alleles of essential protein kinases in the fission yeast Schizosaccharomyces pombe, *Cell Cycle 10*, 3527-3532.

[74] Treiber, D. K., and Shah, N. P. (2013) Ins and Outs of Kinase DFG Motifs, *Chem. Biol. 20*, 745-746.

[75] Borsello, T., Centeno, C., Riederer, I. M., Haefliger, J. A., and Riederer, B. M. (2007) Phosphorylation-dependent dimerization and subcellular localization of islet-brain 1/c-Jun N-terminal kinase-interacting protein 1, *J. Neurosci. Res. 85*, 3632-3641.

[76] Nihalani, D., Wong, H. N., and Holzman, L. B. (2003) Recruitment of JNK to JIP1 and JNK-dependent JIP1 Phosphorylation Regulates JNK Module Dynamics and Activation, *J. Biol. Chem. 278*, 28694-28702.

[77] Zalatan, J. G., Coyle, S. M., Rajan, S., Sidhu, S. S., and Lim, W. A. (2012) Conformational Control of the Ste5 Scaffold Protein Insulates Against MAP Kinase Misactivation, *Science 337*, 1218-1222.

[78] Cohen-Katsenelson, K., Wasserman, T., Khateb, S., Whitmarsh, A. J., and Aronheim, A. (2011) Docking interactions of the JNK scaffold protein WDR62, *Biochem. J. 439*, 381-390.

[79] Witzel, F., Maddison, L., and Bluthgen, N. (2012) How scaffolds shape MAPK signaling: what we know and opportunities for systems approaches, *Front Physiol 3*, 475.

[80] Invitrogen. (2017) Conquer Cell Counting, pp 1-12, Thermo Fisher Scientific, https://assets.thermofisher.com/TFS-Assets/LSG/brochures/countess-II-automated-cell-counters-brochure.pdf.

[81] Taylor, S. S., Keshwani, M. M., Steichen, J. M., and Kornev, A. P. (2012) Evolution of the eukaryotic protein kinases as dynamic molecular switches, *Philos. Trans. R. Soc., B 367*, 2517-2528.

[82] Golkowski, M., Vidadala, R. S. R., Lombard, C. K., Suh, H. W., Maly, D. J., and Ong, S.-E. (2017) Kinobead and Single-Shot LC-MS Profiling Identifies Selective PKD Inhibitors, *J. Proteome Res. 16*, 1216-1227.

[83] Umezawa, T. (2015) Screening of Kinase Substrates Using Kinase Knockout Mutants, *Methods Mol. Biol. 1306*, 59-69.

[84] Iyer, G. H., Garrod, S., Woods, V. L., and Taylor, S. S. (2005) Catalytic Independent Functions of a Protein Kinase as Revealed by a Kinase-dead Mutant: Study of the Lys72His Mutant of cAMP-dependent Kinase, *J. Mol. Biol. 351*, 1110-1122.

[85] Uitdehaag, J. C. M., Verkaar, F., Alwan, H., de Man, J., Buijsman, R. C., and Zaman, G. J. R. (2012) A guide to picking the most selective kinase inhibitor tool compounds for pharmacological validation of drug targets, Br. *J. Pharmacol. 166*, 858-876.

[86] Bradshaw, R. A., and Dennis, E. A. (2004) *Handbook of Cell Signaling*, Volume 2, Elsevier.

[87] Gautier, A., Juillerat, A., Heinis, C., Correa, I. R., Jr., Kindermann, M., Beaufils, F., and Johnsson, K. (2008) An engineered protein tag for multiprotein labeling in living cells, *Chem Biol. 15*, 128-136.

[88] Keppler, A., Gendreizig, S., Gronemeyer, T., Pick, H., Vogel, H., and Johnsson, K. (2003) A general method for the covalent labeling of fusion proteins with small molecules in vivo, *Nat. Biotechnol. 21*, 86-89.

[89] Juillerat, A., Gronemeyer, T., Keppler, A., Gendreizig, S., Pick, H., Vogel, H., and Johnsson, K. (2003) Directed Evolution of O6-Alkylguanine-DNA Alkyltransferase for Efficient Labeling of Fusion Proteins with Small Molecules In Vivo, *Chem. Biol. 10*, 313-317.

[90] Juillerat, A., Heinis, C., Sielaff, I., Barnikow, J., Jaccard, H., Kunz, B., Terskikh, A., and Johnsson, K. (2005) Engineering substrate specificity of O6-alkylguanine-DNA alkyltransferase for specific protein labeling in living cells, *ChemBioChem 6*, 1263-1269.

[91] Gronemeyer, T., Chidley, C., Juillerat, A., Heinis, C., and Johnsson, K. (2006) Directed evolution of O6-alkylguanine-DNA alkyltransferase for applications in protein labeling, *Protein Eng., Des. Sel. 19*, 309-316.

[92] Mizutani, S. (2010) HaloTag: a novel protein labeling technology for cell imaging and protein analysis, *Saibo 42*, 128-130.

[93] Srikun, D., Albers, A. E., Nam, C. I., Iavarone, A. T., and Chang, C. J. (2010) Organelle-Targetable Fluorescent Probes for Imaging Hydrogen Peroxide in Living Cells via SNAP-Tag Protein Labeling, *J. Am. Chem. Soc. 132*, 4455-4465.

[94] Barr, F. A., Sillje, H. H. W., and Nigg, E. A. (2004) Polo-like kinases and the orchestration of cell division, *Nat. Rev. Mol. Cell Biol. 5*, 429-441.

[95] Ji, J.-H., and Jang, Y.-J. (2006) Screening of domain-specific target proteins of polo-like kinase 1: construction and application of centrosome/kinetochore-specific targeting peptide, *J. Biochem. Mol. Biol. 39*, 709-716.

[96] Garcia-Alvarez, B., de Carcer, G., Ibanez, S., Bragado-Nilsson, E., and Montoya, G. (2007) Molecular and structural basis of polo-like kinase 1 substrate recognition: implications in centrosomal localization, *Proc. Natl. Acad. Sci. U. S. A. 104*, 3107-3112.

[97] Li, H., Wang, Y., and Liu, X. (2008) Plk1-dependent phosphorylation regulates functions of DNA topoisomerase IIalpha in cell cycle progression, *J. Biol. Chem. 283*, 6209-6221.

[98] Macurek, L., Lindqvist, A., Lim, D., Lampson, M. A., Klompmaker, R., Freire, R., Clouin, C., Taylor, S. S., Yaffe, M. B., and Medema, R. H. (2008) Polo-like kinase-1 is activated by aurora A to promote checkpoint recovery, *Nature 455*, 119-123.

[99] Liu, D., Davydenko, O., and Lampson, M. A. (2012) Polo-like kinase-1 regulates kinetochore-microtubule dynamics and spindle checkpoint silencing, *J. Cell Biol. 198*, 491-499.

[100] Colicino, E. G., Garrastegui, A. M., Freshour, J., Santra, P., Post, D. E., Kotula, L., and Hehnly, H. (2018) Gravin regulates centrosome function through PLK1, *Mol. Biol. Cell 29*, 532-541.

[101] Vaid, R., Sharma, N., Chauhan, S., Deshta, A., Dev, K., and Sourirajan, A. (2016) Functions of Polo-Like Kinases: A Journey From Yeast To Humans, *Protein Pept. Lett. 23*, 185-197.

[102] Marumoto, T., Zhang, D., and Saya, H. (2005) Aurora-A - A guardian of poles, *Nat. Rev. Cancer 5*, 42-50.

[103] Katayama, H., Sasai, K., Kloc, M., Brinkley, B. R., and Sen, S. (2008) Aurora kinase-A regulates kinetochore/chromatin associated microtubule assembly in human cells, *Cell Cycle 7*, 2691-2704.

[104] DeLuca, J. G. (2017) Aurora A Kinase Function at Kinetochores, *Cold Spring Harb. Symp. Quant. Biol. 82*, 91-99.

[105] DeLuca, K. F., Meppelink, A., Broad, A. J., Mick, J. E., Peersen, O. B., Pektas, S., Lens, S. M. A., and DeLuca, J. G. (2018) Aurora A kinase phosphorylates Hec1 to regulate metaphase kinetochore-microtubule dynamics, *J. Cell Biol. 217*, 163-177.

[106] Damodaran, A. P., Vaufrey, L., Gavard, O., and Prigent, C. (2017) Aurora A Kinase Is a Priority Pharmaceutical Target for the Treatment of Cancers, *Trends Pharmacol. Sci. 38*, 687-700.

[107] Maia, A. R. R., van Heesbeen, R. G. H. P., and Medema, R. H. (2014) A growing role for Aurora A in chromosome instability, *Nat. Cell Biol. 16*, 739-741.

[108] Hochegger, H., Hegarat, N., and Pereira-Leal, J. B. (2013) Aurora at the pole and equator: overlapping functions of Aurora kinases in the mitotic spindle, *Open Biol.*, 120185.

[109] Raab, M., Kraemer, A., Hehlgans, S., Sanhaji, M., Kurunci-Csacsko, E., Doetsch, C., Bug, G., Ottmann, O., Becker, S., Pachl, F., Kuster, B., and Strebhardt, K. (2015) Mitotic arrest and slippage induced by pharmacological inhibition of Polo-like kinase 1, *Mol. Oncol. 9*, 140-154.

[110] Kothe, M., Kohls, D., Low, S., Coli, R., Rennie, G. R., Feru, F., Kuhn, C., and Ding, Y.-H. (2007) Selectivity-determining residues in Plk1, *Chem. Biol. Drug Des. 70*, 540-546.

[111] Hill, Z. B., Perera, B. G. K., Andrews, S. S., and Maly, D. J. (2012) Targeting Diverse Signaling Interaction Sites Allows the Rapid Generation of Bivalent Kinase Inhibitors, ACS Chem. Biol. 7, 487-495.

[112] Sells, T. B., Chau, R., Ecsedy, J. A., Gershman, R. E., Hoar, K., Huck, J., Janowick, D. A., Kadambi, V. J., LeRoy, P. J., Stirling, M., Stroud, S. G., Vos, T. J., Weatherhead, G. S., Wysong, D. R., Zhang, M., Balani, S. K., Bolen, J. B., Manfredi, M. G., and Claiborne, C.

F. (2015) MLN8054 and Alisertib (MLN8237): Discovery of Selective Oral Aurora A Inhibitors, *ACS Med. Chem. Lett. 6*, 630-634.

[113] Dodson, C. A., Kosmopoulou, M., Richards, M. W., Atrash, B., Bavetsias, V., Blagg, J., and Bayliss, R. (2010) Crystal structure of an Aurora-A mutant that mimics Aurora-B bound to MLN8054: insights into selectivity and drug design, *Biochem. J. 427*, 19-28.

[114] Gillingham, A. K., and Munro, S. (2000) The PACT domain, a conserved centrosomal targeting motif in the coiled-coil proteins AKAP450 and pericentrin, *EMBO Rep. 1*, 524-529.

[115] Jongsma, M. A., and Litjens, R. H. G. M. (2006) Self-assembling protein arrays on DNA chips by auto-labeling fusion proteins with a single DNA address, *Proteomics 6*, 2650-2655.

[116] Bogomolovas, J., Gasch, A., Labeit, S., Simkovic, F., Rigden, D. J., and Mayans, O. (2014) Titin kinase is an inactive pseudokinase scaffold that supports MuRF1 recruitment to the sarcomeric M-line, *Open Biol. 4*, 140041.